

國立臺灣大學工學院機械工程學研究所

博士論文

Department of Mechanical Engineering

College of Engineering

National Taiwan University

Doctoral Dissertation

變剛性驅動器之發展與應用

Development and Application of Variable Stiffness Actuators



王仁政

Ren-Jeng Wang

指導教授：黃漢邦 博士

Advisor: Han-Pang Huang, Ph.D.

中華民國 101 年 3 月

March 2012

國立臺灣大學博士學位論文
口試委員會審定書

變剛性驅動器之發展與應用

Development and Application of Variable Stiffness
Actuators

本論文係 王仁政 君 (D94522031) 在國立臺灣大學機械工程學系完成之博士學位論文，於民國 101 年 03 月 07 日承下列考試委員審查通過及口試及格，特此證明

口試委員：

黃漢邦

(簽名)

(指導教授)

小菅 - 弘

李雲國

范芳照

孫同欽

蔡得民

系主任

楊耀州

(簽名)

Department of Mechanical Engineering
National Taiwan University
Taipei, TAIWAN, R.O.C.

Date: March 07, 2012

We have carefully read the thesis entitled

"Development and Application of Variable Stiffness Actuators"

submitted by Ren-Jeng Wang in partial fulfillment of the requirement of the degree of **DOCTOR OF PHILOSOPHY** and recommend its acceptance.

Kuei-Fan

Ren-Jeng Wang

Kang-Chau Fan

Chang-Lue Sung

De-Min Tsay

Advisor:

Yang YF

Chairperson

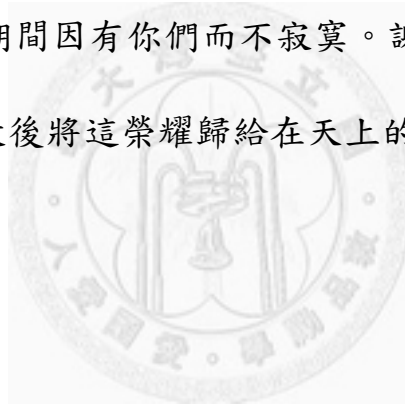
Department of Mechanical Engineering:

Yang YF

致謝

感謝指導教授 黃漢邦老師創立機器人實驗室，使我在機器人領域能有更加的認識。感謝論文口試委員小管一弘教授、王國雄教授、宋震國教授、范光照教授、蔡得民教授，百忙中能撥空給予我指教與建議。。

感謝實驗室的大家 明輝學長、欽仁、子豪、舉樓、聖諺、博任、柏霆、啟舜、聖翔、士益，研究期間因有你們而不寂寞。謝謝一直包容我的爸媽，姐姐，還有我美麗的老婆。最後將這榮耀歸給在天上的父(上帝)，感謝上帝的帶領保守。



敬畏耶和華是智慧的開端

(箴言 9 章 10 節)

摘要

本論文主要的目的，在發展不同於傳統工業機器手臂之擬人形機器手臂整合系統。此系統將可安裝於為不同目的而設計的機器人平台上，應用於不同環境中，取代人類或協助人類工作，甚至與人類進行安全的互動行為。

為了研發出一具備上述功能之多自由度擬人形機器手臂整合系統，本論文主要可分為兩大部分。第一部分將著重於模組化 2 軸驅動系統(DAMA)之機構設計與軟硬體架構建制，並藉由銜接三組該模組化 2 軸驅動系統，完成一擬人形 6 軸機器手臂之建置。而有鑑於傳統的致動器，無法同時滿足操作效能與安全互動之需求，本論文的第二部分將討論具安全互動行為機制的致動器與設計準則，提出可以滿足人機安全互動及提升系統效能的主動變剛性彈性驅動系統，並建立具有此特性之系統廣義線性數學模型，且進一步針對此一模型進行分析與控制器設計。最後分別設計製作出 APVSEA、AVSEA 與 ADEA 可自行調整輸出特性的主動變剛性彈性驅動器，以分別滿足安全與效能之需求。此設計將可取代傳統致動器，安裝於任一機器人系統上，以提升系統之性能。除擬人形機器手臂整合系統外，本文於最後將額外說明主動變剛性彈性驅動系統另一實質應用—手肘關節復健系統(AVSER)。

未來期許以本論文所發展的主動變剛性彈性驅動器來取代傳統致動器設計，安裝於所設計製作的多自由度擬人形機器手臂上，達到具有高操作效能仍可與人類進行安全的互動行為之設計目標。於復健系統則期許發展多關節手腳復健系統，達到具多關節復健功能之最終目標。

關鍵字：模組化 2 軸驅動器、擬人形機器手臂、人機安全互動、主動變剛性彈性驅動器、手肘關節復健系統

ABSTRACT

This dissertation aims to develop an integrated humanoid robot arm system that can be assembled into robot platforms designed for a variety of purposes, assisting, cooperating, and even interacting with humans in different fields and environments.

The dissertation presents the development of this integrated system in two major parts. The first focuses on developing an integrated system for a vertically intersected dual-axis modularized actuator system (DAMA), which is applied to a 6-axis humanoid robot arm. This section does not carefully consider the safety of human-robot interaction. The second part discusses actuation design, focusing on achieving a proper level of safety in human-robot interaction, and proposes a new actuation approach, active variable stiffness elastic actuation (AVSEA). Several active variable stiffness elastic actuators (APVSEA, AVSEA, ADEA) are designed, offering a compromise between proper safety levels and high manipulation performance. The end section of the dissertation describes another application of active variable stiffness elastic actuators—the elbow rehabilitation system (AVSER).

The research discussed involves the creation of a prototype for an active variable stiffness elastic actuator that has adjustable characteristics. It can be adapted to unknown environments and applied to the creation of a humanoid robot arm system that offers high levels of safety and performance.

Keywords: DAMA, Humanoid Robot Arm, Safety Human-Robot Interaction, Active Variable Stiffness Elastic Actuator, Elbow Rehabilitation System.

CONTENT

摘要.....	i
Abstract.....	iii
List of Tables.....	ix
List of Figures.....	xi
Nomenclature.....	xv
CHAPTER 1. Introduction.....	1
1.1. Motivation.....	1
1.2. Overview of the Dissertation.....	3
1.3. Contributions of the Dissertation.....	9
CHAPTER 2. Building a Humanoid Robot Arm.....	13
2.1. Introduction.....	14
2.2. Mechanical Design of a DAMA.....	19
2.2.1. The Concept of a DAMA.....	19
2.2.2. Detailed Structure of a DAMA (High Torque Module).....	19
2.2.3. Detailed Structure of a DAMA (Small Size Module).....	22
2.3. Simulation System.....	24
2.3.1. The Independent Joint Control of the DAMA System.....	24
2.3.2. Control and Simulation of the DAMA System.....	28
2.4. Finite Element Analysis.....	31
2.5. Hardware and Software.....	32
2.6. Experimental Results.....	33
2.7. Summary.....	40
CHAPTER 3. Background and Related Work of Inherently Safe Actuating Mechanisms.....	41
3.1. Introduction.....	42
3.2. Performance and Safety Constrains.....	44
3.2.1. Performance Indices.....	44
3.2.2. Safety Criteria.....	46
3.3. Pre-existing Compliant and Safety Actuator Design.....	50
3.3.1. Cable-and-Cylinder Drive Transmissions.....	50
3.3.2. Series Elastic Actuators (SEA).....	51
3.3.3. Programmed Impedance Actuators.....	53
3.3.4. Variable Stiffness Actuators.....	54

3.3.5. Parallel Coupled Micro-Macro Actuators (DM2).....	56
3.3.6. Antagonistic Pneumatic Artificial Muscle.....	56
3.3.7. Safe Link Mechanism and Safe Joint Mechanism.....	57
3.4. Summary.....	59
CHAPTER 4. APVSEA—An Active-Passive Variable Stiffness Elastic Actuator for Safety Robot Systems.....	63
4.1. Introduction.....	64
4.2. Precise Position Movement Actuation / Safe Actuation	65
4.2.1. Motor-Ball screw Drive System	65
4.2.2. Passive Variable Stiffness Serial Configuration.....	66
4.2.3. Active Variable Stiffness Serial Configuration.....	67
4.2.4. Active-Passive Variable Stiffness Elastic Actuator (APVSEA).....	69
4.3. Design of an Active-Passive Variable Stiffness Elastic Actuator (APVSEA)	71
4.4. System Experiment Evaluation.....	75
4.4.1. Adaptive Compliant Property	75
4.4.2. Active Variable Stiffness Property.....	78
4.4.3. Safe Robot System.....	79
4.5. Summary.....	80
CHAPTER 5. AVSEA—Active Variable Stiffness Elastic Actuator : Design and Application for Safe Physical Human-Robot Interaction	83
5.1. Introduction.....	84
5.2. Precise Position Movement Actuation / Safe Actuation	84
5.2.1. Motor-Ball screw Drive System	85
5.2.2. Active Variable Stiffness Serial Configuration.....	88
5.2.3. Active Variable Stiffness Elastic Actuator (AVSEA).....	90
5.3. Design of an Active Variable Stiffness Elastic Actuator.....	91
5.4. System Experiment Evaluation.....	96
5.4.1. Adaptive Compliant Property	96
5.4.2. Active Variable Stiffness Property.....	98
5.4.3. Response to Position Command with Variable Stiffness.....	98
5.4.4. Head Injury Criterion (HIC)	100
5.5. Summary.....	102
CHAPTER 6. ADEA—Active Variable Stiffness Differential Elastic Actuator : Design and Application for Safe Robotics.....	103
6.1. Introduction.....	104

6.2.	General Idea of the Active Variable Stiffness Differential Elastic Actuator (ADEA).....	105
6.2.1.	Active Variable Stiffness Element — Leaf spring.....	105
6.2.2.	Mathematical Description of the Active Variable Stiffness Differential Elastic Actuator (ADEA).....	106
6.3.	Design, Working Principle and Modeling of the ADEA.....	108
6.3.1.	Mechanical Design and Working Principle.....	109
6.3.2.	Mechanism Modeling of the ADEA System.....	111
6.3.3.	Analysis of the ADEA System.....	113
6.4.	System Experiment Evaluation.....	115
6.4.1.	Adaptive Compliant Property of ADEA.....	116
6.4.2.	Active Variable Stiffness Property of ADEA.....	117
6.4.3.	Response to Position Command with Variable Stiffness.....	118
6.4.4.	Head Injury Criterion (HIC).....	119
6.5.	Summary.....	121
CHAPTER 7.	Application : Rehabilitation System.....	123
7.1.	Introduction.....	124
7.2.	New Rehabilitation Robot System—Active Variable Stiffness Exoskeleton Robot (AVSER).....	128
7.3.	Principle and Design of the Active Variable Stiffness Elastic Exoskeleton Robot (AVSER).....	130
7.4.	System Experiment Evaluation.....	130
7.5.	Summary.....	137
CHAPTER 8.	Conclusions and Future Works.....	139
8.1.	Conclusions.....	139
8.2.	Future Works.....	140
8.2.1.	Active Variable Stiffness Elastic Actuator.....	141
8.2.2.	Humanoid Robot System Design.....	141
8.2.3.	Rehabilitation System.....	142
8.2.4.	Exoskeleton System.....	142
References	144

LIST OF TABLES

Table 2-1 Specification of the DAMA.....	34
Table 2-2 Specification of the 6-axis humanoid robot arm.....	37
Table 4-1 Specification of the APVSEA.....	77
Table 4-2 The Estimated HIC and v_{\max} for APVSEA and SEA.....	80
Table 5-1 Specification of AVSEA.....	97
Table 6-1 Specification of the ADEA.....	115
Table 7-1 Specification of the AVSER.....	132



LIST OF FIGURES

Figure 2-1 Poly Bot [2]	15
Figure 2-2 Micro-robot [6].....	15
Figure 2-3 Odin [8]	16
Figure 2-4 Modular Robot [9].....	16
Figure 2-5 KRVM [10]	16
Figure 2-6 Roombots [16].....	16
Figure 2-7 (a) The kinematics of the 6-axis humanoid robot arm, and (b) the concept of the 6-axis humanoid robot arm with three DAMAs.....	18
Figure 2-8 The Vertically Intersected Dual Axes Modularized Actuator System (DAMA) with high torque capability: (a) the DAMA outward appearance, (b) the detailed structure of the DAMA, (c) the Joint 01 system of the DAMA, and (d) the Joint 02 system of the DAMA.	21
Figure 2-9 The Vertically Intersected Dual Axes Modularized Actuator System (DAMA) with small size capability: (a) the DAMA outward appearance, (b) the detailed structure of the DAMA, (c) the Joint 01 system, and (d) the Joint 02 system.	23
Figure 2-10 (a) The Simulation System of the DAMA, and (b) the ADAMS software Simulation System.	29
Figure 2-11 Simulation results and the average tracking errors: (a) the joint 01 system of the DAMA, and (b) the joint 02 system of the DAMA.....	30
Figure 2-12 Finite element analysis of two key components of the DAMA.	32
Figure 2-13 (a) Experimental setup for the DAMA, and (b) the angular positions and the error curves of two independent joints of the DAMA.	35
Figure 2-14 The Workspace of the 6-axis robot arm.	37
Figure 2-15 (a) Experimental setup, and (b) trajectory planning for the 6-axis robot arm.	38
Figure 2-16 The 6-axis humanoid robot arm simulation and control system.	38
Figure 2-17 Experimental results: (a) the 6-axis humanoid robot arm with circle motion, and (b) the 6-axis humanoid robot arm with five-angle star motion.	39
Figure 3-1 Head injury criteria as a function of effective inertia and interface stiffness [40].....	49
Figure 3-2 The Barrett WAM robot [42].....	51
Figure 3-3 Different kinds of Series Elastic Actuators.	53
Figure 3-4 Mechanical Impedance Adjuster where linear spring and brake	

systems are directly built [54][58]	55
Figure 3-5 Appearance of the Variable Stiffness Actuator [61]	55
Figure 3-6 An Actuator with Mechanically Adjustable Series Compliance [52].....	55
Figure 3-7 Distributed Elastically Coupled Macro Mini Actuation (DECMMA) [40]	58
Figure 3-8 Artificial muscles in antagonistic pairs	58
Figure 3-9 Prototype and operation of the safe joint mechanism [84]	58
Figure 4-1 Motor-Ball screw Drive System.....	67
Figure 4-2 Passive variable stiffness serial configuration.	67
Figure 4-3 Active Variable Stiffness Serial Configuration.	70
Figure 4-4 The relationship between the block movement and the force on the block.....	70
Figure 4-5 The relationship between the block movement and the force on the block.....	70
Figure 4-6 3D model of Active-Passive Variable Stiffness Elastic Actuator.	73
Figure 4-7 Front view of Active-Passive Variable Stiffness Elastic Actuator.....	74
Figure 4-8 3D model of Main structure of APVSEA.	74
Figure 4-9 3D model of Main structure of APVSEA when APVSEA with external forces.	74
Figure 4-10 Active-Passive Variable Stiffness Elastic Actuator (APVSEA).	77
Figure 4-11 Adaptive compliant property for Active-Passive Variable Stiffness Elastic Actuator.	77
Figure 4-12 Response to position command with various stiffness.....	78
Figure 4-13 Measure stiffness of the APVSEA.	78
Figure 4-14 Experiment setup for hitting-object experiment.	80
Figure 5-1 Motor-Ball screw Drive System.....	87
Figure 5-2 A block assembly (with propelling shave and fixed pulley).	87
Figure 5-3 New Motor-Ball screw Drive System (with block assembly).....	88
Figure 5-4 A beam system.....	89
Figure 5-5 Schematic of active variable stiffness serial configuration. By changing the position of the moving plant, the active variable stiffness serial configuration has ability to obtain the effective length of leaf spring (l), change of the effective length of the leaf spring results in changing stiffness.....	89
Figure 5-6 A concept of the Active Variable Stiffness Elastic Actuator (AVSEA).	90
Figure 5-7 Control topology of the AVSEA. The AVSEA consists of two	

DC-motors: one is used to control the position of the joint and the other is used to adjust the stiffness of the APVSEA. Each motor is controlled by a simple PID controller.	90
Figure 5-8 3D model of Active Variable Stiffness Elastic Actuator (AVSEA).	93
Figure 5-9 Top view of AVSEA (3-D model of new motor-ball screw drive system)	93
Figure 5-10 3-D model of active variable stiffness serial configuration of AVSEA ...	94
Figure 5-11 3D model of the Motor-Ball screw drive system of AVSEA; (a) the concept of the Motor-Ball screw drive system of AVSEA, (b) the cross-section diagram of the Motor-Ball screw drive system of AVSEA, (c) the detail structure of the Motor-Ball screw drive system of AVSEA, (d) the Motor-Ball screw drive system of AVSEA with external forces.	94
Figure 5-12 Active Variable Stiffness Elastic Actuator (AVSEA).	97
Figure 5-13 Adaptive compliant property for Active Variable Stiffness Elastic Actuator.	99
Figure 5-14 Measure stiffness of the AVSEA.	99
Figure 5-15 Response to position command with variable stiffness.	100
Figure 5-16 The head Injury Criterion (HIC) for SEA and AVSEA. An HIC of 100 is a suitable value to normal operation of a machine physically interacting with humans. The model parameters for AVSEA are: Maximum $K_{transm} = 3000\text{kN/m}$ (Equivalent to rigid joint stiffness), Minimum $K_{transm} = 0.95\text{kN/m}$, $\gamma = 3000\text{kN/m}$, $K_{cov} = 25\text{kN/m}$, $M_{oper} = 4\text{kg}$, $M_{rotor} = 0.7\text{kg}$ and $M_{link} = 0.5\text{kg}$	102
Figure 6-1 The Active Variable Stiffness Differential Elastic Actuator (ADEA) ...	104
Figure 6-2 The Concept of a Beam System.	106
Figure 6-3 The four bar linkage system of the ADEA.	108
Figure 6-4 The symmetric roller system of the ADEA.	108
Figure 6-5 The detail structure of the ADEA.	110
Figure 6-6 3D model of the ADEA.	111
Figure 6-7 A Simplified ADEA Model.	112
Figure 6-8 Simulation Frequency Response with End Free.	114
Figure 6-9 Simulation Frequency Response without any Actuator Force.	115
Figure 6-10 Active Variable Stiffness Differential Elastic Actuator (ADEA).	116
Figure 6-11 Adaptive compliant property for the ADEA.	117
Figure 6-12 Measure stiffness of the ADEA.	119

Figure 6-13 Response to position command with variable stiffness.	119
Figure 6-14 The head Injury Criterion (HIC) for SEA and ADEA. An HIC of 100 is a suitable value to normal operation of a machine physically interacting with humans. The model parameters for ADEA are: Maximum $K_{transm} = 3000\text{kN/m}$ (Equivalent to rigid joint stiffness), Minimum $K_{transm} = 0.95\text{kN/m}$, $\gamma = 3000\text{kN/m}$, $K_{cov} = 25\text{kN/m}$, $M_{oper} = 4\text{kg}$, $M_{rotor} = 0.7\text{kg}$ and $M_{link} = 0.5\text{kg}$	121
Figure 7-1 The Active Variable Stiffness Exoskeleton Robot System.....	129
Figure 7-2 Rehabilitation Robot System.....	129
Figure 7-3 3D model of AVSEA	131
Figure 7-4 3D model of AVSER.	131
Figure 7-5 Active Variable Stiffness Exoskeleton Robot System (AVSER).....	133
Figure 7-6 Rehabilitation exercise setup.....	133
Figure 7-7 Active Variable Stiffness Exoskeleton Robot System (AVSER).....	134
Figure 7-8 Experiment results of different rehabilitation exercise modes.....	137
Figure 8-1 The multi-Axial rehabilitation system (a) 3D model of the system, (b) The system has elastic elements and functions of variable stiffness to meet the demand for safe upper limbs rehabilitation.....	142

NOMENCLATURE

Notations

e_b	Back electromotive force
f_{eff}	Effective viscous friction coefficient of the combined motor and load referred to the motor shaft
f_m	Viscous-friction coefficient of the motor referred to the motor shaft
f_L	Viscous-friction coefficient of the load referred to the load shaft
i_a	Armature current
J_{eff}	Effective moment of inertia of the f the combined motor and load referred to the motor shaft
J_L	Moment of inertia of the load referred to the load shaft
J_m	Moment of inertia of the motor referred to the motor shaft
K_a	Torque constant of the motor
K_b	Back emf constant
K_p	Position feedback gain
K_v	Error derivative feedback gain
K_I	Integral gain
L_a	Armature inductance
n	Reduction ratio of the gear train
R_a	Armature resistance
V_a	Applied voltage
θ_m	Angular displacements of the motor shaft
θ_L	Load shaft in radian
τ	Torque delivered by the motor
τ_m	Torque dissipated by the motor
τ_L	Load torque referred to the load shaft
τ_L^*	Torque dissipated by the load referred to the motor shaft

Acronyms

ADEA	Active Variable Stiffness Differential Elastic Actuator
APVSEA	Active-Passive Variable Stiffness Elastic Actuator
AVSEA	Active Variable Stiffness Elastic Actuator
AVSER	Active Variable Stiffness Exoskeleton Robotic System
DAMA	A Vertically Intersected Dual Axes Modularized Actuator System
DOF	Degree of Freedom
DECMMA	Distributed Elastically Coupled Macro Mini Actuation
EMG	Electromyogram
HIC	Head Injury Criterion
SEA	Series Elastic Actuator
SJM	Safe joint mechanism
SLM	Safe link mechanism



CHAPTER 1. INTRODUCTION

1.1. Motivation

The field of robotics currently involves a wide range of applications that can be employed in different fields and environments. One of the most important issues in modern robotics, and also one of the most challenging, is to make robots more versatile in terms of their ability to handle unpredictable and difficult tasks. A great amount of research has been carried out that aims to enhance the dexterity and functionality of robots. The development of an integrated system for a humanoid robot arm, taking into account mechanical design, solvability of kinematics, trajectory generation, control theorems, and a compromise between safety and performance, is thus critical. An excellently designed humanoid robot arm system can be assembled and integrated into either a movable platform or a fixed platform to fulfill diverse tasks.

The development of a humanoid robot system involves the following two areas:

(1) Hardware Design

Hardware design involves mechanical and control architecture design, seriously

influencing operation performance as well as other crucial issues. Mechanical design, involving mechanical component design, arrangement of actuators and sensors, distribution of masses, and analyses of kinematics and dynamics, is crucial to the performance of a humanoid robot. Control architecture design, involving control and communication modules, motor signal process modules, driver modules, and sensor systems, is also crucial, particularly with regard to real-time performance and control algorithm realization. An overall control system can be divided into several sub-systems, each designed for different purposes that suit a variety of potential situations.

(2) Software Development

The software used by a humanoid robot arm, which includes a user interface, control algorithm, trajectory planning, and task planners, determines its responses. Integrated industrial manipulator systems that take both hardware and software design into account have long existed, whereas humanoid robots that are able to physically assist humans in various environments are still being developed. Most existing unfolding robot arms have only one design consideration, such as performance or safety. This integrative humanoid robot system, consisting of rigid links, electrical servo actuators, tough covers, high-ratio reduction devices, and position sensors, can

only interact with people and environments under safety constraints, and moves slowly through carefully planned motions, applying multiple control strategies.

Human-robot-environment interaction includes a wide range of applications, and may involve robots operating in unstructured environments, sharing workspaces, and engaging in close physical cooperation with humans, which means that safety issues are a primary concern.

1.2. Overview of the Dissertation

This dissertation is divided into two main parts. The first part, presented in Chapter 2 focuses on developing the integrated system for a rigid humanoid robot arm without carefully considering the safety level of human-robot interaction. The second part, which presented in Chapters 3 through 6, concentrates on the development of an alternative actuation approach, and of critical modular mechanism components, making compromises that allow humanoid robot arms to interact with people and execute complex motions safely in unstructured environments. In Chapter 7, another application of active variable stiffness elastic actuators, the elbow rehabilitation system (AVSER), is described. Chapter 8 presents conclusions and directions for future work.

The chapters in this dissertation can be briefly described as follows:

Chapter 1 Introduction

This chapter gives a brief statement about the motivation, overview, and contributions of this dissertation, and discusses essential elements of the construction of an integrated humanoid robot arm system from the broad perspective of modern robotics.

Chapter 2 Building a Humanoid Robot Arm

The beginning of this chapter describes current robotics technology, focusing especially on the design of robot manipulators. This dissertation develops a vertically intersected dual-axis modularized actuator system (DAMA), and applies it to a 6-axis humanoid robot arm. This DAMA system consists of two independent joints, and is refined using finite element analysis. In this chapter, it is demonstrated how a novel DAMA modular system can be used to easily construct a mechanism with any degree of freedom, achieving a modular or reconfigurable system by using the DAMA module. The system's dynamic properties are observed based on simulations with ADAMS and MATLAB software packages. This chapter also covers the development of the hardware and software systems of the DAMA. The hardware architecture is composed of a microprocessor, an RS-232 to CAN Bus Module, and two

independent-joint controller modules. The software control system is written in Visual C++. The system employs a simple but effective PID scheme to independently control the DAMA's two joints. The experimental results show that for an S curve and circle trajectory input position command, the DAMA and the 6-axis humanoid robot arm, which is formed by the DAMA module, are able to effectively track commands. This means that the DAMA can be used as a generic module for multiple-degrees-of-freedom systems.

Chapter 3 Background and Related Work of Inherently Safe Actuating Mechanisms

In this chapter, the focus shifts to a different field, that of human-robot interaction, with the aim of developing an intrinsically-safe method of robot actuation and a control strategy that takes both capacity for performance and safety of motion into account. Critical qualitative and quantitative indices for measuring performance and safety are discussed, with reference to the evaluation and development of a robotic system and actuator design. A brief introduction to pre-existing compliant actuators and their design concepts is also presented.

Chapter 4 APVSEA - An Active-Passive Variable Stiffness Elastic Actuator for Robot System Safety

In classical robotics applications, robotic systems consist of servo motors, as well

as high-ratio reduction and rigid links. Mechanical designers prefer to design robotic applications that are as stiff as possible, so that robots can be manipulated with greater speed and precision. Unfortunately, such robotic applications are often unable to meet safety requirements in their interactions with people, and in environments where the safety of humans and protection of robots is fundamental. This dissertation presents an active-passive variable stiffness elastic actuator (APVSEA) which is designed for safe robot systems. The APVSEA consists of two DC motors. One is used to control the position of the robot's joint, while the other is used to adjust the stiffness of the system. Stiffness is generated by two antagonistically nonlinear springs, and by changing the preload length of the springs, the APVSEA is able to minimize heavy forces of impact due to shocks, safely interact with the user, and become as stiff as is needed to make precise position movements and trajectory tracking control easier. This chapter presents experiment results to show that the APVSEA is capable of allowing both precise position movements and safe human-robot interaction.

Chapter 5 AVSEA- Active Variable Stiffness Elastic Actuator : Design and Application for Safe Human-Robot Physical Interaction

This dissertation also presents an active variable stiffness elastic actuator (AVSEA) that is designed to allow for safe human-robot physical interaction. The AVSEA consists of two DC motors. One is used to control the position of the joint and

the other is used to adjust the stiffness of the system. The stiffness is generated by a leaf spring. By changing the effective length of the leaf spring, the AVSEA has the ability to minimize the force of heavy impacts due to shocks, safely interact with users, and become as stiff as necessary to more easily allow precise position movements and trajectory tracking control. Experimental results are presented to show that AVSEA is capable of enabling precise position movements to be carried out while also ensuring safe human-robot interaction.

Chapter 6 ADEA- Active Variable Stiffness Differential Elastic Actuator : Design and Application for Robot Safety

In addition to the above, this dissertation presents an active variable stiffness differential elastic actuator (ADEA) that is designed for application in robotic systems and, more generally, in machines designed to interact with people and environments under safety constraints. The ADEA consists of two DC motors that independently drive two antagonistic worm gears. By changing the synchronization and differentiation in angle displacement of these two gears, the ADEA has the capacity to minimize heavy impacts due to shocks, safely interact with users, and become as stiff as is necessary to make precise position movements. In addition, the ADEA allows for fast motion control while guaranteeing the safety of human operators in worst-case impact situations through its dynamically variable stiffness. This chapter presents

experimental results to demonstrate the performance and safety capabilities of a one-link arm actuated by the ADEA.

Chapter 7 Application : Rehabilitation System

The dissertation introduces an active variable stiffness exoskeleton robotic system (AVSER) with the AVSEA, improving the safety of human-robot interaction and produces a unique capacity for adjustable stiffness that meets demands for safe active-passive elbow rehabilitation. The AVSEA consists of two DC motors. One is used to control the position of the joint, while the other is used to adjust the stiffness of the system. The stiffness is generated by a leaf spring. By shortening the effective length of the leaf spring, the AVSEA is able to reduce stiffness automatically, which moves the AVSER from active (assistive) motion to passive (resistance) rehabilitation during the process of therapy. In this chapter, the mechanical design, modeling, and control algorithms are described in detail. The capacity of the proposed AVSER with electromyogram (EMG) signal feedback is verified through rehabilitation exercise experiments to demonstrate the efficacy of the system.

Chapter 8 Conclusions and Future Work

This chapter briefly gives a summary of the dissertation, offers some concluding remarks and outlines work to be carried out in the future.

1.3. Contributions of the Dissertation

The contributions of this dissertation are

(1) Design of a Vertically Intersected Dual-Axis Modularized Actuator System

The dissertation presents the design of a vertically intersected dual-axis modularized actuator system (DAMA) and its application to a 6-axis humanoid robot arm. This DAMA system possesses some special characteristics, including the following:

- Each DAMA consists of a pair of two DOF atoms, with two units.
- Each DAMA has an on-board microprocessor and communication system.
- Each DAMA has the ability to connect to, disconnect from, and rotate around its neighbors.
- Each DAMA possesses enough power to rotate its neighbors.
- The shape of the DAMA is in pot form, mimicking the appearance of a human arm.

(2) Design of a 6-Axis Humanoid Robot Arm

As part of this dissertation, a 6-axis humanoid robot arm has been built, which consists of three DAMAs, two high torque modules for the shoulder and upper part, and one small module for the lower part. The arm possesses some special

characteristics, such as:

- Human form, allowing it to work with objects designed for people more easily.
- Human-like structure and integration of simple kinematics.
- Partial utilization of harmonic drives, improving precision and efficiency.
- Quick and flexible construction.
- Simple wire systems, constructed using DAMAs.

These characteristics can also serve as useful design objectives for the development and examination of more advanced theories and algorithms.

(3) Development of Actuation Compromise between Safety and Performance

Several intrinsically safe intelligent actuators have been designed, which ensure both high performance and safe motion capacities. A linear model and a series of manipulations have been used to check the performance of the system and its benefits for designers.

(4) Design of Intrinsically Safe Intelligent Actuator Mechanisms

By changing the stiffness of actuators, the system is able to minimize high impact forces due to shocks, safely interact with users, and become as stiff as is needed to make precise position movements or trajectory tracking control easier. This

dissertation presents an APVSEA whose stiffness is generated by two antagonistically nonlinear springs, an AVSEA whose stiffness is generated by a leaf spring, and an ADEA whose stiffness is generated by the synchronization and differentiation of angle displacement in two antagonistic worm gears. These intrinsically safe intelligent actuators allow for high performance within safety constraints.

(5) Design of Rehabilitation System Mechanism

The dissertation introduces an AVSER with the AVSEA, which improves the safety of human-robot interaction and produces a unique capacity for adjustable stiffness that meets safe active-passive elbow rehabilitation demands. The mechanical design and control algorithms are described in detail. The capacity of the proposed AVSER with electromyogram (EMG) signal feedback is verified through rehabilitation exercise experiments that demonstrate the efficacy of the system.

CHAPTER 2. BUILDING A HUMANOID ROBOT ARM

A Vertically Intersected Dual-Axis Modularized Actuator System (DAMA) is developed and applied to a 6-axis humanoid robot arm in this dissertation. The DAMA consists of a two-independent-joint system, and the system structure is further refined using finite element analysis. It will be shown that the novel DAMA modular system can be used to easily construct a mechanism with any degrees of freedom. In other words, a modular or reconfigurable system can be achieved using the DAMA module. Based on simulations with ADAMS and MATLAB software packages, the system dynamic properties can be observed. In addition, the hardware and software systems of the DAMA are developed. The hardware architecture is composed of a microprocessor, an RS-232 to CAN Bus Module, and two independent-joint controller modules. The software control system is written in Visual C++. The system employs a simple but effective PID scheme to independently control the DAMA's two joints. The experimental results show that for an S curve and circle trajectory input position command, the DAMA and the 6-axis humanoid robot arm, which is formed by the

DAMA module, can track the command well. Hence, the DAMA can be used as a generic module for multiple-degrees-of-freedom systems

2.1. Introduction

A modular robot can be defined as a robotic system constructed from a set of standard components. Modular robots are of interest because they permit the construction of a wide variety of specialized robots from a set of standard components. Due to the adaptability of the modular robot, it can pass through narrow passageways, reshape itself into a legged robot and walk over rubble, and climb stairs or even on desks by self-reconfiguration. Another application is space/planetary exploration, where unpredictable terrains on a planet have to be explored by a robot before human beings are sent. There are two types of connection methods between modules, manual and self-reconfigurable.

For the manual type, two modular reconfigurable robots are connected by the user; and various types of modular systems have been proposed, CEBOT [1], PolyPod [2][3], Tetrobot [4], RBR [5], Micro-robot [6], Modular Robot Manipulators with Preloadable Modules [7], Odin [8], New Independently-Mobile Reconfigurable Modular Robot [9]. Less effort has been made in the field of self-reconfigurable modular robots, which can autonomously change their configurations. The modular

self-reconfigurable robot is proposed in order to make the system adaptable to different given tasks and unknown environments. Several self-reconfigurable robots have been proposed, KRVM [10], Modular Robotic System [11], Self-reconfigurable robots [12], M-TRAN [13], Switchable bonding mechanism [14], [15], Roombots [16]. In the studies above, the software and hardware designs of the module are important issues. In recent years, humanoid robot technology has gradually matured. The main purpose of humanoid robots is to help people in operations, or even to replace people in dangerous jobs, such as repairing machines, experimenting with chemical treatments, and achieving precision in work. In humanoid robot arms design, many researchers have focused on developing a 6-axis robot arm that looks like a human arm. HRP [17], BHR-01 [18], KHR-3 [19], MAHRU [20], and BHR-02 [21] are well-known 6-axis human-size humanoid robot arms. However, in those robots, the structures of the robot arms are complex.

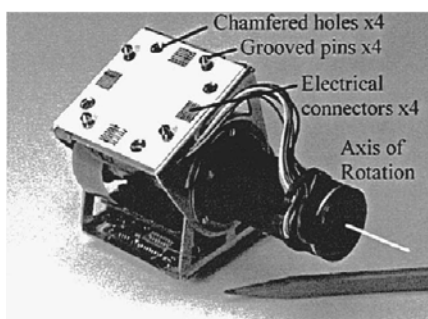


Figure 2-1 Poly Bot [2]



Figure 2-2 Micro-robot [6]



Figure 2-3 Odin [8]



Figure 2-4 Modular Robot [9]

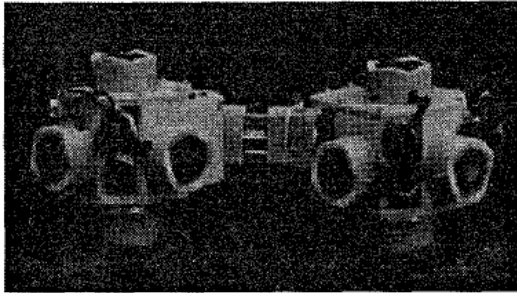


Figure 2-5 KRVM [10]

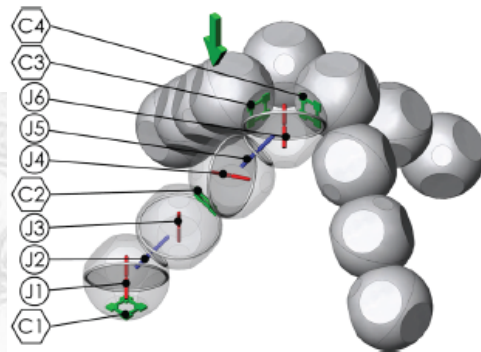


Figure 2-6 Roombots [16]

In addition, the development of microprocessors, microelectronics, and communication method, proceeds very rapidly. A humanoid robot consists of a multiple-degree-of-freedom mechanism, and is very complicated. Some robots have been designed with centralized control architectures, such as IEEE-1394, local ISA, VME, RS-232, and PCI bus. Their communication interfaces have high communication speed, but the wire systems are too heavy and complicated. Other robots have been designed with distributed control architecture using CAN-Bus [22],

Ethernet [23], or Ethernet-CAN-USB [24] to achieve real-time control.

The goal of this dissertation is to design a Vertically Intersected Dual Axes Modularized Actuator System (DAMA) with CAN-Bus communication system that can build humanoid robot arm systems more flexibly and quickly with low manufacturing and maintenance costs. The kinematics of the 6-axis humanoid robot arm is shown in Figure 2-7(a) and the concept of the 6-axis humanoid robot arm with three DAMAs is shown in Figure 2-7(b). Therefore, we consider the following parameters:

- Each DAMA consists of a pair of two-DOF atoms (with two units).
- Each DAMA has an on-board microprocessor and communication system.
- Each DAMA has ability to connect, disconnect and rotate around its neighbors.
- Each DAMA can offer enough power to rotate its neighbors.
- The shape of each DAMA is in a pot form to mimic the appearance of a human arm.
- The robot arms which consist of DAMAs can be constructed quickly and flexibly.
- The wire systems of the robot arms constructed using DAMAs are simple.

This chapter is structured as follows. Section 2 presents the main idea of a DAMA, and the mechanical structure and properties of the DAMA will be introduced. Dynamic simulation of the DAMA is shown in Section 3. In Section 4, finite element analysis for the key components of the DAMA is briefed. The hardware and software of the DAMA control system are discussed and implemented in Section 5. Section 6 presents experimental results to show that each joint of DAMA is capable of providing precise position movement. Finally, summary are made in Section 7.

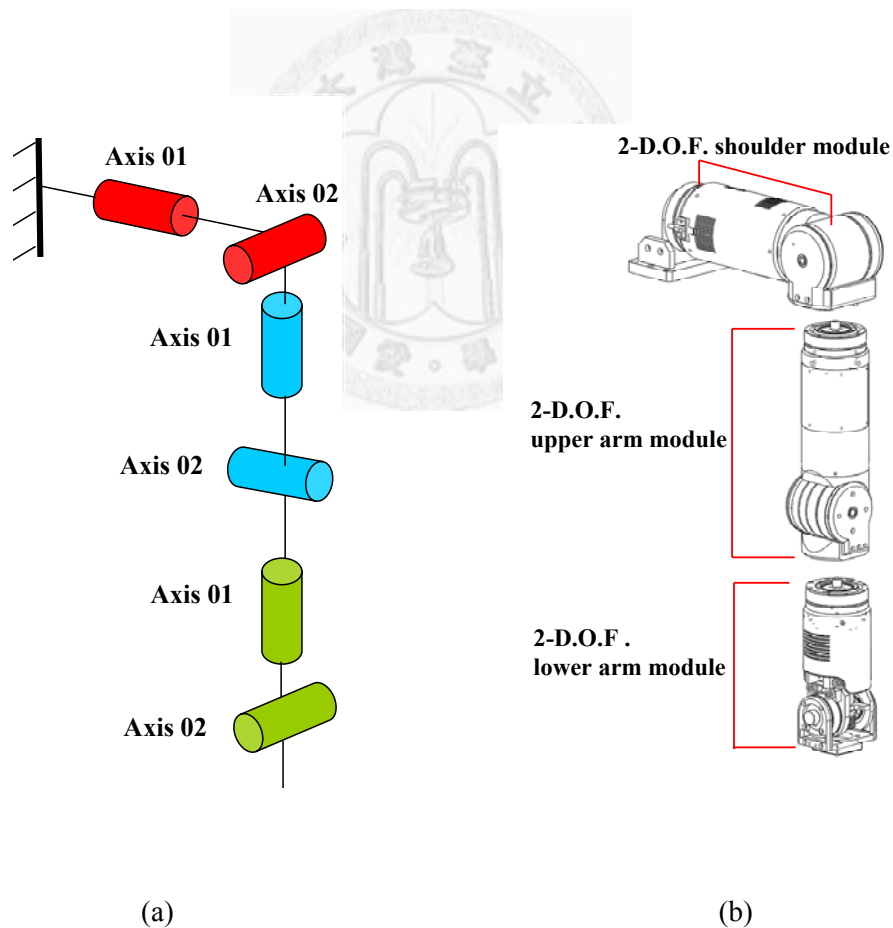


Figure 2-7 (a) The kinematics of the 6-axis humanoid robot arm, and (b) the concept of the 6-axis humanoid robot arm with three DAMAs.

2.2. Mechanical Design of a DAMA

A modular robot can be defined as a robotic system constructed from a set of standard components. Modular robots are of interest because they permit the construction of a wide variety of specialized robots. In this section, the concept and the detailed structure of the DAMA are presented.

2.2.1. The Concept of a DAMA

The main concept of a DAMA is a vertically intersected, dual-axis structure and some specific designs make it modularized. It can serve as a modular two-axis actuator. Hence, a multiple-degree-of-freedom (DOFs) mechanism, such as humanoid robot arms, can be configured in terms of a DAMA. However, for a humanoid robot system, each part has its unique standards. For example, in a humanoid robot arm, the shoulder part is focused on high power and high torque, but the wrist part should pay attention to the size of the mechanism. To satisfy such requirements, two types of DAMAs, a high torque module and a small size module, will be developed in this dissertation.

2.2.2. Detailed Structure of a DAMA (High Torque Module)

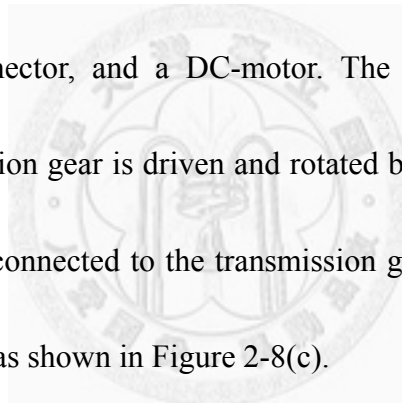
The DAMA with high torque capability is composed of four parts: the Joint 01 system, the Joint 02 system, an exoskeleton, and two circuit boards, as shown in

Figure 2-8(a) and Figure 2-8(b). Joint 01 and Joint 02 form two independent axes.

Namely, the DAMA is characterized by dual axes, high output torque, and precise position movement. In order to mimic the appearance of a human arm, the shape of a DAMA is in a regular pot form. Therefore, it is a big challenge to arrange all components in such a particular space.

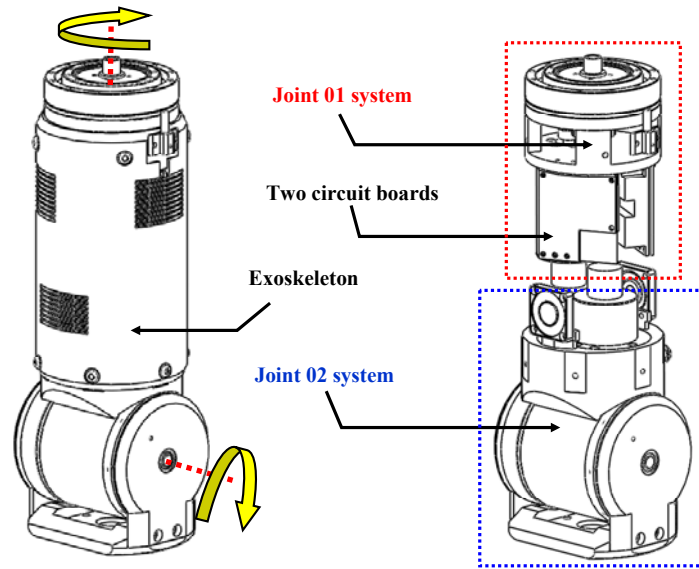
Joint 01 System

Joint 01 of the DAMA with high torque capability consists of a harmonic drive, a transmission gear, a connector, and a DC-motor. The DC-motor is fixed on the connector, and a transmission gear is driven and rotated by the DC-motor. Hence, the harmonic drive, which is connected to the transmission gear, will be driven and then the output link be rotated, as shown in Figure 2-8(c).



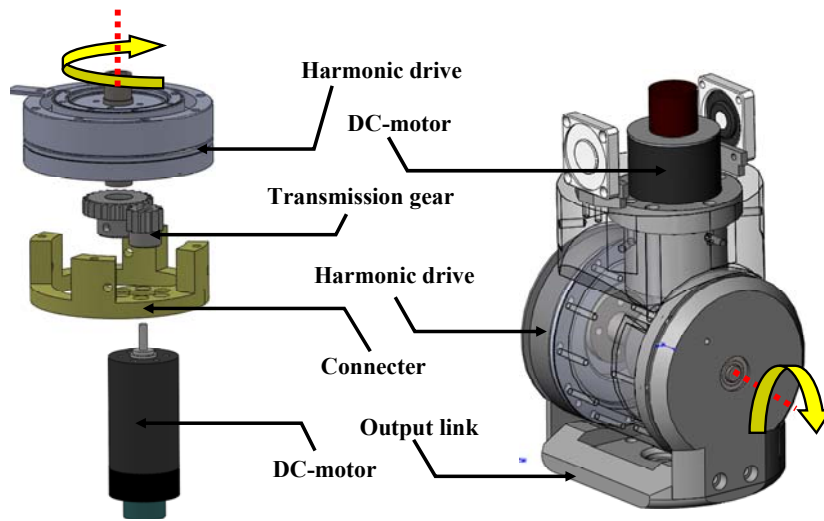
Joint 02 System

Similar to Joint 01, joint 02 of DAMA with high torque capability is mainly composed of a harmonic drive, a transmission gear, a connector, and a DC-motor. To fit some components in the exoskeleton to shape the DAMA like a drum, the DC-motor of the Joint 02 system is installed on the side and parallel to the DC-motor of Joint 01. The transmission gear is used to drive and rotate the harmonic drive, and the output link is rotated, as shown in Figure 2-8(d).



(a)

(b)



(c)

(d)

Figure 2-8 The Vertically Intersected Dual Axes Modularized Actuator System (DAMA) with high torque capability: (a) the DAMA outward appearance, (b) the detailed structure of the DAMA, (c) the Joint 01 system of the DAMA, and (d) the Joint 02 system of the DAMA.

Exoskeleton

The DAMA has two independent rotation systems. The exoskeleton is used to connect the Joint 01 system and the Joint 02 system in order to form a complete two-axis actuator. The exoskeleton is made of aluminum to reduce the weight of DAMA, and keeps joint 01 and joint 02 systems in the right location

2.2.3. Detailed Structure of a DAMA (Small Size Module)

The DAMA with small size capability is composed of five main parts: the Joint 01 system, the Joint 02 system, a tension adjuster, an exoskeleton, and two circuit boards, as shown in Figure 2-9(a) and (b). Joint 01 and Joint 02 form two independent axes. Namely, the DAMA is characterized by dual axes, precise position movement, and easy control.

Joint 02 System

Joint 02 of the DAMA with small size capability is a cable driven system, as shown in Figure 2-9(c). In the cable system, a screw, a DC-motor and a cable are connected. The cable passes through a pulley system and connects to the tension adjuster. When the DC-motor drives the screw, the cable fixed on the screw is pulled, and the output link is rotated by the connection of the cable to the tension adjuster.

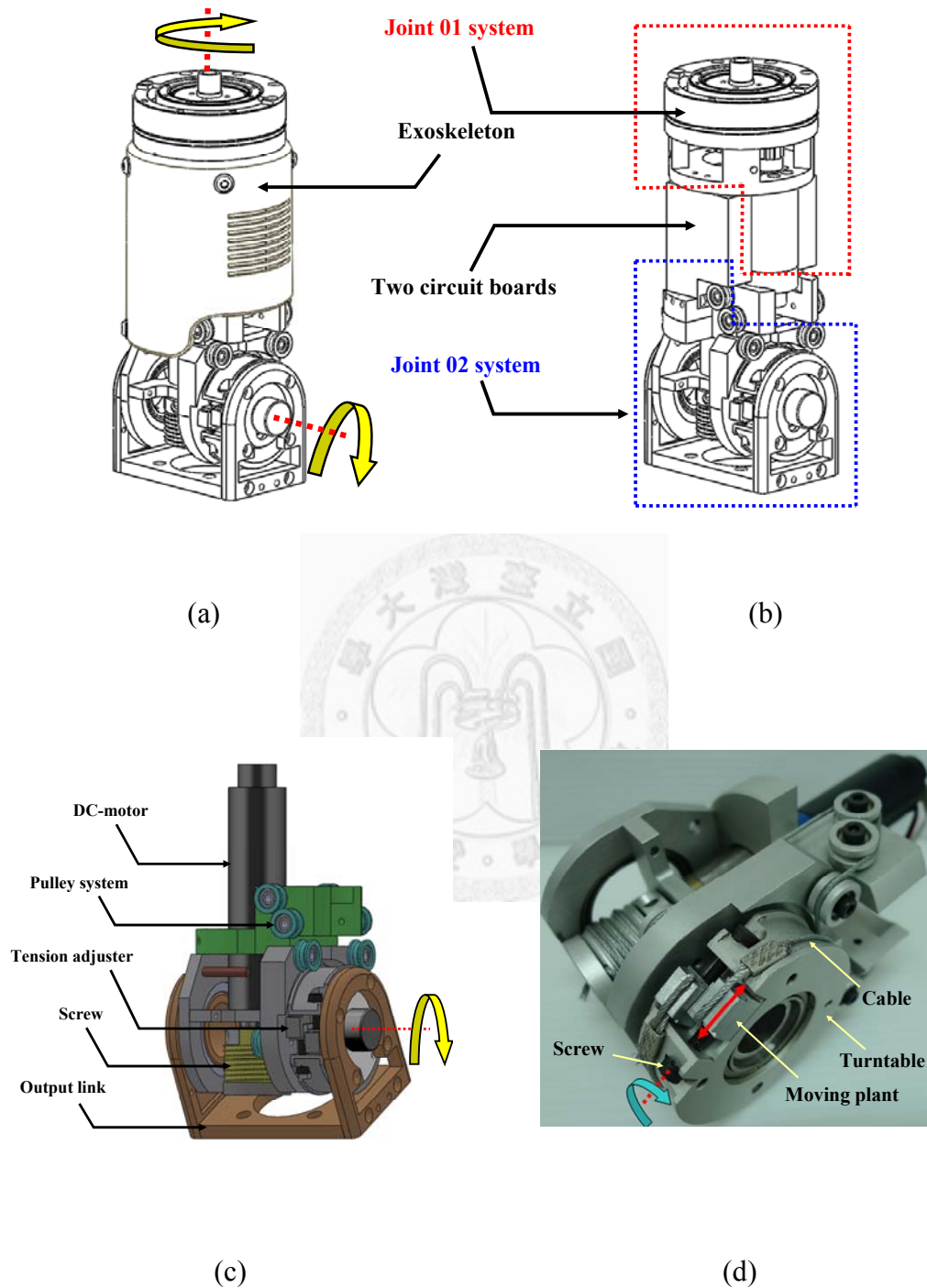


Figure 2-9 The Vertically Intersected Dual Axes Modularized Actuator System (DAMA) with small size capability: (a) the DAMA outward appearance, (b) the detailed structure of the DAMA, (c) the Joint 01 system, and (d) the Joint 02 system.

Tension Adjuster

To keep Joint 02 as stiff as possible with precise position movement, a tension adjuster is designed to adjust the cable tension, as shown in Figure 2-9(d). The tension adjuster consists of a turntable, two antagonistic screws, and two moving plants. Each moving plant is fixed on the screw, and one end of the cable is fixed on the moving plant. By turning the screw, the moving plant will move to adjust the cable tension.

2.3. Simulation System

In this dissertation the MATLAB/Control software and ADAMS/Simulation are integrated to simulate the dynamic behaviors of the DAMA system.

2.3.1. The Independent Joint Control of the DAMA System

Most robot manipulators are electrically actuated. Electrically driven manipulators are constructed with a DC permanent magnet torque motor for each joint. The motor shaft is coupled to a gear train to the load of the link. So the relationship between motor shaft and load shaft can be described as

$$\frac{\theta_L}{\theta_m} = n < 1, \quad (2-1)$$

where n is the reduction ratio of the gear train and θ_m and θ_L are the angular displacements of the motor shaft and load shaft in radian respectively. When a load is

attached to the output gear, the torque developed at the motor shaft can be described as

$$\tau(t) = \tau_m(t) + \tau_L^*(t) , \quad (2-2)$$

where $\tau(t)$ is the torque delivered by the motor, $\tau_m(t)$ is the torque dissipated by the motor, and $\tau_L^*(t)$ is the torque dissipated by the load referred to the motor shaft.

The motor torque referred to the motor shaft $\tau_m(t)$ and the load torque referred to the load shaft $\tau_L(t)$ can be written as

$$\tau_m(t) = J_m \ddot{\theta}_m(t) + f_m \dot{\theta}_m(t) , \quad (2-3)$$

$$\tau_L(t) = J_L \ddot{\theta}_L(t) + f_L \dot{\theta}_L(t) , \quad (2-4)$$

where J_m and f_m are the moment of inertia and the viscous-friction coefficient of the motor referred to the motor shaft, respectively, and J_L and f_L are the moment of inertia and the viscous-friction coefficient of the load referred to the load shaft.

From conservation of work, the torque $\tau_L^*(t)$ can be described as

$$\tau_L^*(t) = n\tau_L(t) = n^2 [J_L \ddot{\theta}_m(t) + f_L \dot{\theta}_m(t)] . \quad (2-5)$$

the torque delivered by the motor $\tau(t)$ can be described as

$$\tau(t) = \tau_m(t) + \tau_L^*(t) = J_{\text{eff}} \ddot{\theta}_m(t) + f_{\text{eff}} \dot{\theta}_m(t) , \quad (2-6)$$

where $J_{\text{eff}} = J_m + n^2 J_L$ and $f_{\text{eff}} = f_m + n^2 f_L$ are the effective moment of inertia and the effective viscous friction coefficient of the combined motor and load referred to the motor shaft. The torque $\tau(t)$ increases linearly with armature current. That is

$$\tau(t) = K_a i_a(t) , \quad (2-7)$$

where K_a is the torque constant of the motor and $i_a(t)$ is the armature current.

Applying Kirchoff's voltage law to the armature circuit, we obtain

$$V_a(t) = R_a i_a(t) + L_a \frac{di_a(t)}{dt} + e_b(t) , \quad (2-8)$$

where R_a is the armature resistance, L_a is the armature inductance, and $e_b(t)$ is the back electromotive force (emf) which can be described as

$$e_b(t) = K_b \dot{\theta}_m(t) , \quad (2-9)$$

where K_b is the back emf constant. Taking the Laplace transform of Eq. (2-9) and solving for $I_a(s)$, the Laplace transform of $\tau(t)$ can be obtained as:

$$T(s) = K_a I_a(s) = K_a \left[\frac{V_a(s) - sK_b \Theta_m(s)}{R_a + sL_a} \right] . \quad (2-10)$$

taking the Laplace transform of Eq. (2-6), we obtain

$$T(s) = s^2 J_{\text{eff}} \Theta_m(s) + s f_{\text{eff}} \Theta_m(s). \quad (2-11)$$

from Eq. (2-1), (2-10) and (2-11), the transfer function from the armature voltage

$V_a(s)$ to the angular displacement of the load $\Theta_L(s)$ can be described as

$$\frac{\Theta_L(s)}{V_a(s)} = \frac{nK_a}{s \left[s^2 J_{\text{eff}} L_a + (L_a f_{\text{eff}} + R_a J_{\text{eff}}) s + R_a f_{\text{eff}} + K_a K_b \right]}. \quad (2-12)$$

since the electrical time constant of the motor is much smaller than the mechanical time constant, the armature inductance can be neglected. Eq. (2-12) can be simplified as

$$\frac{\Theta_L(s)}{V_a(s)} = \frac{nK}{s(T_m s + 1)}, \quad (2-13)$$

where

$$K = \frac{K_a}{R_a f_{\text{eff}} + K_a K_b}, \quad (2-14)$$

$$T_m = \frac{R_a J_{\text{eff}}}{R_a f_{\text{eff}} + K_a K_b}. \quad (2-15)$$

the output of the control system is the angular displacement (Θ_L). The transfer

function between the applied voltage and angular displacement can be described as

$$\frac{\Theta_L(s)}{V_a(s)} = \frac{nK_a}{s(sR_aJ_{eff} + R_aJ_{eff} + K_aK_b)}. \quad (2-16)$$

the angular displacement of the joint is controlled to track a preplanned trajectory. We obtain the closed-loop transfer function relating the actual angular displacement $\Theta_L(s)$ to the desired angular displacement $\Theta_L^d(s)$ as

$$\frac{\Theta_L(s)}{\Theta_L^d(s)} = \frac{K_aK_v s + K_aK_p}{s^2R_aJ_{eff} + s(R_aJ_{eff} + K_aK_b + K_aK_v) + K_aK_p}, \quad (2-17)$$

where K_p is the position feedback gain, K_v is the error derivative feedback gain, and K_i is the integral gain.

2.3.2. Control and Simulation of the DAMA System

The performance of the DAMA with PID controller is simulated by the Simulation System. It is illustrated in Figure 2-10(a). This simulation method integrates two different simulators that exchange data and parameters with each other at each step. It provides a convenient way to simulate complicated models. In the simulation system, the proposed PID controller is built by using MATLAB/Simulink software to control the mechanism with physical and dynamic properties, and the model of the DAMA is developed by using ADAMS software to observe the dynamic behaviors of the mechanism. The ADAMS model is treated as a control plant.

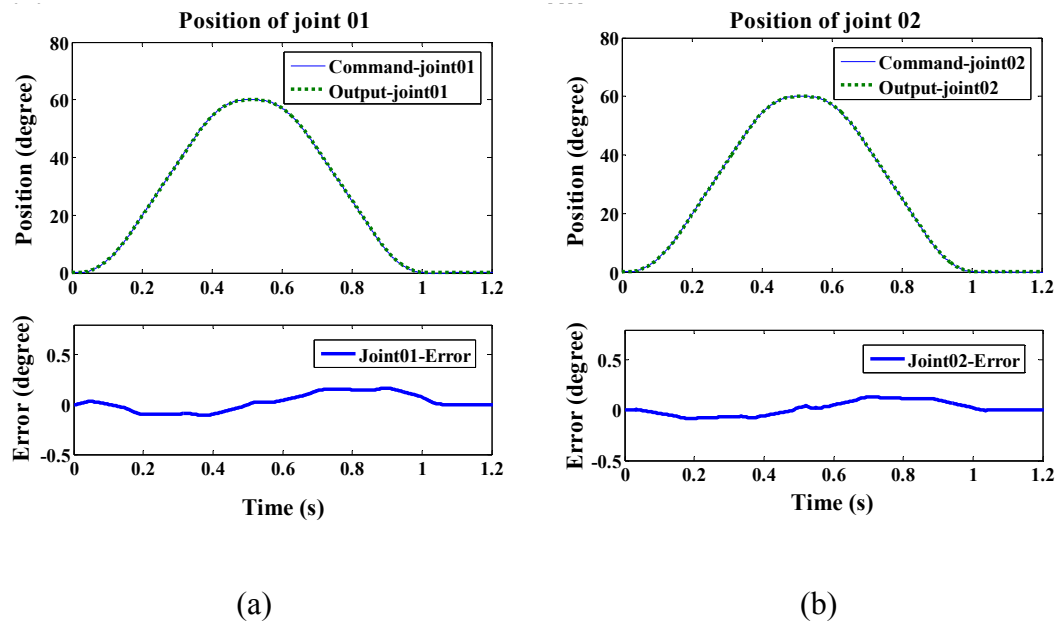


Figure 2-11 Simulation results and the average tracking errors: (a) the joint 01 system of the DAMA, and (b) the joint 02 system of the DAMA.

It receives control command from the controller and gives the response. The simulation system can provide necessary data for researchers to reduce the development cycle and cost. The 3D models constructed from Solidworks and the ADAMS simulation are shown in Figure 2-10(b). The simulation under the MATLAB/Control software is based on the model implemented in the ADAMS/Simulation dynamic environment. The input trajectories of Joint 01 and Joint 02 are an angular displacement of 60 degrees with maximum angular velocity of 120 degrees/sec. For each DAMA joint, a simple PID controller is used to control the angular displacement. The simulation results show that the average tracking errors of

Joint 01 are under 0.15° and Joint 02 are under 0.16° , as shown in Figure 2-11(a) and Figure 2-11(b), respectively. In other words, the position movement of each joint is almost the same as the desired command.

2.4. Finite Element Analysis

To reduce the weight of the DAMA, finite element analysis is used to analyze several important components. Figure 2-12 shows two key components: the exoskeleton component and the rotation support component. The exoskeleton component connects the Joint 01 and Joint 02 systems, and the rotation support component keeps the rotation mechanism from bending. In this dissertation, we use ADAMS simulation software to mimic the dynamic property of the DAMA to get the force and torque applied to each part and the two joints of the DAMA. Those data are used in the finite element analysis to remove the unnecessary portions of the two key components to reduce weight. Then, the displacement, stress, and strain of the two key components are further analyzed to make sure that the DAMA structure is strong and safe enough.

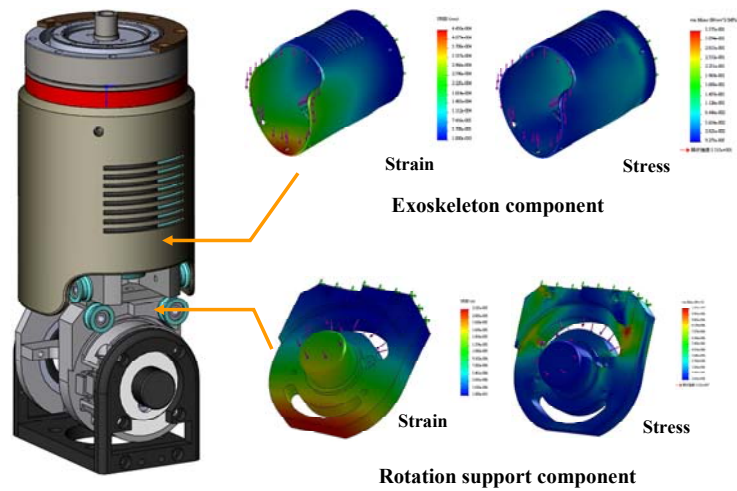


Figure 2-12 Finite element analysis of two key components of the DAMA.

2.5. Hardware and Software

Hardware Architecture

The DAMA hardware is composed of a microprocessor, a USB to RS-232 module, an RS-232 to CAN Bus Module, and an independent-joint controller module.

Each control module captures the position information from potentiometers and encoders and forces information from the current. The joint control module utilizes dsPIC30F4011 as a microprocessor and IC LMD18201 is used as the driver between the controller and the motor.

Software of Human Interaction

The computer is implemented as the trajectory planner and the user interface. To easily manipulate the two-axis robot, the user interface is written in Visual C++. For

the trajectory planner, the main functions are interpolation, inverse kinematics, file open, and file save. Finally, the trajectory command and the position data back to the computer will give the human interface for the user.

2.6. Experimental Results

In this section, experiments were conducted to evaluate the dynamic properties of the DAMA module and the 6-axis humanoid robot arm, which was constructed using three DAMA units. S curve and circle trajectory input position commands were used as the trajectory commands for these two systems.

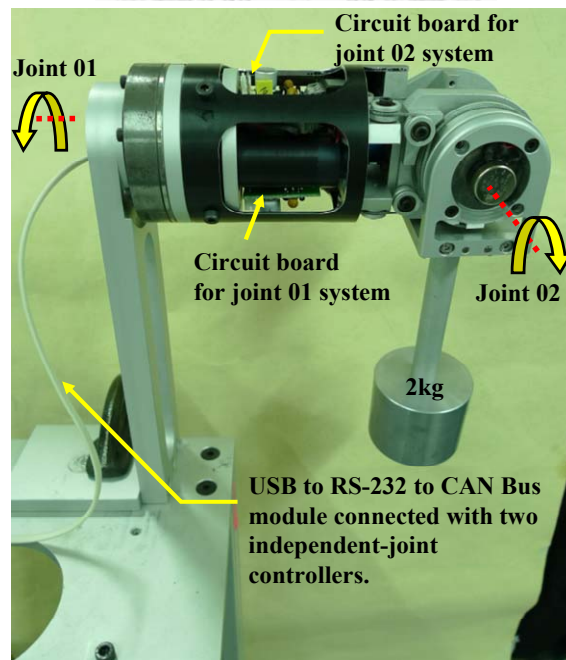
Implementation of the DAMA

The DAMA was fixed on a table and a 2 kg object attached to the endpoint of Joint 02's output link, as given in Figure 2-13(a). A microprocessor served as the trajectory planner and user interface. The trajectory inputs of joint01 and 02 were angular displacement of 60 degrees with maximum angular velocity of 100 degrees/sec. The two joints of DAMA are controlled by a simple PID controller. The design parameters, some detailed specification of DAMA and the PID gains of two independent joints are listed in Table 2-1. The angular positions and the error curves of the two independent joints (joint 01 and joint 02) of the DAMA are shown in

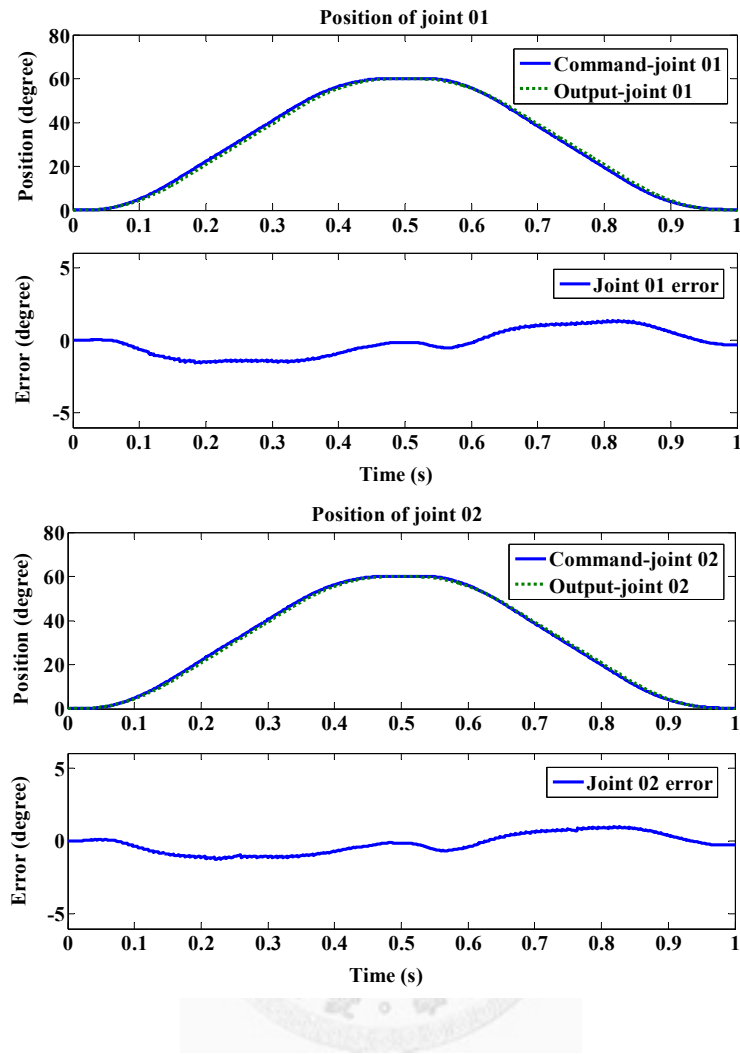
Figure 2-13(b). A slight time delay between the command position and actual position is due to inherent sampling. In addition, for a planned S curve trajectory, the end point of the DAMA can track the actual position very well.

Table 2-1 Specification of the DAMA.

Parameter	Value
Weight	1.6 kg
Degree of freedom	2 D.O.F.
Maximum output torque (for each joint)	200 N-m
Maximum output speed (for each joint)	240 (deg. /second)
Maximum movement (for joint 01)	$\pm 360^\circ$
Maximum movement (for joint 02)	$\pm 95^\circ$
The PID gains of the two joints	KP1: 1000, KI1: 0.01 KD1:200
	KP2: 1000, KI2: 0.01 KD2:200



(a)



(b)

Figure 2-13 (a) Experimental setup for the DAMA, and (b) the angular positions and the error curves of two independent joints of the DAMA.

Implementation of the 6-axis Humanoid Robot Arm

In this dissertation, a 6-axis humanoid robot arm, which consists of three DAMAs (two high torque modules for the shoulder and upper part, and one small size module for the lower part) has been built. The design parameters and some detailed

specification of the 6-axis humanoid robot arm are listed in Table 2-2 and the workspace of the 6-axis humanoid robot arm is shown in Figure 2-14. The 6-axis humanoid robot arm is fixed on a table. The hardware architecture is composed of a notebook computer, a USB to RS-232 module, an RS-232 to CAN Bus Module, and six independent-joint controller modules, as given in Figure 2-15(a). The software is written in Visual C++. The system employs a simple, but effective, PID scheme to independently control the six joints of the robot arm. Figure 2-15(b) shows the trajectory planning for 6 joints of the 6-axis humanoid robot arm. A circle with a 20-cm radius and a five-angle star in the workspace are used as the trajectory input to illustrate the capability of the 6-axis humanoid robot arm. In this dissertation, we also built a simulation system to simulate the movement of the 6-axis humanoid robot arm before real implementation. The DH rule and inverse kinematics for the robot arm are written with MATLAB software. Figure 2-16 shows the flow path of the robot arm simulation and control system. Figure 2-17(a) shows the experimental results of the 6-axis humanoid robot arm with circle motion. In order to show the experimental results more clearly, a flashlight was fixed on the endpoint of the robot arm, and a camera was used to record the trajectory of the robot arm. Figure 2-17(b) shows the experimental results of the 6-axis humanoid robot arm with five-angle star motion.

Table 2-2 Specification of the 6-axis humanoid robot arm.

Parameter	Value	
Weight	7 kg	
Degree of freedom	6 DOFs	
Movable range	Shoulder	Pitch -180° to 180° Yaw -20° to 200° Roll -180° to 180°
	Elbow	Pitch 0° to 120°
	Wrist	roll -180° to 180°
		Yaw -90° to 90°
End speed	1.5 m/s	
Payload	3.5 kg	

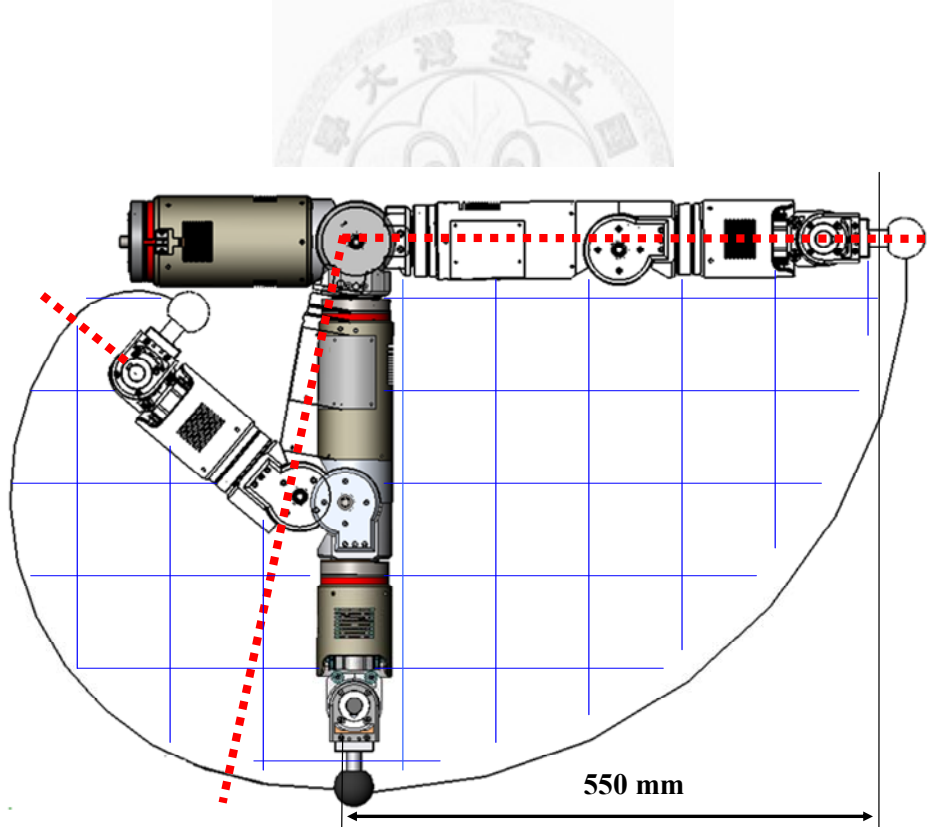


Figure 2-14 The Workspace of the 6-axis robot arm.

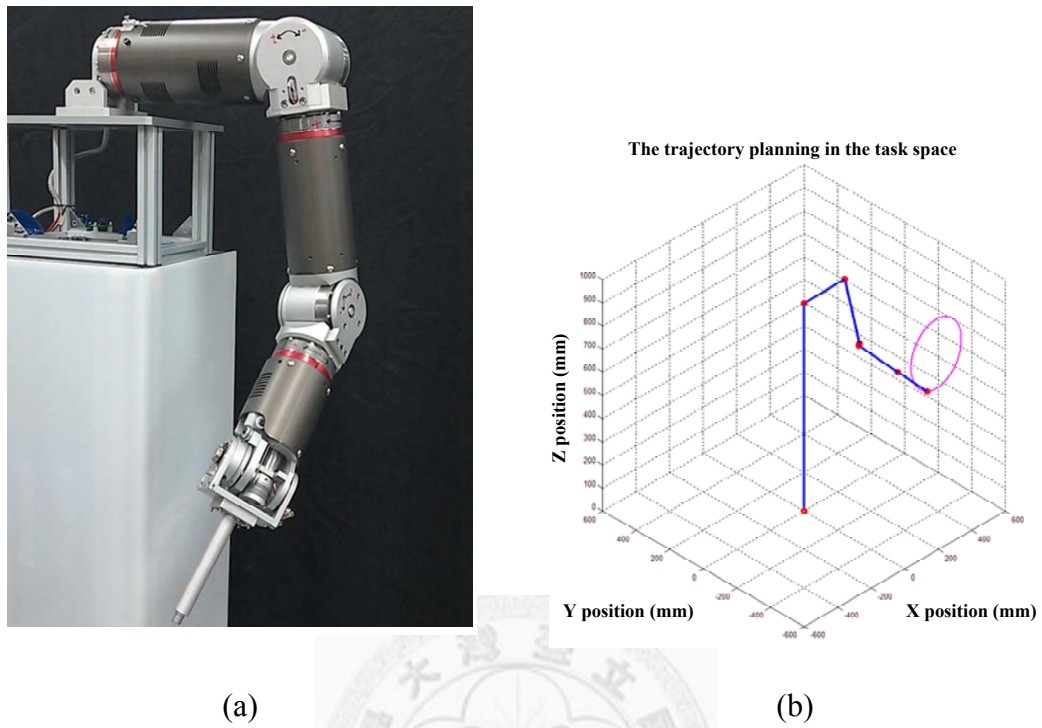


Figure 2-15 (a) Experimental setup, and (b) trajectory planning for the 6-axis robot arm.

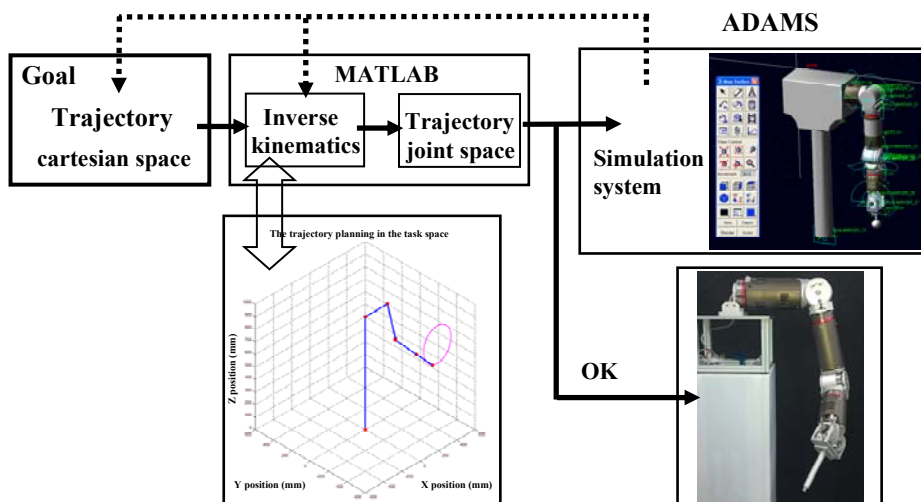
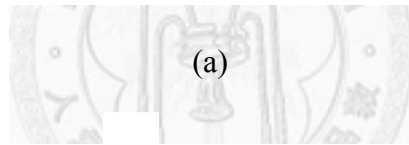
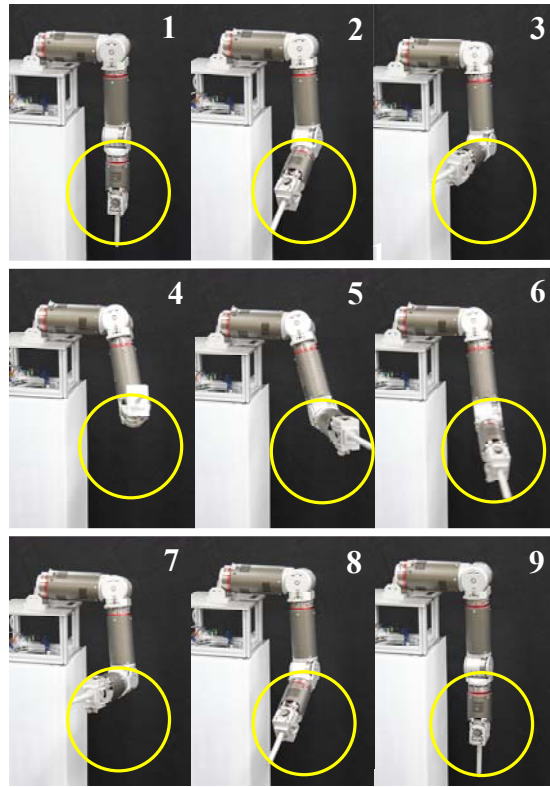
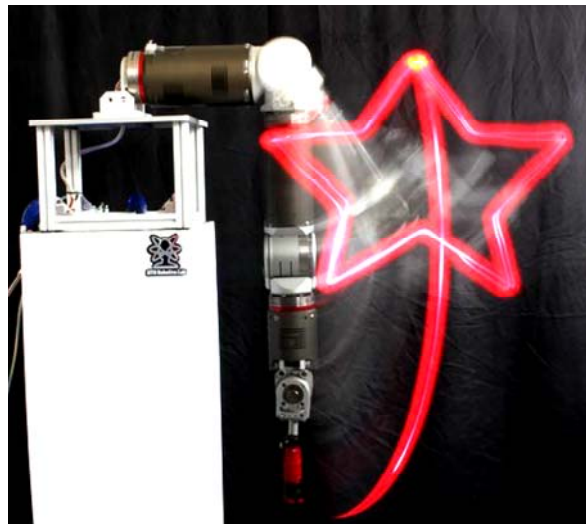


Figure 2-16 The 6-axis humanoid robot arm simulation and control system.



(a)

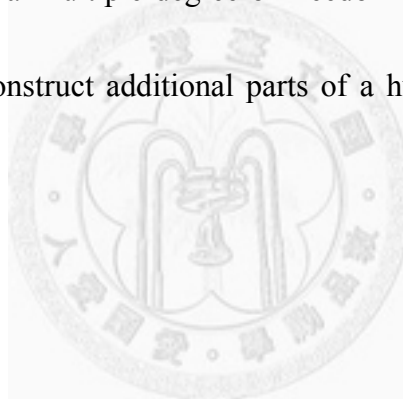


(b)

Figure 2-17 Experimental results: (a) the 6-axis humanoid robot arm with circle motion, and (b) the 6-axis humanoid robot arm with five-angle star motion.

2.7. Summary

In this chapter, a vertically intersected dual-axis modularized actuator system (DAMA) has been designed and applied to humanoid robot arms. Due to its compact and modular design, the DAMA can be used as a building block to configure a complex system. The experimental results show that the DAMA and the 6-axis humanoid robot arm can track commands very well. Hence, the DAMA can be used as a generic module for a multiple-degree-of-freedom system. In the future, the DAMA will be used to construct additional parts of a humanoid robot, such as the neck, trunk, and legs.



CHAPTER 3. BACKGROUND AND RELATED WORK OF INHERENTLY SAFE ACTUATING MECHANISMS

In the preceding chapters, we have developed an integrative humanoid robot system to execute dexterous functions, a trajectory planning method to produce smooth trajectories and a robust control algorithm to perform fast and precise controlled responses. In short, all of these efforts lead the robot to look like human beings and move like human beings. Whereas, this integrative humanoid robot system, consisting of rigid links, electrical servo actuators, tough covers, high-ratio reduction devices, position sensors but any torque sensor, causes the robot hardly interact with people and environments under safety constraints or move slowly with careful motion planning results and multiple control strategies.

Since the human-robot-environment interaction embraces a wide range of applications, safety issue is becoming a primary concern when the robot is supposed to operate in an unstructured environment, share the workspace with the human, and allow close physical cooperation. In the following chapters, we will focus on the different field, the human-robot-environment interaction, to develop intrinsically safe

robot actuation and its control strategy that can look after both sides of the capacity of good performance and safe motion.

3.1. Introduction

In fact, the development of robots as mechanical workers that can support human labor and assist human daily activities by physical interaction, informational interaction, etc, has been expected for a long time. That is why, recently, the field of physical human-robot interaction (pHRI), considering the trade-off between safety and performance, emerges from the modern robotics as a focused effort to design manipulators that are intrinsically safe for human interaction [25].

However, most of the real-world robots are fast, strong and powerful without any capacity of interaction with humans, say industrial robots; on the contrary, others are slow, weak and powerless without capacity of dealing with versatile tasks, say entertainment robots. Therefore, through whole task execution, how a robot achieves good performances in accuracy and promptness under the safe condition is becoming one of the most important issues in this field. To achieve safety and efficiency, one must employ manifold strategy, involving all aspects of robot design including the mechanical, electrical, and control and software architecture.

Traditionally, modifying controllers of rigid robots (stiffness, impedance control, collision detector, etc.) by additional sensors (position, velocity, force, contact, proximity, etc) have demonstrated the effectiveness to achieve safe manipulation [26].

Anyhow, there are intrinsic limitations of a controller to alter the dynamic behavior of robots because of the unmatched mechanical bandwidth. Furthermore, the natural dynamics of the system is engineered and utilized to where possible, while the software control system adds energy lost in the mechanism, and creates extrinsic dynamic behavior. Intuitively, a rigid and powerful structure of the robot with modified controllers and additional sensors would do its performance and safety a favor; nevertheless lightweight and compliant structures are more suitable for safe operation.

To have a compliant robot, intrinsically safe for humans and unstructured environment interaction, researchers have utilized either compliant actuators or joints, complying with this compliant requirement, such as a series elastic actuator (SEA) [27]–[29], a series damper actuator [30], a compliant structure [31], etc; on the contrary, it suffers from some intrinsically problems for the elastic property notwithstanding [27][28][29][32][33]. The most critical one of these properties is a stiffness constant of the series elastic component dominates bandwidth and payload

capacity of the overall system and the safety level of the human-robot-environment interaction: to wit, a compromise between the safety and performance is difficult to make. In order to determinate the trade-off of these two aspects of robotic system or actuator design, some qualitative and quantitative indices to measure the performance and safety will be mentioned in the following section.

3.2. Performance and Safety Constrains

To evaluate a robot system and/or actuator design, some critical qualitative and quantitative indices to measure the performance and safety defined or mentioned in [34]–[36] are shown in the following.

3.2.1. Performance Indices

Power Density and Force Density

Force density or power density is regarded as an actuator's ability to generate force or deliver power to the robot per unit mass and unit volume of the actuator, respectively. An actuator's having high force and power density means that the small size actuator or robot system can output much energy. Therefore, utilizing lightweight actuators with high force and power densities prevents a robot system possessing an over-burdening structure but allows it to possess quick responses.

Dynamic Range

The dynamic range is the maximum output force divided by the minimum resolvable output force increment of the actuator, implying how sensitive the actuator is to small forces with respect to its full force output capability. A large dynamic range is desirable.

Backdrivability

Backdrivability is a measure of how accurately a force or motion applied at the output end of a mechanical transmission is reproduced at the input end. For instance, good backdrivability means that a person can grab the end-tip of the robot arm and move it around effortlessly [35].

Mechanical Output Impedance

Mechanical Output impedance is defined as the minimum amount of force an actuator outputs for a given load motion, either displacement or velocity. Ideally, the actuator should be a pure force source of which the impedance is zero and internal dynamics can be negligible. An actuator with low impedance is sometimes referred to as being backdrivable, thus can dramatically reduce the coupled dynamic effect between the actuator and the corresponding inertial loading [34].

Bandwidth

The force bandwidth is a measure of how quickly the actuator can generate commanded forces. There are two ways to measure the dynamics response, say small and large force bandwidth (saturation bandwidth). They are defined as the frequency range over which the actuator can sinusoidally oscillate at a force amplitude equivalent to maximum output force at steady state with respect to a minimum or maximum input. For the servomotor, the large force bandwidth is defined at the natural frequency of the spring and reflected motor inertia [34].

It is worth mentioning that the existing actuation technologies, say electro-magnetic, hydraulic, and pneumatic actuators with power and torque capabilities required for different complicated tasks, have serious deficiencies, unfortunately limiting their inherent safety and/or performance characteristics. Therefore, it is so difficult to simultaneously achieve safety and performance characteristics with a single actuator or traditional robot design [34].

3.2.2. Safety Criteria

Safety criterions for designing robots provide important judgments to compromise on the safety and performances. For a typical robot, the margin available

for designing to satisfy both safety and performance requirements is the intersection of the ranges of tip-velocity and payload values of acceptable designs. Since the tip-velocity and payload values determine how to design a safe robot, several safety criteria based on these two factors have been developed. For example, to represent human safety associated with the dynamic collision, the head injury criterion (HIC) [37], quantitatively measuring head injury risks in car crash situations, is used to evaluate the tolerate level of human-robot impact in many researches [25][38][39], and defined as

$$HIC \equiv \frac{\max}{T} \left\{ T \left[\frac{1}{T} \int_0^T a(\tau) d\tau \right]^{2.5} \right\} \quad (3.1)$$

where time interval T is equal to or less than the time of impact and a is the acceleration in the unit of gravitational acceleration g . A HIC value equal to or greater than 1000 is typically associated with extremely severe head injury; less than 100 considered suitable to normal operation of a machine physically interacting with humans. It can be solved numerically or analytically, whereas a simple and easy approximate HIC value can be also obtained by introducing a compound inertia M_{rob} and a modified form relevant for compliant manipulators [38], such as

$$HIC = 2 \left(\frac{2}{\pi} \right)^2 \left(\frac{K_{cov}}{M_{oper}} \right)^3 \left(\frac{M_{rob}}{M_{rob} + M_{oper}} \right)^4 v_{max}^{\frac{5}{2}} \quad (3.2)$$

where the impacted operator mass is M_{oper} , K_{cov} is the lumped stiffness of a compliant cover on the arm, and a compound inertia M_{rob} is defined as

$$M_{rob}(K_T) = M_{link} + \frac{K_T}{K_T + \gamma} M_{motor} \quad (3.3)$$

where γ is the rigid joint stiffness regarded as 3000, and provides well fit approximation. Note that low transmission stiffness K_T serves to decouple the rotor mass M_{motor} from the link mass M_{link} , dominating the major effect of the M_{rob} .

Moreover, the acceptable velocity under the safety constraint can be shown as

$$v_{max} = \left[\frac{HIC_{max}}{2 \left(\frac{2}{\pi} \right)^{\frac{3}{2}} \left(\frac{K_{cov}}{M_{oper}} \right)^{\frac{3}{4}} \left(\frac{M_{rob}(K_{transm})}{M_{rob}(K_{transm}) + M_{oper}} \right)^{\frac{7}{4}}} \right]^{\frac{2}{5}} \quad (3.4)$$

where the maximum tolerated HIC_{max} could be chosen as less than 100, a suitable value to normal operation of a machine physically interacting with humans.

From the above equations, under the safety constraint, a manipulator's acceptable velocity regarded as a important performance index can be improved in a number of ways, say lowering K_{cov} through a soft cover, limiting the velocity commands v_{safe} , lowering K_T via passive compliance, and designing for a lightweight manipulator to reduce mass M_{link} . shows a plot of the head injury

criterion as a function of effective inertia and interface stiffness of the PUMA 560, the addition of a compliant covering can reduce impact loading. However, the amount of compliant material required to reduce impact loads to a safe level can be substantial. Clearly, adding large amounts of compliant covering is impractical [40]. Anyhow, a high-ratio reduction transmission device placed between a motor and a link to amplify the output capacity enlarges the effect of the rotor mass (or inertial), and becomes a critical factor in pHRI problems, and thus lowering K_T via passive compliance is the most effective way to design a robot well compromising performances with a high safety level.

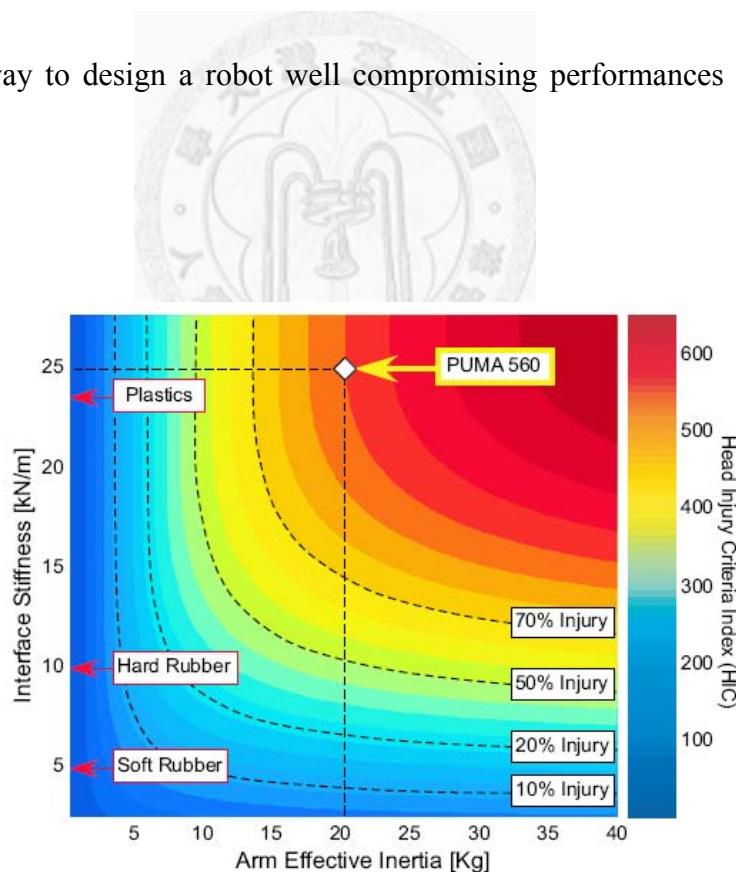


Figure 3-1 Head injury criteria as a function of effective inertia and interface stiffness [40]

3.3. Pre-existing Compliant and Safety Actuator Design

Recently, several techniques and approaches have been devised to efficiently keep a robot arm with intrinsically safe robot actuation, but some intrinsic performance limitation can be only overcome by modifying the mechanical design and introducing a somewhat more complicated actuation mechanism. Therefore, this section briefly introduces pre-existing compliant actuators and their design concepts in this context.

3.3.1. Cable-and-Cylinder Drive Transmissions

As a cable-drive robot arm proposed by [35][41][42], the WAM arm, uniquely exhibiting zero backlash with low friction and low inertia, endows the robot with good open-loop “backdrivability.” High backdrivability and motion control through joint torque control enable the intrinsic sensing of forces over the whole arm and make it inherently safe to humans. Although, these actuation devices have shown the effectiveness to promise them a well safety level of the human-robot interaction, the size and reduction ratio are limited because that huge transmission mechanisms, cylinders, must have a larger diameter than the shaft of the motor and be separate from the motor shaft for an unavoidable rational distance to provide, in part, the desired reduction.

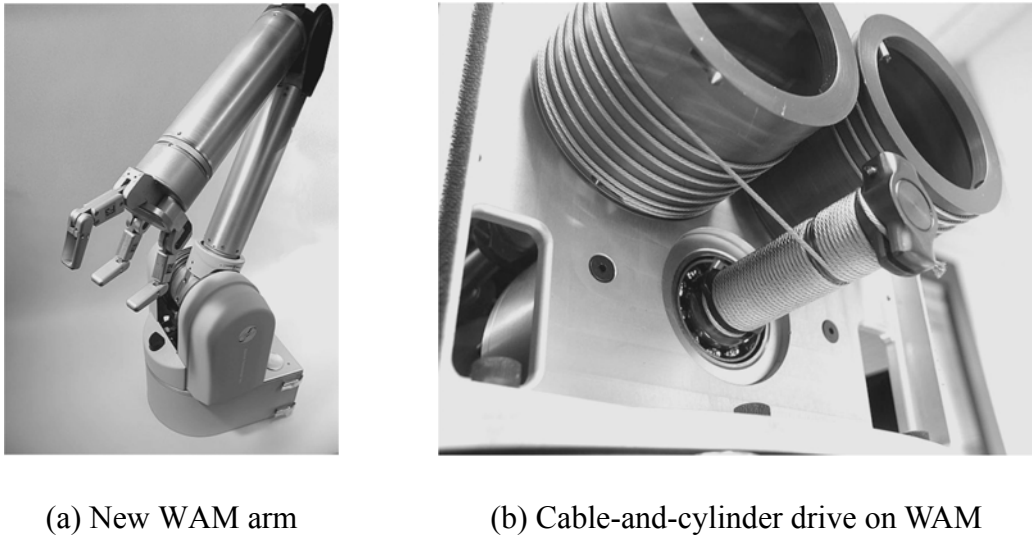


Figure 3-2 The Barrett WAM robot [42]

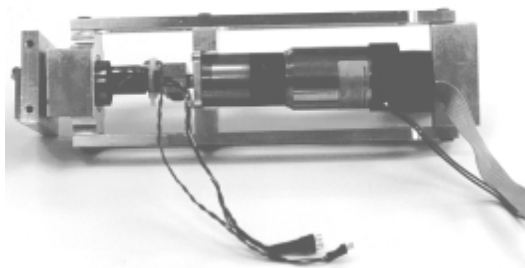
3.3.2. Series Elastic Actuators (SEA)

These actuators use low impedance or high compliant and/or viscous elements in series between transmission mechanisms and loads, and moreover, both linear and rotary SEA designs have been presented in [27][28][43][44][45]. To control the spring deflection, the linear version requires a precision ball screw, allowing good and precise mechanical transmission reduction but making the system expensive and limitative in its stroke. A conventional rotary SEA requires custom-made torsional springs, hard to fabricate and limiting the operational range, and its spring deflection is generally measured by strain-gauge sensors, cumbersome to mount and maintain. What is more, both these linear and rotary SEA versions present joint integration problems, and therefore, a compact, easily-mountable and cheaper actuator maintaining the features

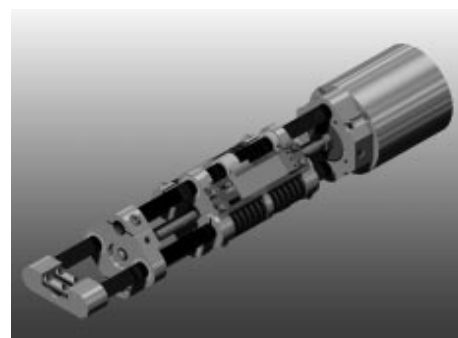
of the SEA has been designed in [44]. However, the operational range is also limited.

Besides, non-collocation of the sensors and transducers limits their utilization for precise and fast force control tasks [34].

In [27], a new compact high performance actuator design especially adapted for the integration of robotic mechanisms is presented and makes use of a mechanical differential as a central element. Differential coupling between intrinsically high impedance plus a transducer and an intrinsically low impedance spring element provides the same benefits as serial coupling but with a relative smaller size than the preceding designs. Recently, the SEA has been design in hand [47] and leg rehabilitation exercise [46][48][49][50].

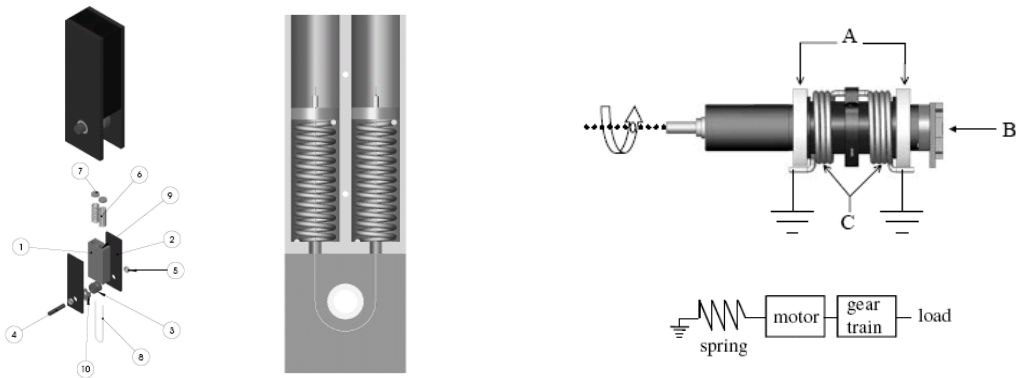


(a) One rotational SEA [29]

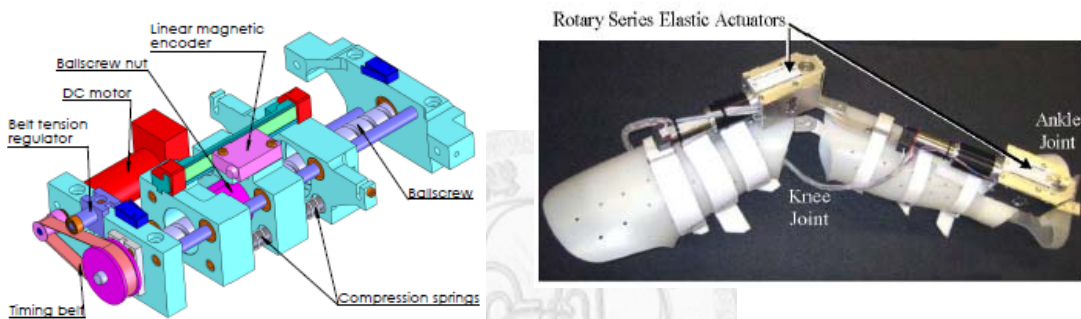


(b) An linear electric series elastic actuator [28]

3.3 PRE-EXISTING COMPLIANT AND SAFETY ACTUATOR DESIGN



(c) A simple and scalable force Actuator [44] (d) Force Sensing Compliant Actuator [43]



(e) Hand Rehabilitation System [47] (f) Rotary Series Elastic Actuator [48]

Figure 3-3 Different kinds of Series Elastic Actuators.

3.3.3. Programmed Impedance Actuators

In passive dynamic systems, motion is modulated by interaction between the mechanism and the environment instead of being forced to follow pre-planned trajectories by the actuators, and namely, the environment is used to guide motion. An approach has been proposed to concentrate on the development of an integrated actuator containing force and position control within a single unit including an integrated control system and programming interface [46] or a form of impedance

control addressing the issue of stability as well as providing programmability of robots for interactive tasks [52].

3.3.4. Variable Stiffness Actuators

Variable stiffness actuators use a variable stiffness transmission mechanism to vary mechanical stiffness of the given system. Most of the proposed implementations make use of two non-linear mechanical springs working in antagonistic configuration with one additional actuator applied in the design system, allowing changing the mechanical impedance of the actuator during motion [53]–[57][113]. However, this kind of variable stiffness actuators has to use two matched actuators, and sacrifices lots of output capacities to achieve the function of changing mechanical stiffness [58]–[63].

Some of the pre-existing variable compliant/stiffness actuators change the stiffness by the linear quadratic relation between the output and input angles or displacements, and also show the different characteristics corresponding to the different level of the pre-tension [52][64][65][66][67][68], whereas the magnitude of output force is associated with certain initially determined specified impedance. Further, some mechanical elements based upon the concept of structure controlled stiffness have be proposed in [69].

3.3 PRE-EXISTING COMPLIANT AND SAFETY ACTUATOR DESIGN

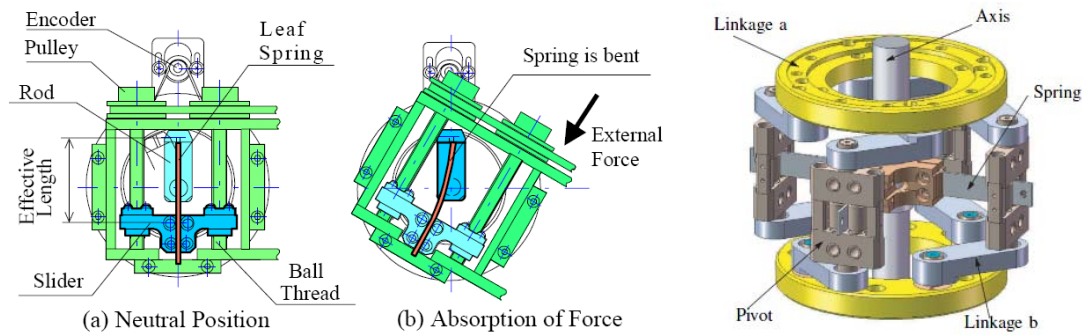


Figure 3-4 Mechanical Impedance Adjuster where linear spring and brake systems are directly built [54][58]

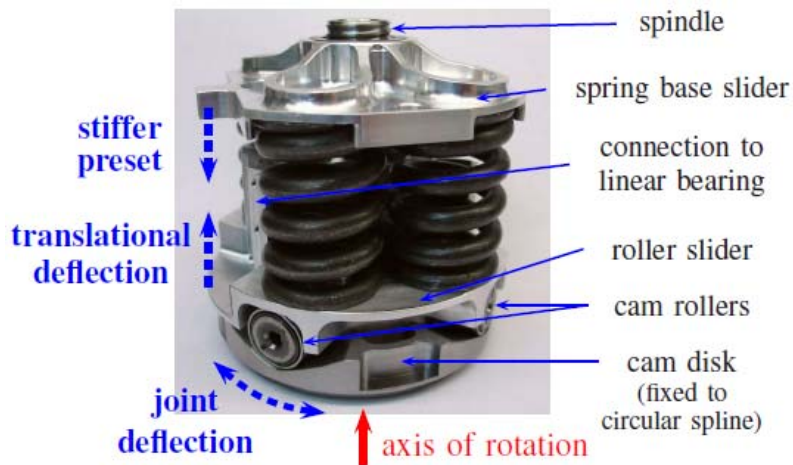


Figure 3-5 Appearance of the Variable Stiffness Actuator [61]



Figure 3-6 An Actuator with Mechanically Adjustable Series Compliance [52]

3.3.5. Parallel Coupled Micro-Macro Actuators (DM2)

This kind of actuators uses a high power series elastic actuator in parallel with a low power direct drive transducer. The serial elastic actuator contributes for low frequencies and high amplitude forces, while the direct drive actuator contributes for high frequencies and low power forces [40][72][73]. In order for the DM2 approach to work properly, both the high- and low-frequency actuators must have zero or near-zero impedance. This is due to the fact that during power transfer, the actuator torques will be added nondestructively only if their respective impedance is zero. In particular, only if each actuator does not have significant impedance within the frequency range of the opposing actuator can the DM2 concept work. The second part of the DM2 actuation approach, differing from previous attempts at coupled actuation, is to distribute the low- and high-frequency actuators to locations on the manipulator where their effect on contact impedance is minimized while their contribution to control bandwidth is maximized. Whereas, the separate design of the DM2 does not make the design compact but complicated.

3.3.6. Antagonistic Pneumatic Artificial Muscle

Most of the proposed implementations of this kind of actuators make use of two non-linear mechanical pneumatic artificial muscles in antagonistic configuration

[38][74]. Pneumatic actuators are inherently elastic components, leading to their successful use on several robots. However, pneumatic actuators are also inherently difficult to control, energetically loss, and difficult to power without an external compressor. Electrical actuation allows for much more precise control, and allows for easier tether-free operation [34][52][75]–[78].

3.3.7. Safe Link Mechanism and Safe Joint Mechanism

The safe link mechanism(SLM) and the safe joint mechanism(SJM), passive safety mechanisms proposed in [39][79][80][81][101][102] respectively, are composed of linear springs, slider mechanisms, and transmission shafts and utilize the concept of the transmission angle of the four-bar linkage and the characteristics of the slider mechanism in combination with the springs to perform nonlinear characteristics. The main contribution of these proposed devices are the variable stiffness capability to develop a nonlinear spring capacity that stiffness remains very high and then will become very low when external force acting on the end-effector is over the critical impact force. However, the critical impact force is inherently fixed without considering the payload variations and operation velocity during the manipulation, so that the SLM and the SJM cannot hold any heavy object leading total external force acting on the end-effector over the critical impact force whether it hurts people or not,

say that these proposed SLM and SJM cannot be used for the manipulator required a large payload capacity and much positioning accuracy.

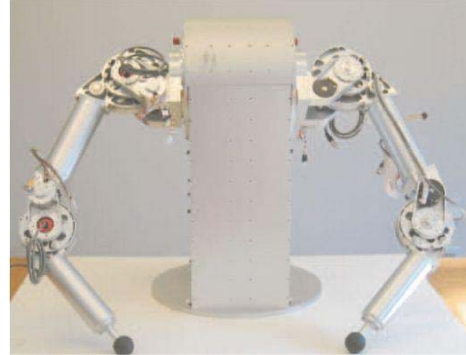
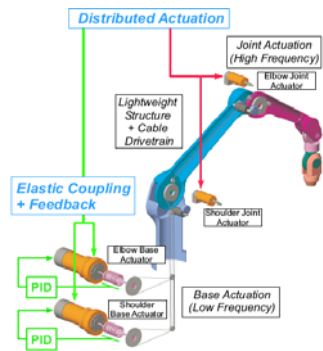
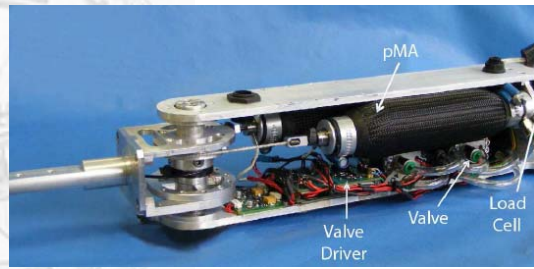


Figure 3-7 Distributed Elastically Coupled Macro Mini Actuation (DECMMA) [40]



(a) Pleated pneumatic artificial muscle [74]

(b) Pneumatic artificial muscle [76]

Figure 3-8 Artificial muscles in antagonistic pairs

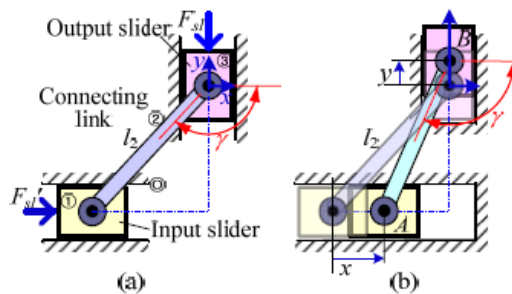
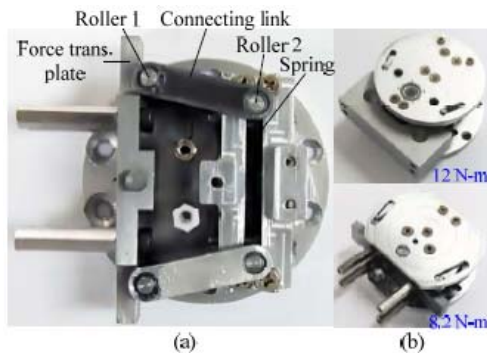


Figure 3-9 Prototype and operation of the safe joint mechanism [81]

3.4. Summary

To sum up, there are two factors to reduce the impedance of robot systems, playing an important role in the human-robot interaction, say one is the passive component placing in series between the actuator and the output link, and the other is the active control tracking the difference between the desired reference input and the output response. Furthermore, with these two factors, the overall system can be regarded as a compliant control system with general equivalent impedance.

Compared to other actuators, series elastic actuators have the following properties [27][28][29][32][33], such as

1. Low reflected inertia
2. Backlash phenomenon elimination
3. Shock tolerance
4. More accurate force and stable force control
5. Less damage to the environment
6. Energy storage
7. Low loop gain of the closed-loop system
8. Robust to the changing load

Specifically, the above-mentioned properties depend on the stiffness constant of series elastic components of a series elastic actuator, that is, a soft series elastic component can contribute to

- reduce the stiction effect and nonlinear friction
- increase the range of the control gain so that stability of force control is improved
- reduce the large force bandwidth and burden capacity
- decrease the output impedance contributing to safe human-robot interaction

On the other hand, a hard series elastic component can contribute to

- increase the operation bandwidth so that improve the overall performance
- decrease deflection and therefore decrease the damping effect
- increase the large force bandwidth and burden capacity
- increase the output impedance contributing to safe human-robot interaction

As the aforementioned properties, designing a SEA system should always find out a maximum allowable output impedance and a maximum tolerable stiction on the SEA system to define the upper bound of the spring constant, and a minimum acceptable large force bandwidth to define the lower bound of the spring constant [34].

3.4 SUMMARY

Generally speaking, series elastic actuators and other few publications found on this subject show that high performance actuators is somehow difficult to implement, particularly within compact volumes and large force/power outputs.



CHAPTER 4. APVSEA—AN ACTIVE-PASSIVE VARIABLE STIFFNESS ELASTIC ACTUATOR FOR SAFETY ROBOT SYSTEMS

For classical robotic applications, robotic systems consist of servo motors, high-ratio reduction and rigid links; mechanical designers prefer to designing robotic applications as stiff as possible to make robots manipulate with remarkable speed and precise position movements. However, these robotic applications can hardly interact with people and environments under safety constraints. It poses the very fundamental problem of ensuring safety to humans and protecting the robot. This chapter presents an active-passive variable stiffness elastic actuator (APVSEA) which is designed for safety robot systems. The APVSEA consists of two DC-motors: one is used to control the position of the joint and the other is used to adjust the stiffness of the system. The stiffness is generated by two antagonistically nonlinear springs. By changing the preload length of the two antagonistically nonlinear springs, APVSEA has the ability to minimize large impact forces due to shocks, to safely interact with the user and/or become as stiff as possible to make precise position movements or trajectory tracking

control easier. Experiment results are presented to show that APVSEA is capable of providing precise position movements while offering safe human-robot interaction.

4.1. Introduction

To development of robots that can work alongside humans in our homes and workspaces to assist human daily activities through physical interaction, informational interaction, etc., has been ongoing for a long time. That is the reason why the research on physical human-robot interaction that considers the trade-off between safety and performance has emerged in the field of modern robotics.

An active-passive variable stiffness elastic actuator (APVSEA), designed for safety robot systems is presented in this chapter. It discusses in detail the APVSEA mechanism, the stiffness adjuster and comparative performances between an actuator with maximum and minimum stiffness. This chapter is structured as follows: section 4.2 presents the main ideas of precise position movement actuation and active-passive variable stiffness actuator (safe actuation). In section 4.3, the design of an active-passive variable stiffness elastic actuator (APVSEA) is explained. The APVSEA consists of two DC-motors, one ball screw, one screw and four variable stiffness springs. The rotation of the axis is measured by an encoder which is fixed on the output link. Section 4.4 presents experiment results to show that APVSEA is

capable of providing precise position movements and safer human-robot interaction.

Finally, the summary are made in Section 4.5.

4.2. Precise Position Movement Actuation / Safe Actuation

The precise position movement actuation and safe actuation are presented in this section. The main concept of the precise position movement actuation is the use of a ball-screw and time belt for greater efficiency and making accurate reservations. For the safe actuation, active and passive variable stiffness serial configurations (adaptable compliance) are discussed.

4.2.1. Motor-Ball screw Drive System

To keep the ability of the actuator to make precise position movements and trajectory tracking control easier, as in classic robotic systems, a motor-ball screw drive system was designed, as shown in Figure 4-1. Note that a ball-screw is driven and rotated by a DC-motor01; because the ball screw is rotated, the moving plant which is fixed on the ball screw will advance or draw back in its own axial direction. There is a time belt fixed on the moving plant and connected with the output link; when the DC-motor01 drives the ball screw, the moving plant is moved. Finally, the

output link is rotated and moves because of the time belt which is connected to the moving plant.

4.2.2. Passive Variable Stiffness Serial Configuration

The design of a passive variable stiffness serial configuration can be expressed by the series combination. In order to explain the properties of the passive variable stiffness serial configuration, a simple spring system with a linear spring is used, as shown in Figure 4-2. x is the position of the moving plant (block), and x_p is the position where no forces are generated. The forces on the block are given by:

$$F = k \cdot (x_p - x), \quad \text{if } x \leq x_p \quad (4-1)$$

Differentiating Eq. (4-1) with respect to the position x , the stiffness is expressed as:

$$K = \frac{dF}{dx} = -k \quad (4-2)$$

This result shows that the stiffness of the compliance is uncontrollable.

When the springs with a quadratic characteristic are used, the force is expressed as:

$$\begin{aligned} F &= k \cdot (x_p - x)^2 \\ &= k \cdot x_p^2 - 2k \cdot x_p \cdot x + k \cdot x^2 \end{aligned} \quad (4-3)$$

The stiffness of the nonlinear spring compliance system is obtained

$$K = \frac{dF}{dx} = 2kx - 2k \cdot x_p \quad (4-4)$$

Where the stiffness varies as a linear function of the block position x .

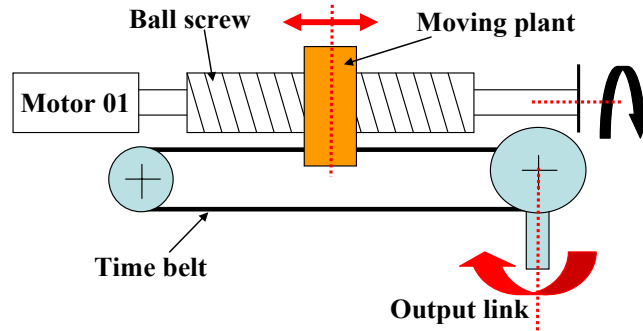


Figure 4-1 Motor-Ball screw Drive System.

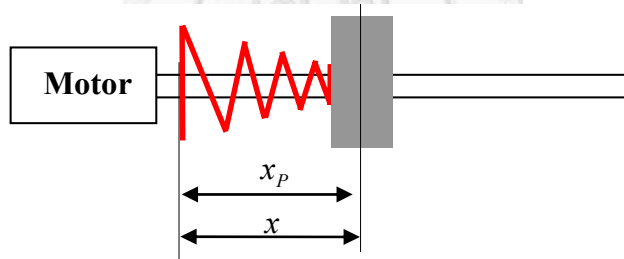


Figure 4-2 Passive variable stiffness serial configuration.

4.2.3. Active Variable Stiffness Serial Configuration

From Eq. (4-4), the stiffness of the nonlinear spring compliance system is dependent on the position of the block. In order to obtain the ability to control the stiffness of the spring compliance system so as not to depend on the position of the block, a new structure model, active variable stiffness serial configuration, was built.

To explain the properties of the active variable stiffness serial configuration, a simple linear antagonistic setup with two linear springs having the same spring constant is used, as shown in Figure 4-3. x is the position of the moving plant (block), x_p is the position where no forces are generated, and x_{oA} and x_{oB} are the controllable position (preload distance of the spring). The forces on the block equal the sum of the forces of both springs:

$$\begin{aligned} F &= k(x_{oA} + (x_p - x)) - k(x_{oB} + (x - x_p)) \\ &= -2kx + k(x_{oA} - x_{oB}) + 2kx_p \end{aligned} \quad (4-5)$$

differentiating Eq. (4-5) with respect to the position x , the stiffness becomes

$$k = \frac{dF}{dx} = -2k \quad (4-6)$$

this result shows that the stiffness of the compliance is uncontrollable.

When the springs with a quadratic characteristic are used, the force is expressed as:

$$\begin{aligned} F &= k(x_{oA} + (x_p - x))^2 - k(x_{oB} + (x - x_p))^2 \\ &= -2kx(x_{oA} + x_{oB}) + k(x_{oA}^2 - x_{oB}^2) + 2k(x_{oA} \cdot x_p + x_{oB} \cdot x_p) \end{aligned} \quad (4-7)$$

the stiffness of the nonlinear spring compliance system, active variable stiffness serial configuration, is obtained:

$$K = \frac{dF}{dx} = -2k(x_{oA} + x_{oB}) \quad (4-8)$$

Figure 4-4 shows the relation between the block movement and the force on the block ($k=1, x_p=6$), where the control parameters x_{oA} and x_{oB} are ($x_{oA}=1,2,3$ and $x_{oB}=1,2,3$). Note that the stiffness of the active variable stiffness serial configuration is controllable.

4.2.4. Active-Passive Variable Stiffness Elastic Actuator (APVSEA)

A motor-ball screw drive system has the property of making precise position movements and the active-passive variable stiffness serial configurations has the ability to minimize large impact forces due to shocks, thereby safely interacting with the user. In this dissertation, the main idea of the active-passive variable stiffness elastic actuator designed for safety robot systems is to combine these two important properties. As shown in Figure 4-5, there is a connector between the motor-ball screw precise drive system and the active-passive variable stiffness serial configuration; the connector connects these two configurations, and as a result, an active-passive variable stiffness elastic actuator was build. The actuator has the ability to minimize large impact forces due to shocks, thereby safely interacting with the user and/or

becoming as stiff as possible to make precise position movements or trajectory tracking control easier.

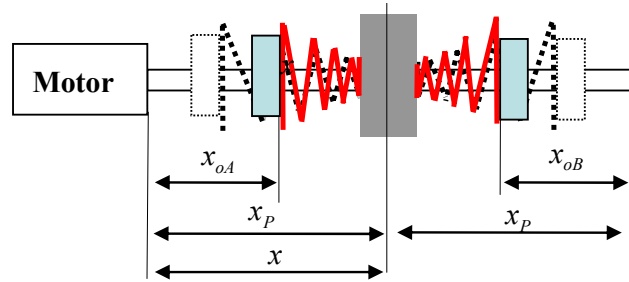


Figure 4-3 Active Variable Stiffness Serial Configuration.

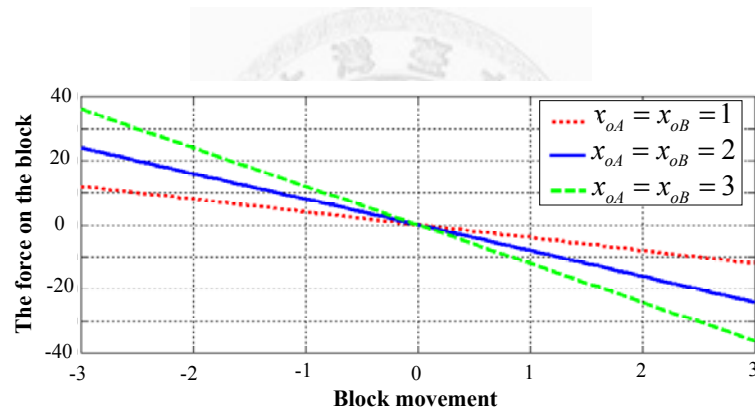


Figure 4-4 The relationship between the block movement and the force on the block.

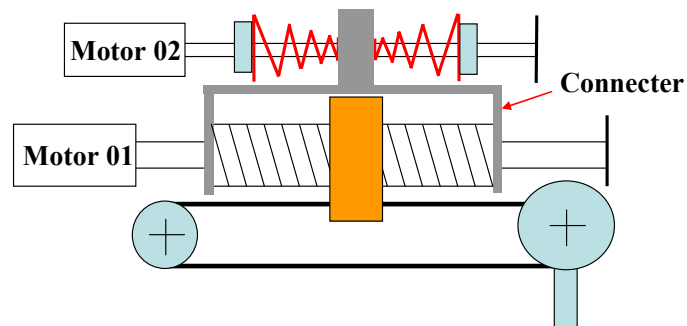


Figure 4-5 The relationship between the block movement and the force on the block.

4.3. Design of an Active-Passive Variable Stiffness Elastic Actuator (APVSEA)

The two main mechanisms, a motor-ball screw system and an active-passive variable stiffness serial configuration, are designed to obtain the two desired characteristics of APVSEA, namely: accurate movement and safety in human-robot interaction.

In the motor-ball screw system, a ball screw is driven and rotated by the DC-motor01 and a moving plant is placed on the ball screw. When the ball screw is rotated by the DC-motor01, the moving plant will advance or draw back in its own axial direction. There is a timing belt02 fixed onto the moving plant and connected with the output link; when the moving plant moves, the output link will move and then rotate. According to the abovementioned moving structure, the APVSEA has the ability to move accurately; the 3-D model of APVSEA is shown in Figure 4-7. In the active-passive variable stiffness serial configuration, a screw is rotated by a DC-motor02, and two moving plants02 move in opposite directions on the screw. There are two variable stiffness springs between the moving plant02 and connector; when two moving plants02 are moved by the screw, the preload length of the variable stiffness springs will be changed; the 3-D model of APVSEA is shown in Figure 4-8.

The APVSEA has the ability to minimize large impact forces due to shocks, to safely interact with the user and/or to become as stiff as possible to make precise position movements or trajectory tracking control easier. The key point of the APVSEA mechanical structure is the relation between input shaft and ball screw.

In the APVSEA actuator design, an input shaft passes through the center of the ball screw. When the input shaft is driven and rotated by the DC-motor, the ball screw will be driven and rotated. When the ball screw is rotated, the moving plant, which is fixed on the ball screw, will advance or draw back in its own axial direction. There is a time belt fixed on the moving plant and connected to the output link; when the DC-motor drives the input shaft, the ball screw is rotated and the moving plant is moved. Finally, the output link is rotated because the time belt, which is connected to the moving plant with the output link, is moved. According to the abovementioned moving theories, the APVSEA has the ability to make precise position movements or trajectory tracking control easier, as shown in Figure 4-9.

In addition, when external forces, impacts or shocks are exerted on the output link, the external forces will push/pull the moving plant by the time belt; then all of the structures, including connector, ball screw and moving plant will be moved. Because the input shaft goes through the center of the ball screw, the ball screw will

4.3 DESIGN OF AN ACTIVE-PASSIVE VARIABLE STIFFNESS ELASTIC ACTUATOR (APVSEA)

slide in the same axial direction as the input shaft, as shown in Figure 4-10. In all cases, the APVSEA has the ability to minimize large impact forces due to shocks, to safely interact with the user. To sum up, the APVSEA can minimize large impact forces and make precise position movements; the key point is the relation between the input shaft and the ball screw. The ball screw can be rotated by the motor and makes the moving plant move. Besides, the ball screw can also be pushed/pulled by the time belt and slides on the input shaft when external forces are exerted on the output link.

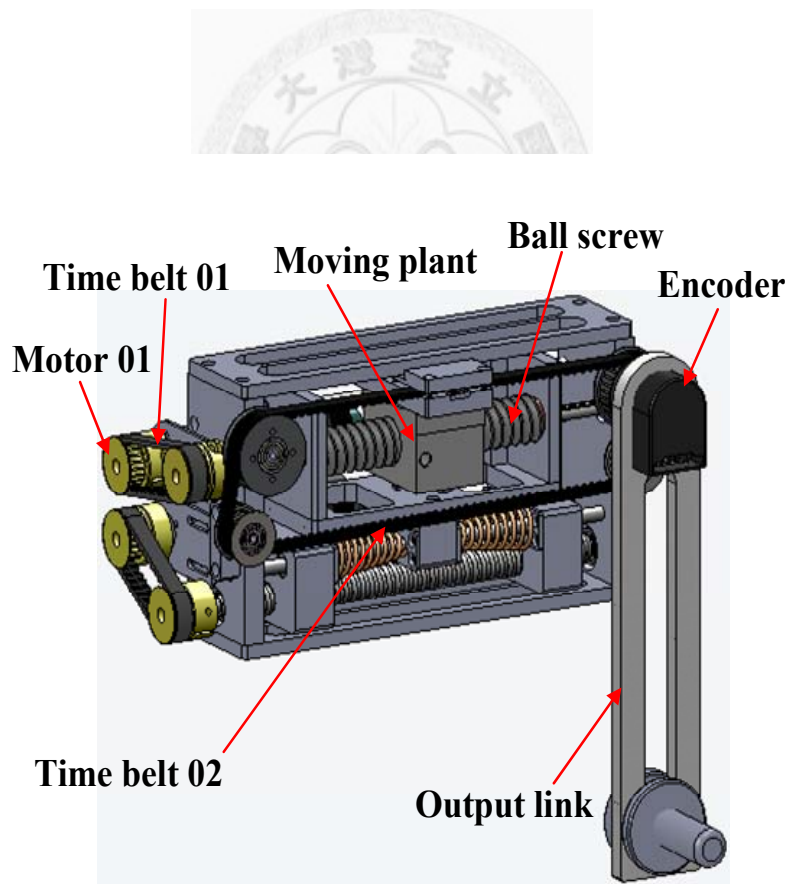


Figure 4-6 3D model of Active-Passive Variable Stiffness Elastic Actuator.

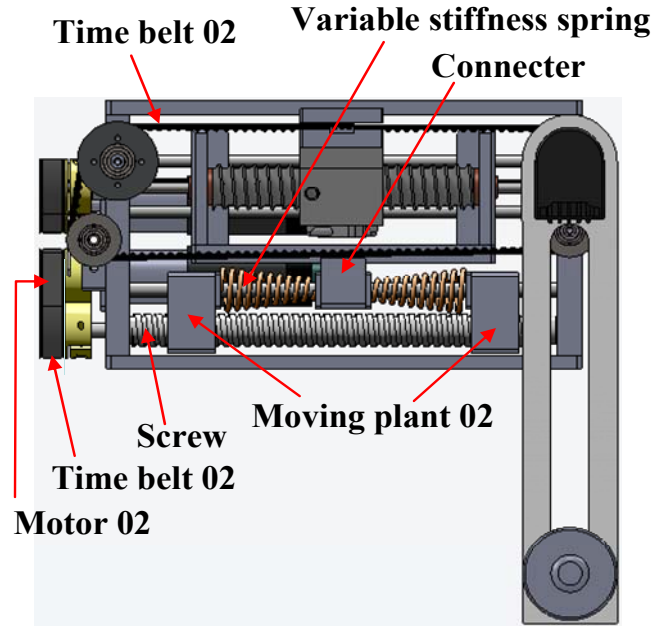


Figure 4-7 Front view of Active-Passive Variable Stiffness Elastic Actuator.

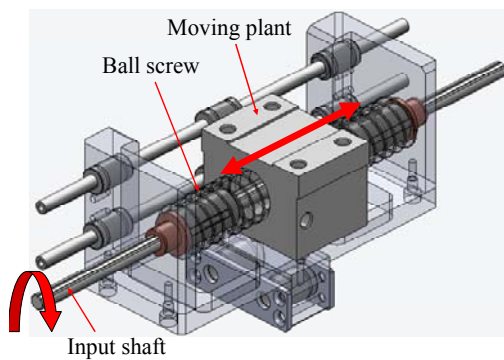


Figure 4-8 3D model of Main structure of APVSEA.

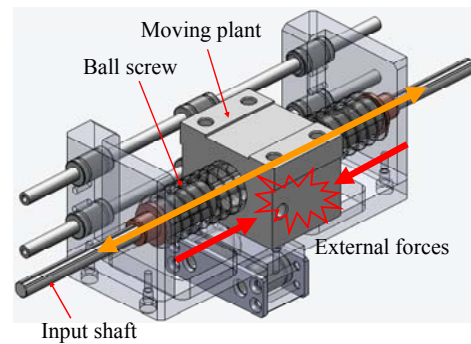


Figure 4-9 3D model of Main structure of APVSEA when APVSEA with external forces.

4.4. System Experiment Evaluation

In this section, experiments were conducted to evaluate the properties and abilities of the active-passive variable stiffness elastic actuator (APVSEA). Figure 4-10 is the picture of the APVSEA which consists of two DC-motors, one ball screw, one screw and four variable stiffness springs. The rotation of the axis is measured by an encoder which is fixed on the output link. Dimensions of the APVSEA, design parameters and some detailed specification are listed in the Table 4-1.

4.4.1. Adaptive Compliant Property

An experiment was designed to interpret the adaptive compliant property of the APVSEA. The experiment comprises four stages. First, by using a simple PID controller, the output link of the APVSEA was rotated and kept in a vertical direction. Second, the output link of APVSEA was manually deflected in a counterclockwise direction away from the 0° (equilibrium point) with the situation whereby the motor was still working. Third, the output link was deflected in a clockwise direction. Fourth, the link was released. As shown in Figure 4-11, the result is a plot of the angle with time and the photograph shows the beginning and finishing position of the APVSEA. The experiment shows that an adaptive compliant configuration was used to make the interaction between robots and humans safer and more natural and that APVSEA has

the ability to interact with people or unknown environments under safety constraints by an adaptive compliance configuration.

The step response of the designed APVSEA system with different preload distance of the nonlinear spring (minimum and maximum) is given in Figure 4-12. The position of the APVSEA changes from 0° to 30° by using a simple PID controller; the result is a plot of the angle with time. As shown in Figure 4-12, when the preload distance of the APVSEA is minimum (stiffness is minimum), vibration due to the position command over 1.4 sec and the actuator is at a 7° angle offset because of the gravity, the precise position movement ability is worse. If the preload distance of the APVSEA is maximum (stiffness is maximum), vibration does not occur, and the APVSEA has good precise position movements. The experiment shows that the APVSEA has the ability to obtain different stiffness by changing the preload distance of the nonlinear spring, and the APVSEA with maximum stiffness shows better response than the APVSEA with minimum.

Table 4-1 Specification of the APVSEA

PARAMETERS	Value
Mass (include two motors)	1.6 kg
Length*Width*Height	150*80*80 mm
DC-motor	2
Max. Output Torque	12.47 Nm
Max. Output Speed	66 rpm
Max. stiffness	Equivalent to rigid joint stiffness
Min. stiffness	4.35 Nm/red.
Max. Output Link Deflection	$\pm 60^\circ$

* The input motors used in this prototype design are Faulhaber DC-micromotor 3257W024CR and 2642W024CR with 23/1 gear head of which reduction ratio is 1:14.

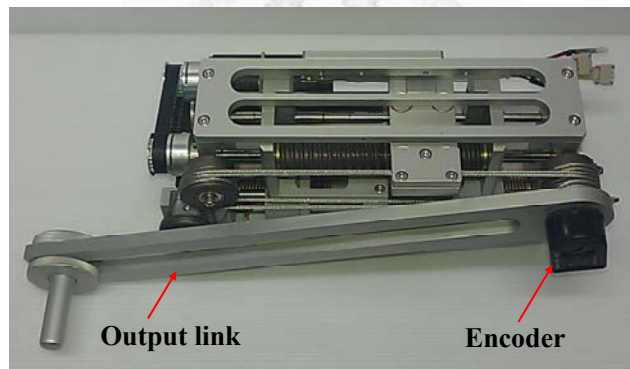


Figure 4-10 Active-Passive Variable Stiffness Elastic Actuator (APVSEA).

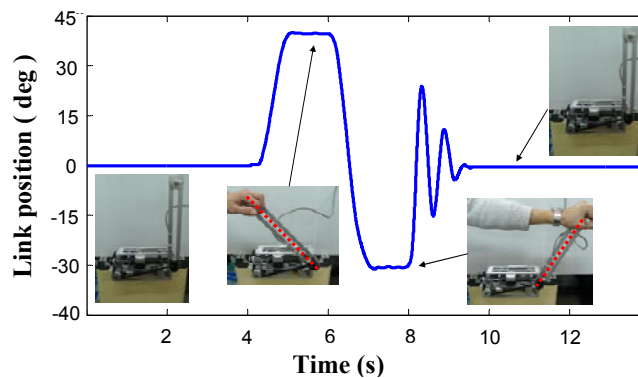


Figure 4-11 Adaptive compliant property for Active-Passive Variable Stiffness Elastic Actuator.

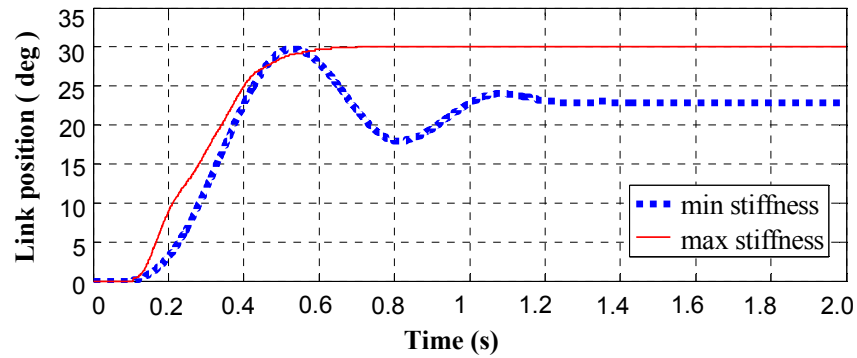


Figure 4-12 Response to position command with various stiffness.

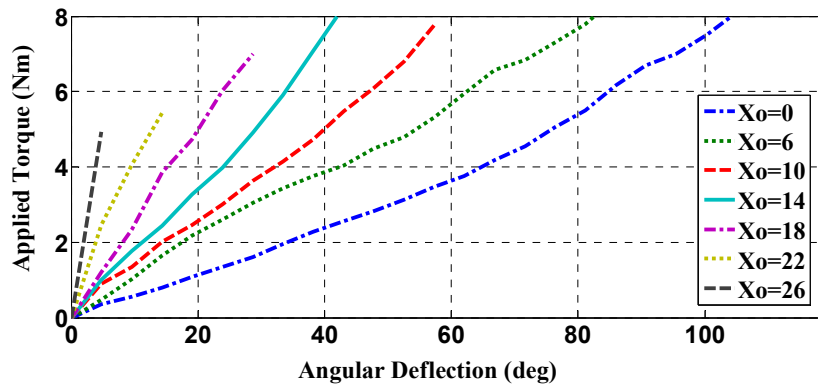


Figure 4-13 Measure stiffness of the APVSEA.

4.4.2. Active Variable Stiffness Property

By changing the preload distance of nonlinear springs, the APVSEA is able to vary the stiffness. In this experiment, a force sensor is used to measure the external force at the end-point of the output link and a potential meter is used to measure the displacement of the nonlinear spring. As shown in Figure 4-13, x_o is the preload distance of nonlinear springs. The stiffness of the APVSEA is changed with the different preload distance of the nonlinear spring.

4.4.3. Safe Robot System

As shown in Figure 4-14, a table-tennis ball and an aluminum cube are hit by the APVSEA output link which is rotated with maximum and minimum stiffness at 2.38rad/s (the preload distance of variable stiffness springs are maximum and minimum); the output link of APVSEA is 500mm long and the objects (table-tennis ball and aluminum cube) are hit at the height of 500mm. The flight distances of the objects are measured. The mean value of the flight distance data is taken after 10 measurements, as shown in Table 4-2. The result shows that for the table-tennis ball and aluminum cube cases, the objects fly farther if the APVSEA has maximum stiffness. The stiffness of APVSEA and flight distances have been shown to be negative correlated to one another. Since the objects are static before being hit by the output link and the mass of the objects does not change, the parameter that affects the objects' flight distance is the acceleration of the objects after collision. Less stiffness leads to less acceleration of the object. Because the safety of the object depends on the objects' acceleration after collision, the experiment implies that it is safer to impact with less stiffness than with higher stiffness.

Table 4-2 The Estimated HIC and v_{\max} for APVSEA and SEA

PARAMETERS	HIC	v_{\max}
APVSEA (Minimum stiffness)	15.29	2.2
APVSEA (Maximum stiffness)	48.74	1.34
SEA	167	0.84

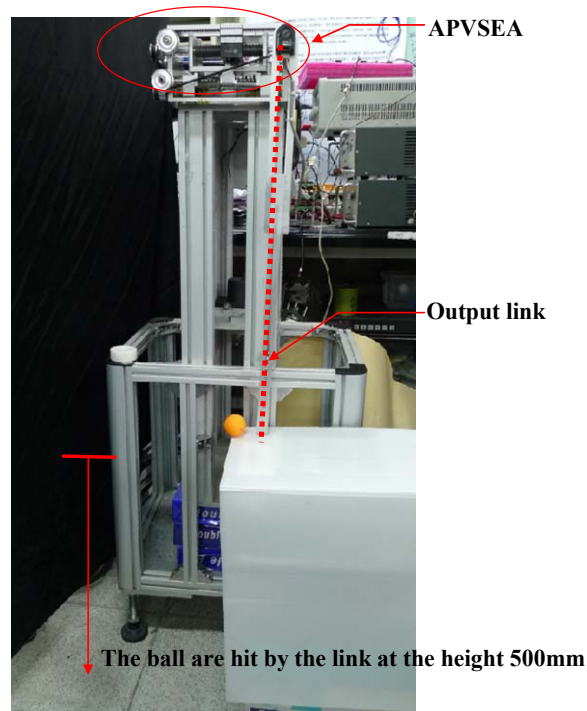


Figure 4-14 Experiment setup for hitting-object experiment.

4.5. Summary

In this chapter, an active-passive variable stiffness elastic actuator for safety robot system was presented. By changing the preload length of the two

antagonistically nonlinear springs, the APVSEA has the ability to minimize large impact forces due to shocks, to safely interact with the user and/or to become as stiff as possible to make precise position movements or trajectory tracking control easier.

The preliminary results obtained from these experiments show that the APVSEA has the capability to interact with people or unknown environments under safety constraints by passive compliance, and also has the ability to obtain different stiffness by changing the preload distance of the nonlinear spring; the APVSEA with maximum stiffness shows better response than the APVSEA with minimum stiffness. When objects were hit by the output link of APVSEA with maximum stiffness, the flight distance of the object was further than in the case of APVSEA with minimum stiffness. Since, the safety of the object depends on the acceleration after the collision, the experiment showed that a joint with less stiffness was safer in case of unexpected impact with humans.

CHAPTER 5. AVSEA—ACTIVE VARIABLE STIFFNESS ELASTIC ACTUATOR : DESIGN AND APPLICATION FOR SAFE PHYSICAL HUMAN-ROBOT INTERACTION

In classical robotic applications, robotic systems consist of servo motors, high-ratio reduction and rigid links; mechanical designers prefer to design robotic applications as stiff as possible to make robots manipulate with remarkable speed and precise position movements. However, these robotic applications can hardly interact with people and environments under safety constraints. It poses the very fundamental problem of ensuring safety to humans and protecting the robot. This chapter presents an Active Variable Stiffness Elastic Actuator (AVSEA) that is designed and application to safe physical human robot interaction. The AVSEA consists of two DC-motors: one is used to control the position of the joint and the other is used to adjust the stiffness of the system. The stiffness is generated by a leaf spring. By changing the effective length of the leaf spring, AVSEA has the ability to minimize large impact forces due to shocks, to safely interact with the user and/or to become as stiff as possible to make precise position movements or trajectory tracking control easier. Experiment results are presented to show that AVSEA is capable of providing

precise position movements while offering safe human-robot interaction.

5.1. Introduction

An active variable stiffness elastic actuator (AVSEA), designed and application to safe physical human robot interaction is presented in this chapter. It discusses in detail the AVSEA mechanism and functions. This chapter is structured as follows: section 5.2 presents the main ideas of precise position movement actuation and active variable stiffness serial configuration (safe actuation). In section 5.3, the design of an active variable stiffness elastic actuator (AVSEA) is explained. Section 5.4 presents experiment results to show that AVSEA is capable of providing precise position movements and safer human-robot interaction. Finally, the summary are made in Section 5.5.

5.2. Precise Position Movement Actuation / Safe Actuation

The precise position movement actuation and safe actuation are presented in this section. The main concept of the precise position movement actuation is the use of a ball-screw for greater efficiency and making accurate reservations. For the safe actuation, an active variable stiffness serial configuration (adaptable compliance) is discussed.

5.2.1. Motor-Ball screw Drive System

To keep the ability of the actuator to make precise position movements and trajectory tracking control easier, as in classic robotic systems, a Motor-Ball screw Drive System was designed, as shown in Figure 5-1. Note that a ball-screw is driven and rotated by a DC-motor01; because the ball screw is rotated, the moving plant which is fixed on the ball screw will advance or draw back in its own axial direction.

There is a cable fixed on the moving plant and connected with the output link; when the DC-motor01 drives the ball screw, the moving plant is moved. Finally, the output link is rotated and moves because of the cable which is connected to the moving plant.

The output link angular displacement of the Motor-Ball screw Drive System (θ_{out}) is given by:

$$\theta_{out} = \theta_m * G \quad (5-1)$$

θ_m is the angular displacement of the DC-motor01, G is the gear reduction ration of the Motor-Ball screw Drive System.

In order to shorten the length of the ball screw to reduce the size of the Motor-Ball screw Drive System, a block assembly with propelling shave and fixed pulley is used, as shown in Figure 5-2. In the block assembly, x_p' is the position of the

propelling shave, and X_p is the position of the propelling shave before the external force is generated. X_E' is the position of the end point of the cable, and X_E is the position of the end point of the cable before the external force is generated. The movement distance between the propelling shave and the end point of the cable is given by:

$$-2(X_p' - X_p) = X_E' - X_E \quad (5-2)$$

By combining Motor-Ball screw Drive System and block assemblies, the New Motor-Ball screw Drive System is presented in this dissertation. As shown in Figure 5-3, the propelling shave of the block assembly is fixed on the moving plant and the end point of the cable is fixed on the output link. When the ball-screw is driven and rotated by a DC-motor01, the moving plant which is fixed on the ball screw will advance or draw back in its own axial direction and the propelling shave fixed on the moving plant will advance or draw back too. Finally, by the block assembly, the output link of New Motor-Ball screw Drive System (with block assembly) is rotated.

The output link angular displacement of the New Motor-Ball screw Drive System with block assembly (θ_{out}') is given by:

$$\theta_{out}' = 2\theta_{out} \quad (5-3)$$

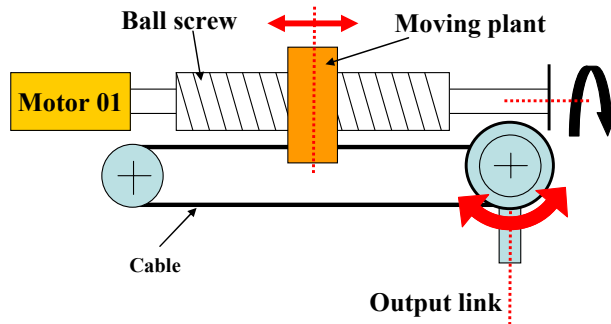


Figure 5-1 Motor-Ball screw Drive System.

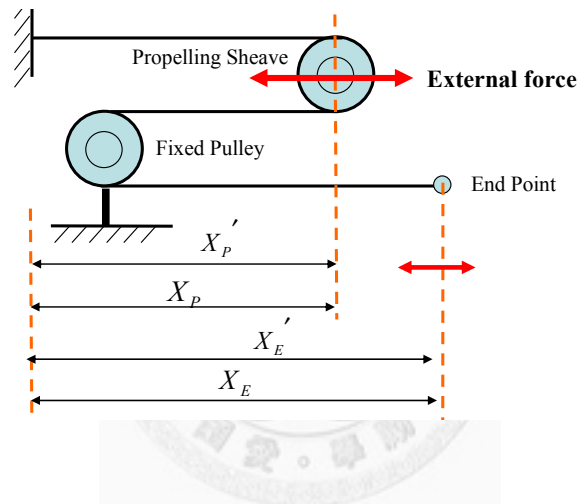


Figure 5-2 A block assembly (with propelling sheave and fixed pulley).

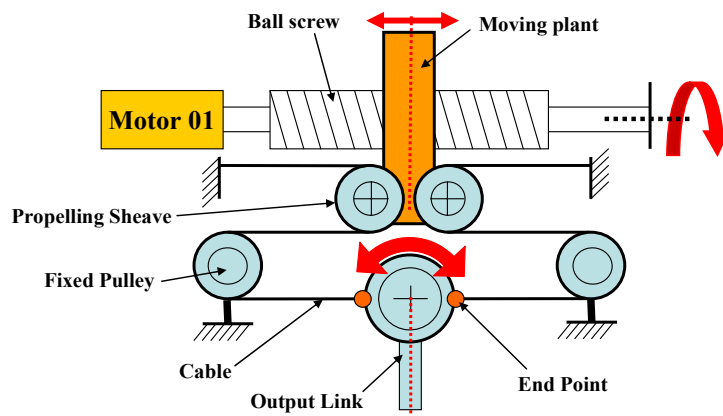


Figure 5-3 New Motor-Ball screw Drive System (with block assembly)

5.2.2. Active Variable Stiffness Serial Configuration

The design of an active variable stiffness serial configuration can be expressed by the series combination. In order to explain the properties of the active variable stiffness serial configuration, a simple beam system is used, as shown in Figure 5-4. P is concentrated load, L is the length of the beam, E is modulus of elasticity (Young's modulus) and I is moment of inertia. The deflection at end point of the beam (δ_b) is given by [17]:

$$\delta_B = \frac{PL^3}{3EI} \quad (5-4)$$

From Eq. (5-4), the deflection at end point of the beam δ_b is changed by the length of the beam L . In this dissertation a leaf spring is used to instead of the beam and in order to obtain the ability to control the deflection at end point of the leaf spring, an active variable stiffness serial configuration is designed, as shown in Figure 5-5. In the active variable stiffness serial configuration, a screw is rotated by a DC-motor02, and a moving plant02 is placed on the screw. When the screw is rotated by the DC-motor02, the moving plant advances or draws back in its own axial direction. By changing the position of the moving plant, the active variable stiffness serial configuration has ability to obtain the effective length of leaf spring (l), change

of the effective length of the leaf spring results in changing stiffness.

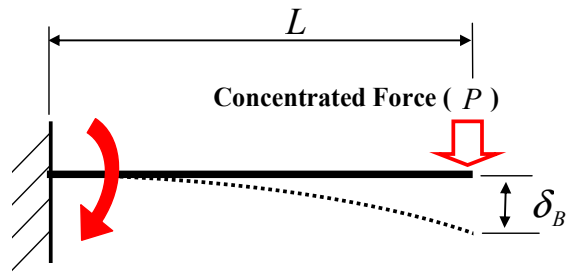


Figure 5-4 A beam system.

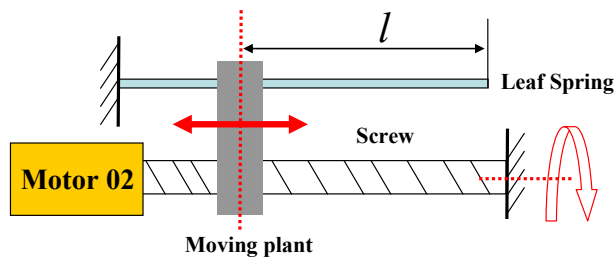


Figure 5-5 Schematic of active variable stiffness serial configuration. By changing the position of the moving plant, the active variable stiffness serial configuration has ability to obtain the effective length of leaf spring (l), change of the effective length of the leaf spring results in changing stiffness.

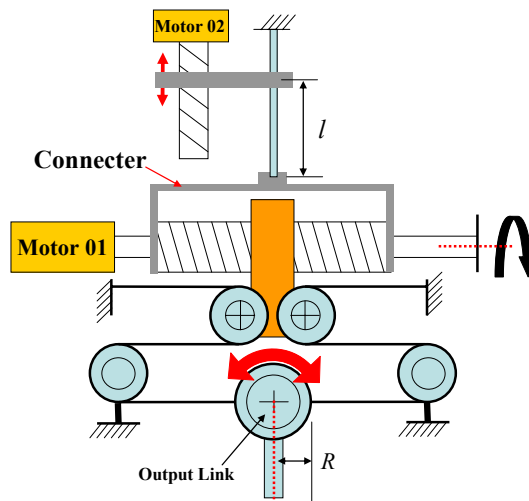


Figure 5-6 A concept of the Active Variable Stiffness Elastic Actuator (AVSEA).

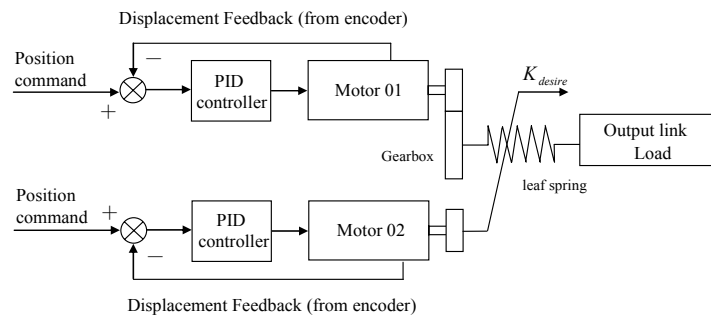


Figure 5-7 Control topology of the AVSEA. The AVSEA consists of two DC-motors: one is used to control the position of the joint and the other is used to adjust the stiffness of the APVSEA. Each motor is controlled by a simple PID controller.

5.2.3. Active Variable Stiffness Elastic Actuator (AVSEA)

The new motor-ball screw drive system has the property of making precise position movements and the active variable stiffness serial configurations has the ability to minimize large impact forces due to shocks, thereby safely interacting with the user. In this dissertation, the main idea of the Active Variable Stiffness Elastic Actuator (AVSEA) that is designed and application to safe physical human robot interaction is to combine these two important properties. As shown in Figure 5-6, there is a connector between the new motor-ball screw drive system and the active variable stiffness serial configuration; the connector connects these two configurations, and as a result, an Active Variable Stiffness Elastic Actuator was build. The actuator has the ability to minimize large impact forces due to shocks and/or becoming as stiff

as possible to make precise position movements or trajectory tracking control easier.

Figure 5-7 depicts the control topology for the AVSEA. The AVSEA consists of two DC-motors: one is used to control the position of the joint and the other is used to control the effective length of the leaf spring to adjust the stiffness of the AVSEA. In the AVSEA, each motor is controlled by a simple PID controller independently. The motor has displacement feedback from an encoder that forms a position closed loop for controlling the motor.

5.3. Design of an Active Variable Stiffness Elastic Actuator

The two main mechanisms, the new motor-ball screw drive system and an active variable stiffness serial configuration, are designed to obtain the two desired characteristics of AVSEA, namely: accurate movement and safe human-robot interaction. The 3-D model of AVSEA is shown in Figure 5-8.

In the new motor-ball screw drive system, a ball screw is driven and rotated by the DC-motor01 and a moving plant is placed on the ball screw. When the ball screw is rotated by the DC-motor01, the moving plant advances or draws back in its own axial direction. There is a cable connected to the propelling shaft, fixed pulley and output link; when the moving plant moves, the output link moves and then rotate. According to the abovementioned moving structure, the AVSEA has the ability to move

accurately. The 3-D model of new motor-ball screw drive system of AVSEA is shown in Figure 5-9.

In the active variable stiffness serial configuration, a screw is rotated by a DC-motor02, and a moving plant02 is placed on the screw. When the screw is rotated by the DC-motor02, the moving plant advances or draws back in its own axial direction. Two rollers are fixed on the moving plant02, these rollers will decide the effective length of leaf spring. According to the abovementioned moving structure, the active variable stiffness serial configuration of AVSEA has the ability to obtain the stiffness as soft as possible to minimize large impact forces due to shocks, to safely interact with the user and/or become as stiff as possible to make precise position movements or trajectory tracking control easier. The 3-D model of active variable stiffness serial configuration is shown in Figure 5-10.

5.3 DESIGN OF AN ACTIVE VARIABLE STIFFNESS ELASTIC ACTUATOR

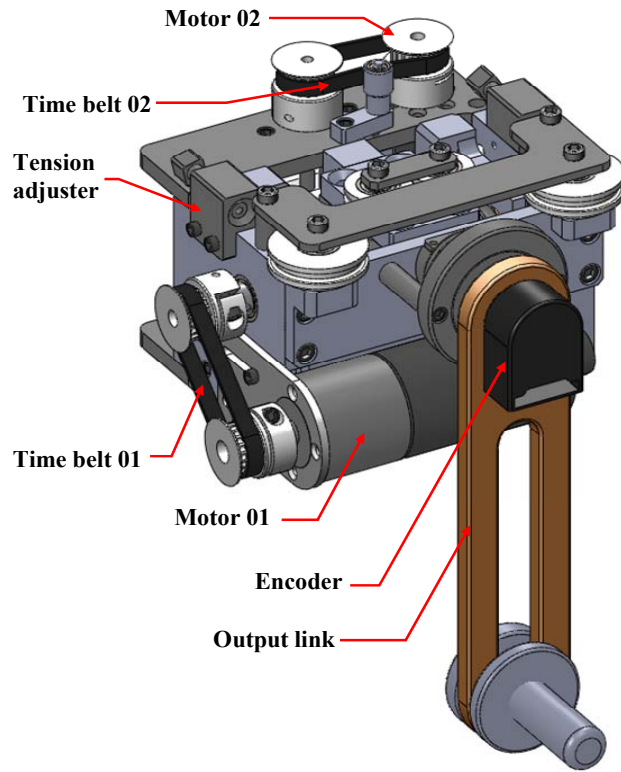


Figure 5-8 3D model of Active Variable Stiffness Elastic Actuator (AVSEA).

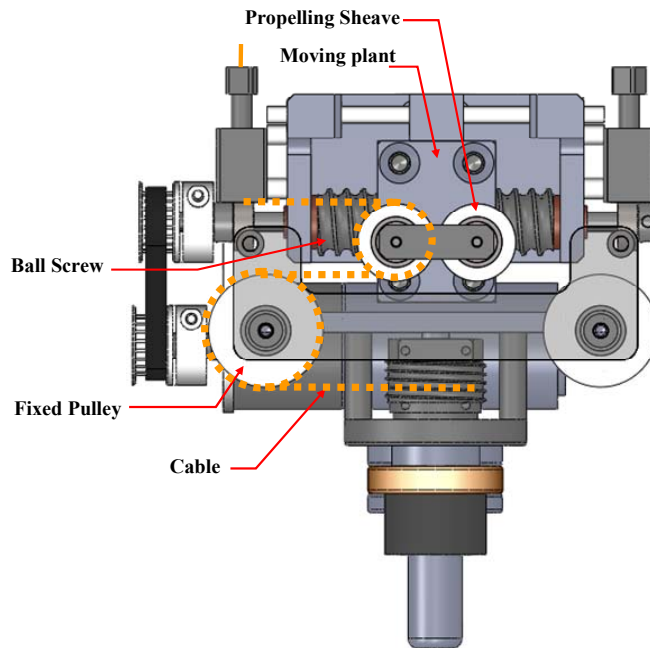


Figure 5-9 Top view of AVSEA (3-D model of new motor-ball screw drive system)

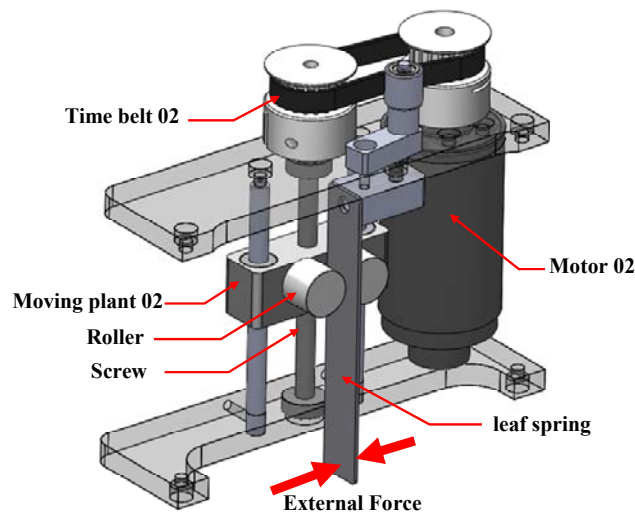


Figure 5-10 3-D model of active variable stiffness serial configuration of AVSEA

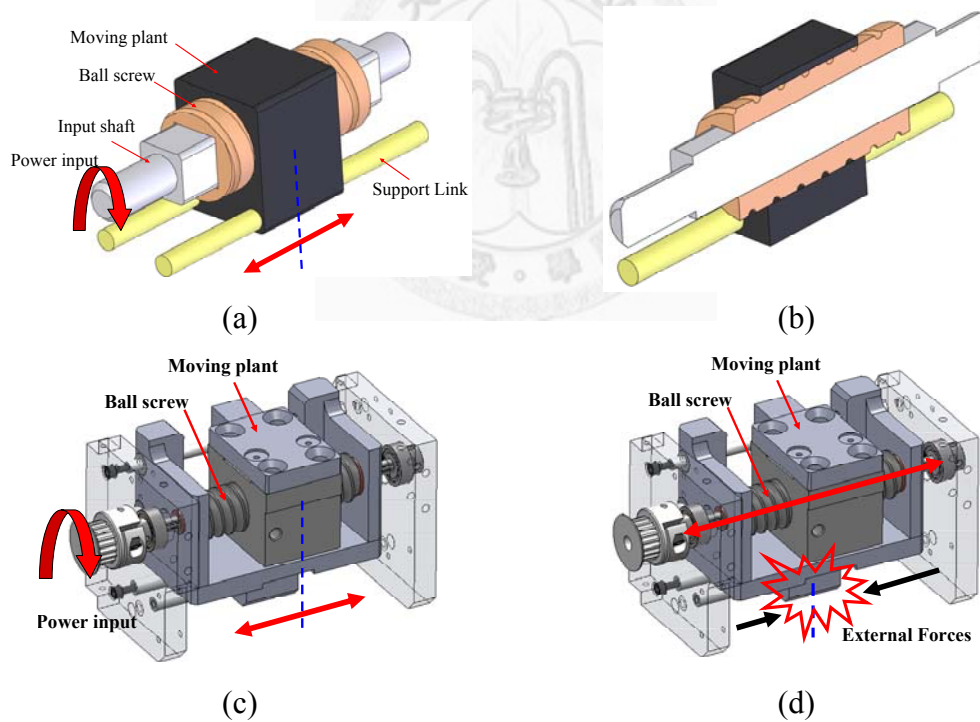


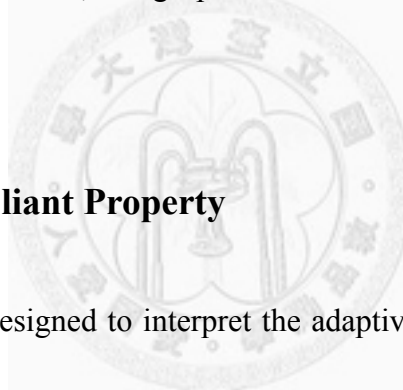
Figure 5-11 3D model of the Motor-Ball screw drive system of AVSEA; (a) the concept of the Motor-Ball screw drive system of AVSEA, (b) the cross-section diagram of the Motor-Ball screw drive system of AVSEA, (c) the detail structure of the Motor-Ball screw drive system of AVSEA, (d) the Motor-Ball screw drive system of AVSEA with external forces.

The key feature of the AVSEA mechanical structure is the relation between the input shaft and the ball screw. The actuation principle of the AVSEA is illustrated in Figure 5-11. Figure 5-11(a) shows the working concept. In the drive system, an input shaft passes through the center of the ball screw. When the input shaft is driven and rotated by the DC-motor 01, the ball screw will be driven and rotated. When the ball screw is rotated, the moving plant, which is fixed on the ball screw, advances or draws back in its own axial direction. There is a time belt fixed on the moving plant and connected to the output link. Then the output link is rotated because the time belt, which is connected to the moving plant with the output link, is moved. According to the abovementioned moving principle, the AVSEA is able to make precise position movements or trajectory tracking control easier. Figure 5-11(b) is the cross-section diagram, and the detailed structure of the Motor-Ball screw drive system of AVSEA is shown in Figure 5-11(c). In addition, when external forces, impacts or shocks are exerted on the output link, the external forces will push/pull the moving plant through the time belt, then all of the structure, including ball screw and moving plant, will be moved. Because the input shaft goes through the center of the ball screw, the ball screw will slide in the same axial direction as the input shaft, as shown in Figure 5-11(d). In all cases, the AVSEA can minimize large impact forces due to shock and

safely interact with the user.

5.4. System Experiment Evaluation

In this section, experiments were conducted to evaluate the properties and abilities of the Active Variable Stiffness Elastic Actuator (AVSEA). Figure 5-12 is the picture of the AVSEA which consists of two DC-motors, one ball screw and a leaf spring. The rotation of the axis is measured by an encoder which is fixed on the output link. Dimensions of the AVSEA, design parameters and some detailed specification are listed in the Table 5-1.



5.4.1. Adaptive Compliant Property

An experiment was designed to interpret the adaptive compliant property of the AVSEA. The experiment comprises four stages. First, by using a simple PID controller, the output link of the AVSEA was rotated and kept in a vertical direction. Second, the output link of AVSEA was manually deflected in a counterclockwise direction away from the 0° (equilibrium point) with the situation whereby the motor was still working. Third, the output link was deflected in a clockwise direction. Fourth, the link was released. As shown in Figure 5-13, the result is a plot of the angle with time and the photograph shows the beginning and finishing position of the AVESA.

Table 5-1 Specification of AVSEA

PARAMETERS	Value
Mass (include two motors)	2.2 kg
Length*Width*Height	120*110*90 mm
DC-motor	2
Max. Output Torque	29 Nm
Max. Output Speed	60 rpm
Max. Stiffness	Equivalent to rigid joint stiffness
Min. Stiffness	0.085Nm/deg
Motion Space	$\pm 150^\circ$
Leaf spring (thickness* width)	3*10 mm
Max. Output Link Deflection	$\pm 40^\circ$

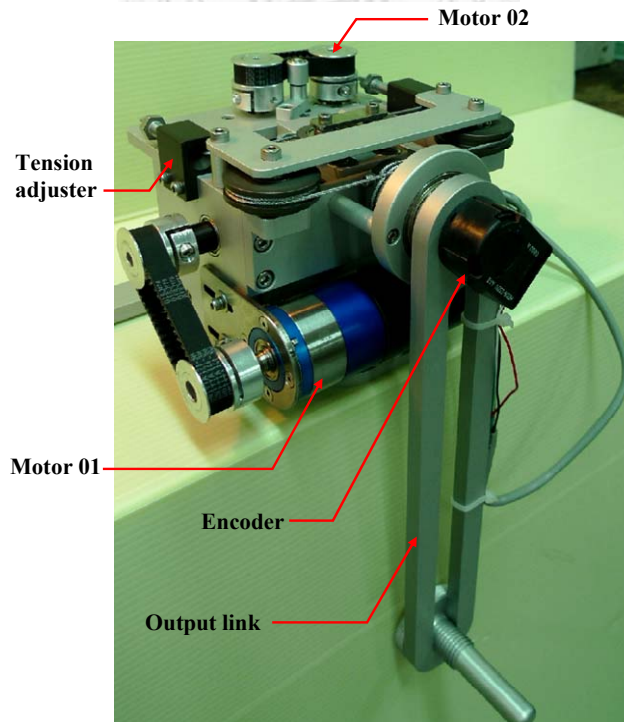


Figure 5-12 Active Variable Stiffness Elastic Actuator (AVSEA).

The experiment shows that an adaptive compliant configuration was used to make the interaction between robots and humans safer and more natural and that AVSEA has the ability to interact with people or unknown environments under safety constraints by an adaptive compliance configuration.

5.4.2. Active Variable Stiffness Property

By changing the effective length of leaf spring, the AVSEA is able to vary the stiffness. In this experiment, a force sensor is used to measure the external force at the end-point of the output link and an encoder is used to measure the angular deflection of the output link. As shown in Figure 5-14, L is the effective length of leaf spring. The stiffness of the AVSEA is changed with the effective length of leaf spring.

5.4.3. Response to Position Command with Variable Stiffness

The step response of the designed AVSEA system with different length of leaf spring (maximum and minimum) is given in Figure 5-15. The position of the AVSEA changes from 0° to 30° by using a simple PID controller; the result is a plot of the angle with time. As shown in Fig. 15, when the length of the leaf spring of the AVSEA is maximum (stiffness is minimum), vibration due to the position command over 0.82 sec and the actuator is at a 5.5° angle offset because of the gravity, the precise position

movement ability is worse. If the length of the leaf spring of the AVSEA is minimum (stiffness is maximum), vibration does not occur, and the AVSEA has good precise position movements. The experiment shows that the AVSEA has the ability to obtain different stiffness by changing the length of the leaf spring of the AVSEA, and the AVSEA with maximum stiffness shows better response than the AVSEA with minimum.

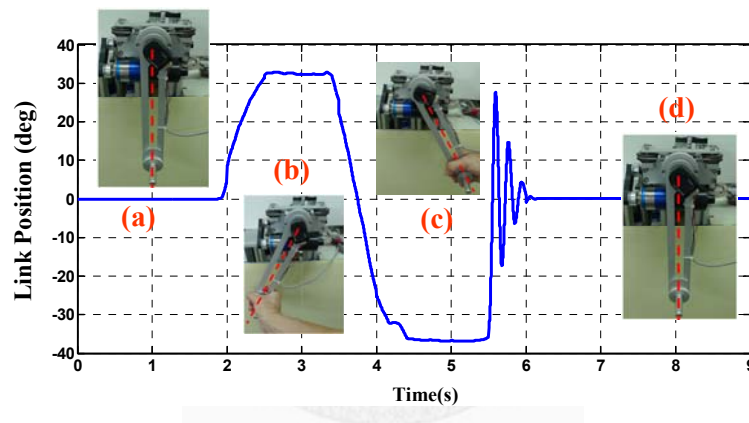


Figure 5-13 Adaptive compliant property for Active Variable Stiffness Elastic Actuator.

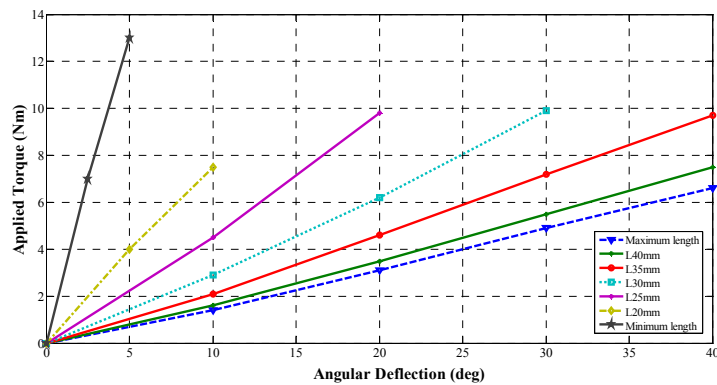


Figure 5-14 Measure stiffness of the AVSEA.

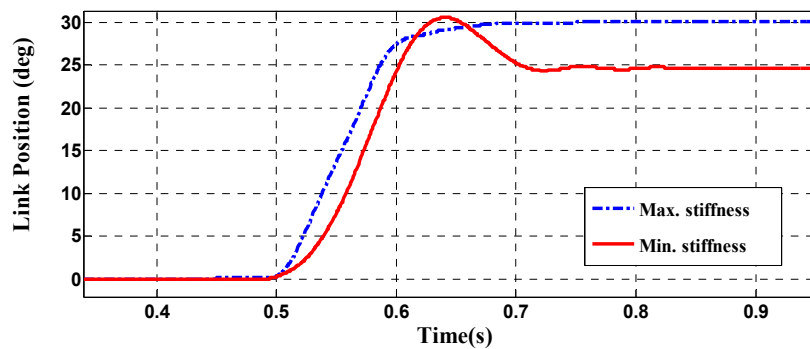


Figure 5-15 Response to position command with variable stiffness.

5.4.4. Head Injury Criterion (HIC)

For a typical robot, the margin available for designing to satisfy both safety and performance requirements is the intersection of the ranges of tip-velocity and payload values of acceptable designs. Since the tip-velocity and payload values determine how to design a safe robot, several safety criteria based on these two factors have been developed. For example, to represent human safety associated with the dynamic collision, the HIC, quantitatively measuring head injury risks in car crash situations, was used to evaluate the tolerant level of human-robot impact in many researches. A HIC value equal to or greater than 1000 is typically associated with extremely severe head injury. The value less than 100 is considered suitable for normal operation of a machine physically interacting with humans. The HIC for compliant manipulators can be given as :

$$HIC = 2\left(\frac{2}{\pi}\right)^{\frac{3}{2}}\left(\frac{K_{cov}}{M_{oper}}\right)^{\frac{3}{4}}\left(\frac{M_{rob}}{M_{rob} + M_{oper}}\right)^{\frac{7}{4}}v_{max}^{\frac{5}{2}} \quad (3.2)$$

where M_{oper} is the impacted operator mass, K_{cov} is the lumped stiffness of a compliant cover on the arm, and v_{max} is the maximum velocity of the end-effector.

The compound inertia M_{rob} is defined as:

$$M_{rob}(K_{transm}) = M_{link} + \frac{K_{transm}}{K_{transm} + \gamma}M_{rotor} \quad (3.3)$$

where γ is the rigid joint stiffness. Note that low transmission stiffness K_{transm} , which decouples the rotor mass M_{rotor} from the link mass M_{link} , dominates the major effect of the M_{rob} . Moreover, the acceptable velocity under the safety constraint can be written as:

$$v_{max} = \left[\frac{HIC_{max}}{2\left(\frac{2}{\pi}\right)^{\frac{3}{2}}\left(\frac{K_{cov}}{M_{oper}}\right)^{\frac{3}{4}}\left(\frac{M_{rob}(K_{transm})}{M_{rob}(K_{transm}) + M_{oper}}\right)^{\frac{7}{4}}} \right]^{\frac{2}{5}} \quad (3.4)$$

where the maximum tolerant max HIC can be chosen less than 100, a suitable value for normal operation of a machine physically interacting with humans. As shown in Figure 5-16, we can see that when $v_{max}=1\text{m/s}$, the HIC of AVSEA is much better than the SEA.

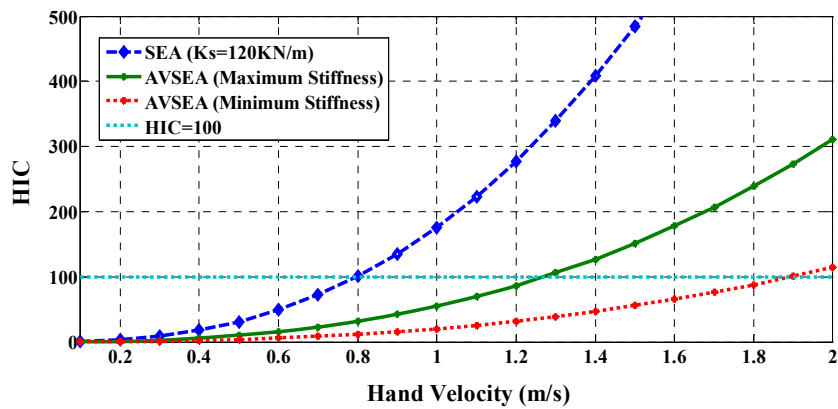


Figure 5-16 The head Injury Criterion (HIC) for SEA and AVSEA. An HIC of 100 is a suitable value to normal operation of a machine physically interacting with humans. The model parameters for AVSEA are: Maximum $K_{transm} = 3000 \text{ kN/m}$ (Equivalent to rigid joint stiffness), Minimum $K_{transm} = 0.95 \text{ kN/m}$, $\gamma = 3000 \text{ kN/m}$, $K_{cov} = 25 \text{ kN/m}$, $M_{oper} = 4 \text{ kg}$, $M_{roor} = 0.7 \text{ kg}$ and $M_{link} = 0.5 \text{ kg}$.

5.5. Summary

In this chapter, an active variable stiffness elastic actuator that is designed and application to safe physical human robot interaction was presented. By changing the effective length of the leaf spring, the AVSEA has the ability to minimize large impact forces due to shocks, to safely interact with the user and/or to become as stiff as possible to make precise position movements or trajectory tracking control easier. The preliminary results obtained from these experiments show that the AVSEA has the capability to interact with people or unknown environments under safety constraints by passive compliance.

CHAPTER 6. ADEA—ACTIVE VARIABLE STIFFNESS DIFFERENTIAL ELASTIC ACTUATOR : DESIGN AND APPLICATION FOR SAFE ROBOTICS

This chapter presents an Active Variable Stiffness Differential Elastic Actuator (ADEA) which is designed and application to robotic systems and more generally for machines that are designed to interact with people and environments under safety constraints. The ADEA consists of two DC-motors to drive two antagonistic worm gears independently. By changing the synchronisation and differentiation of angle displacement of these two antagonistic worm gears, ADEA has the capacity to minimize large impact forces due to shocks, to safely interact with the user or become as stiff as possible to make precise position movements. Besides, the ADEA can achieve fast motion control while guaranteeing safety of human operators in worst-case impact situation because of the stiffness of ADEA is variable dynamically. Experimental results are presented to show performance and safety of a one-link arm actuated by the ADEA.

6.1. Introduction

The major objective of this dissertation is to present an Active Variable Stiffness Differential Elastic Actuator (ADEA) that is designed and application to safe physical human robot interaction, as shown in Figure 6-1. It discusses in detail the ADEA mechanism, performance, properties, and functions. This chapter is structured as follows: Section 6.2 presents the general idea of ADEA. In Section 6.3, the mechanical design, working principle, and modeling of the ADEA are described. Section 6.4 presents experiment results to demonstrate and evaluate the performance and characteristics of ADEA. Finally, the summary are made in Section 6.5.

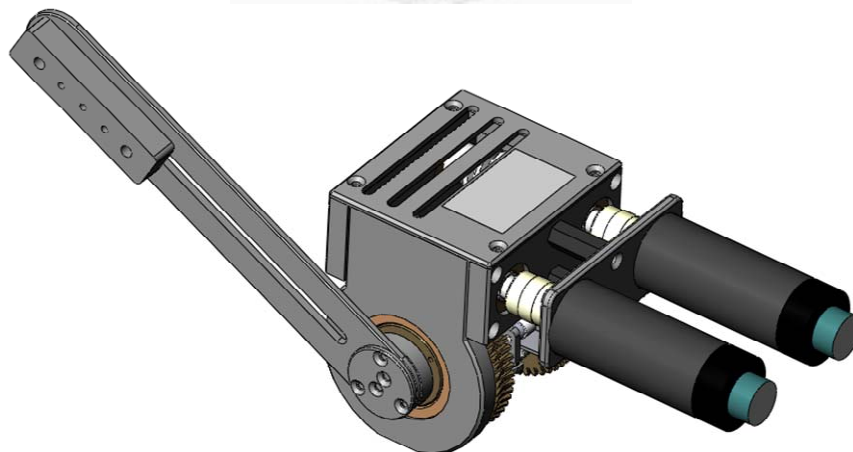


Figure 6-1 The Active Variable Stiffness Differential Elastic Actuator (ADEA)

6.2. General Idea of the Active Variable Stiffness

Differential Elastic Actuator (ADEA)

6.2.1. Active Variable Stiffness Element — Leaf spring

The design of an active variable stiffness serial configuration can be expressed by the series combination. In order to explain the properties of the active variable stiffness serial configuration, a simple beam system is used, as shown in Figure 6-2.

P is concentrated load, L is the length of the beam, E is modulus of elasticity (Young's modulus) and I is moment of inertia. The deflection at end point of the beam (δ_b) is given.

$$\delta_B = \frac{PL^3}{3EI} \quad (6-1)$$

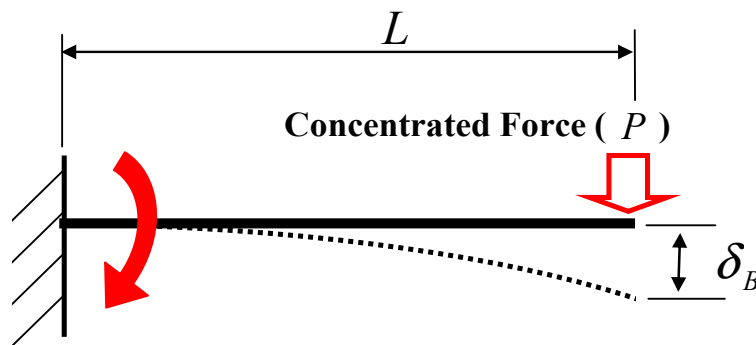


Figure 6-2 The Concept of a Beam System.

From Eq. (6-1), with the same concentrated load (P), the deflection at the end point of the beam (δ_B) is changed by the length of the beam (L). In order to explain the properties of the active variable stiffness serial configuration, a simple beam system is used.

6.2.2. Mathematical Description of the Active Variable Stiffness Differential Elastic Actuator (ADEA)

In this dissertation, a leaf spring is used instead of the beam, and to obtain the ability to control the deflection at the end point of leaf spring, an active variable stiffness differential elastic actuator is designed. In this section, the conception of a four bar linkage is mentioned, as shown in Figure 6-3(a). In the four bar linkage system, the point A and point B are two connect points, and slides on the axis 01 and axis 02. The movement distance of point B (L_b) is equal to the movement distance of point A (L_a) because of the four bar linkage mechanical structure, as shown in Figure 6-3(b). Therefore, the position of the point B can be controlled by the position of the point A. In order to control the position of point A effectively, a symmetric roller system is mentioned in this dissertation. As shown in Figure 6-4(a), there are two rollers rotate coaxial, and these two rollers with a tangent independently, the tangents of two rollers are connected on the connect point. When the Roller01 rotates

counterclockwise direction with θ_1 and the Roller02 rotates clockwise direction with θ_2 , the connect point of the symmetric roller system will move, as shown in Figure 6-4(b). Therefore, by controlling the angle movement of the two symmetric rollers, the system has ability to control position of the connect point.

The conception of the active variable stiffness differential elastic actuator (ADEA) is to combine these two important components (the four bar linkage system and the symmetric roller system). By changing the synchronisation and differentiation of angle displacement of these two symmetric rollers, ADEA has the ability to change the position of the point A. By changing the position of the point A, the ADEA has the ability to obtain an effective length for the leaf spring, and a change in the effective length of the leaf spring results in changing stiffness.

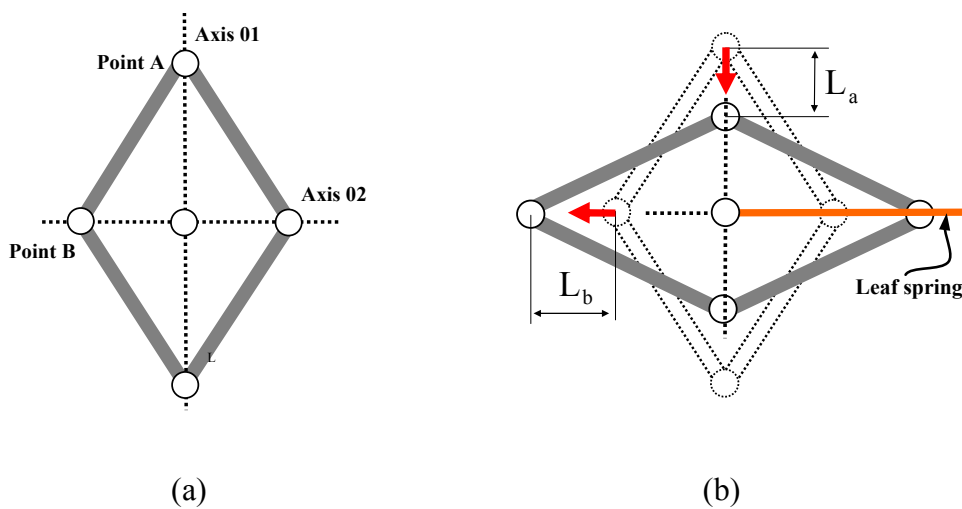


Figure 6-3 The four bar linkage system of the ADEA.

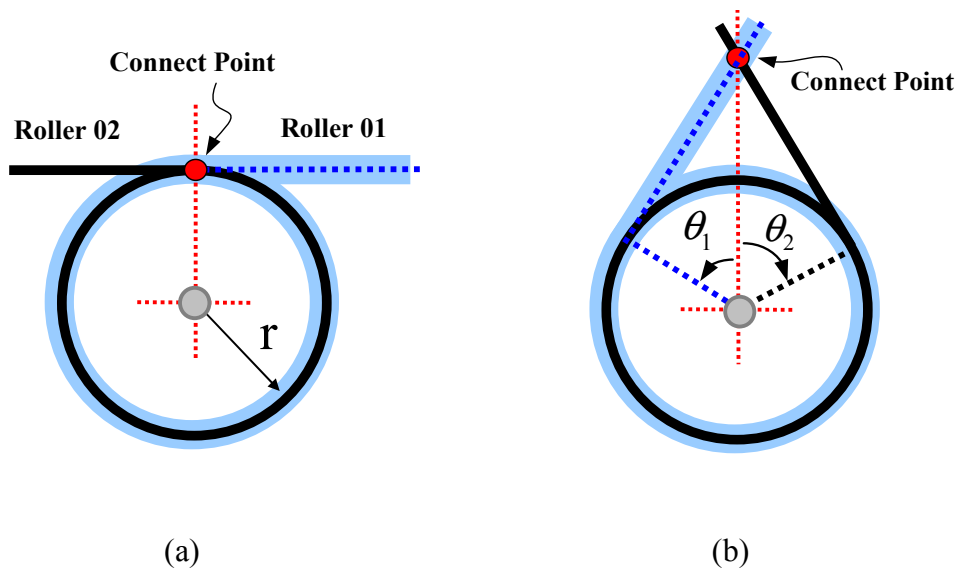


Figure 6-4 The symmetric roller system of the ADEA.

6.3. Design, Working Principle and Modeling of the ADEA

The main idea of this dissertation is to design a mechanism that the angle displacement and the stiffness are controlled dynamically. To reduce design complexity and size of the organization, one possible design is the Active Variable Stiffness Differential Elastic Actuator (ADEA) which with two actuators. In this section the detail structure, working principle, and modeling of the ADEA are described.

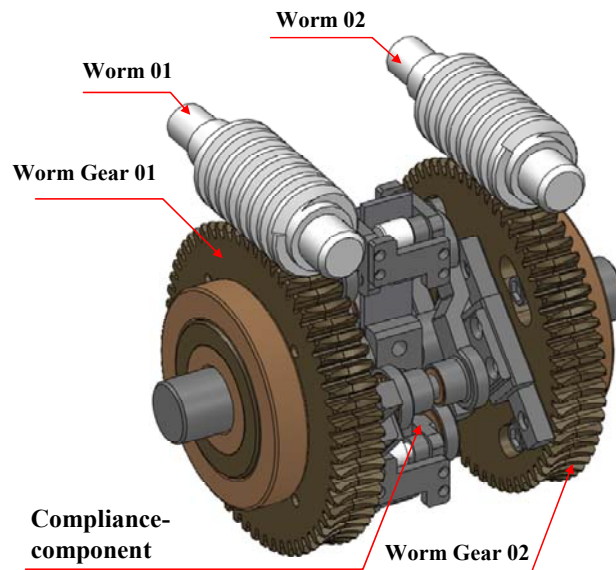
6.3.1. Mechanical Design and Working Principle

As shown in Figure 6-5(a), an Active Variable Stiffness Differential Elastic Actuator (ADEA) with two actuators and leaf springs is designed to obtain two abilities of ADEA; movability and compatibility. In this design, two DC-motors (power input) are connected with two worm-worm gear systems independently

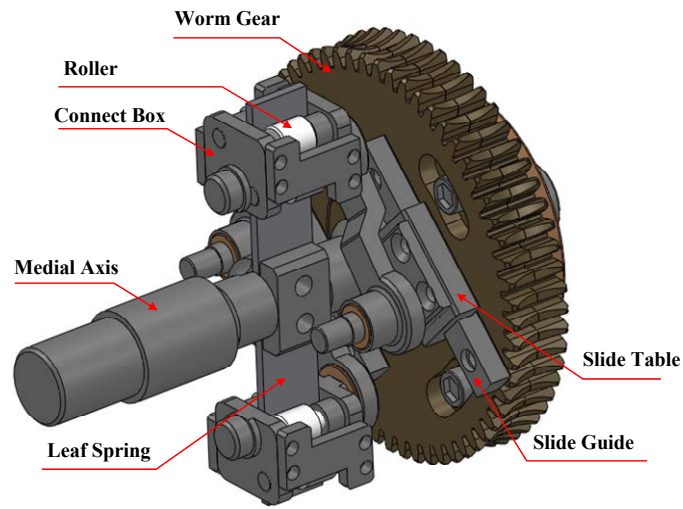
6.3 DESIGN, WORKING PRINCIPLE AND MODELING OF THE ADEA

(worm-worm gear 01, worm-worm gear 02). There is a compliance component between these two antagonistic worm-worm gear systems. In this compliance component, two leaf springs are fixed on and around the media axis at equiangular distance, as shown in Figure 6-5(b). A connect box, combines with several rollers, connects and slides on the leaf spring. By the slide guide, slide table, and support stick, the angel displacement differential of two warm gears is used to define the effect long of leaf spring. By change of the effective length of leaf springs results in changing stiffness of ADEA.

An output link is connected with the medial axis and an encoder is fixed on the rotation joint of ADEA to measure the angle displacement. On the other side of ADEA, a potential meter is fixed and connected between medial axis and warm gear to measure the angle differentia of these two components, as shown in Figure 6-6.



(a)



(b)

Figure 6-5 The detail structure of the ADEA.

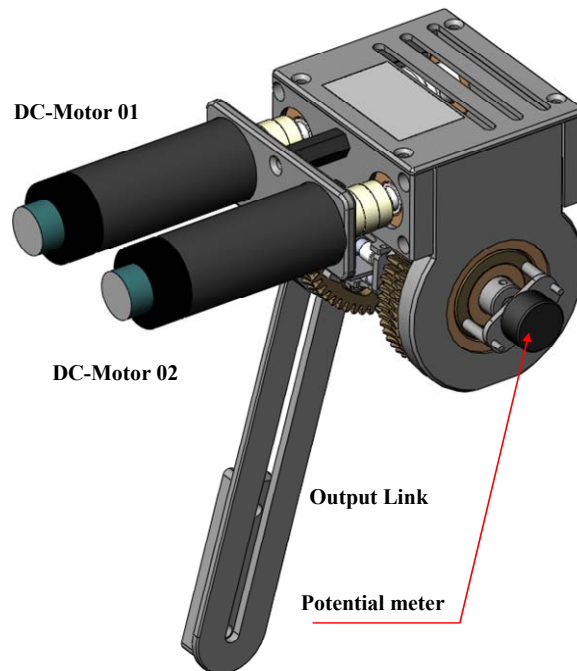


Figure 6-6 3D model of the ADEA.

6.3.2. Mechanism Modeling of the ADEA System

In this dissertation, we assume that the force measurement bandwidth is much higher than the response bandwidth of the actuators, and this is not included in the dynamic model. Considering the force and power density of the actuators through the transmission mechanism ^{$N(\geq 1)$} , the proposed ADEA model contains a reduction device model to evaluate the reduction effect. Furthermore, to obtain a concise model, the equivalent transmission stiffness K_t is used instead of a specified stiffness in the following analysis. The actuator can be modeled using lumped elements. A simplified ADEA model is shown in Figure 6-7. The dynamics of ADEA are further derived below.

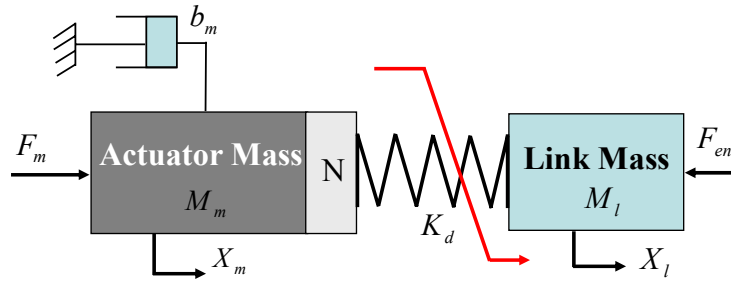


Figure 6-7 A Simplified ADEA Model.

the force on the actuator mass:

$$M_m \ddot{X}_m = -\frac{k_d}{N} \left(\frac{X_m}{N} - X_l \right) - b_m \dot{X}_m + F_m \quad (6-2)$$

the force on the link mass:

$$M_l \ddot{X}_l = k_d \left(\frac{X_m}{N} - X_l \right) - F_{en} \quad (6-3)$$

taking the Laplace transform of Eq. (6-2), (6-3), the transfer function between the two inputs, F_m and F_{en} and the output displacement X_l can be gained, as in the following equation:

$$X_l = \frac{NK_d F_m}{\Delta(s)} - \frac{(M_m N^2 s^2 + b_m N^2 s + k_d) F_{en}}{\Delta(s)} \quad (6-4)$$

where the characteristic equation is

$$\Delta(s) = M_l M_m N^2 s^4 + M_l b_m N^2 s^3 + k_d (M_l + M_m N^2) s^2 + k_d b_m N^2 s \quad (6-5)$$

specifically, the above equation shows that the ADEA is a linear fourth-order system, and two inputs are independent of each other.

6.3.3. Analysis of the ADEA System

As $F_{en} = 0$, the output link moves freely and is driven by the actuator force only, and relating to a changing input, an actuator force, the transform function between the input force actuator force, the transform function between the input force and the output displacement X_l can be shown as follows:

$$\frac{X_l}{F_m} = \frac{-NK_d}{M_l M_m N^2 s^4 + M_l b_m N^2 s^3 + k_d (M_l + M_m N^2) s^2 + k_d b_m N^2 s} \quad (6-6)$$

in Figure 6-8, the bode plot gained by simulation and Eq. (6-6), shows that the

stiffness and reduction ratio affect the bandwidth of the output environmental force. For example, the stiff transmission may permit the system to inherently own quicker responses than the soft one does, and the high reduction may increase the system capacity of the output force responses in the low frequency domain, whereas it may decrease the system capacity of the output force responses in the high frequency domain.

What is more, the output impedance, a measure of how well the system responds to external disturbances and an important factor concerning the physical human-robot interaction (pHRI), can allow one to investigate effects of any environmental force applied to the output link by assuming the actuator input force is equal to zero, namely $F_m = 0$. Then, the output impedance between the environmental force and output displacement is as follows:

$$Z_m = \frac{F_{en}}{V_l} \quad (6-7)$$

$$Z_m = \frac{-[M_l M_m N^2 s^3 + M_l b_m N^2 s^2 + k_d (M_l + M_m N^2) s + k_d b_m N^2]}{M_m N^2 s^2 + b_m N^2 s + k_d} \quad (6-8)$$

In Figure 6-9, the bode plot gained by simulation and Eq. (6-8), shows that the output impedance of the system can be reduced by intentionally decreasing the stiffness of the elastic component to be under the level safe for human-robot interaction. Clearly, transmission stiffness under the safety constraint ensures that the system will never create an unacceptable impact, even over the controllable frequency

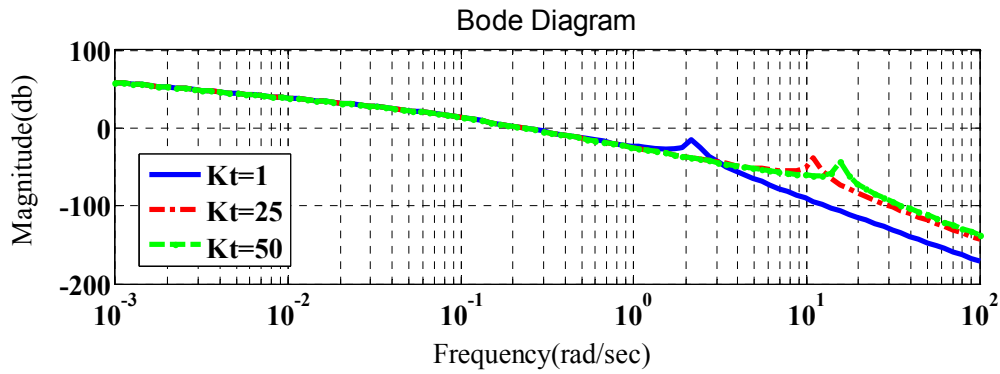


Figure 6-8 Simulation Frequency Response with End Free.

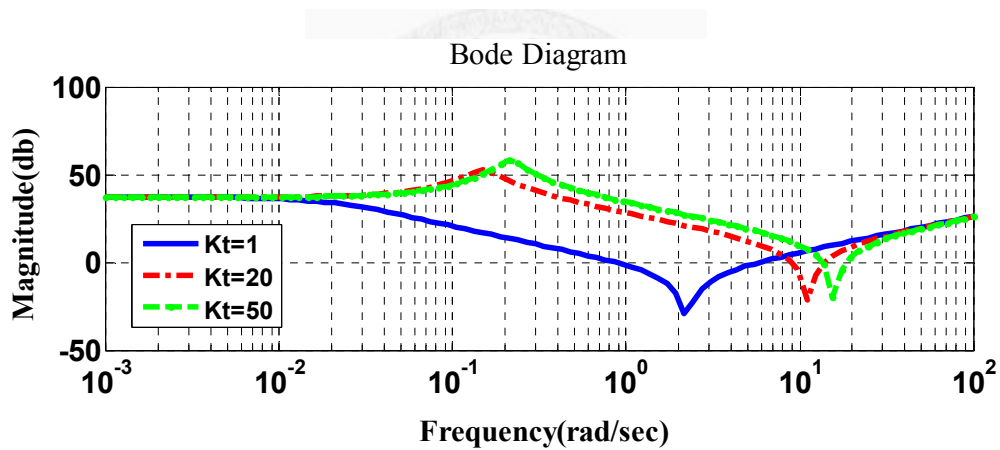


Figure 6-9 Simulation Frequency Response without any Actuator Force.

6.4. System Experiment Evaluation

In this section, experiments were conducted to evaluate the properties and abilities of the Active Variable Stiffness Differential Elastic Actuator (ADEA). Figure 6-10 is the picture of the ADEA which consists of two DC-motors. The rotation of the axis is measured by an encoder which is fixed on the output link. Dimensions of the

ADEA, design parameters and some detailed specification are listed in the Table 6-1.

Table 6-1 Specification of the ADEA

PARAMETERS	Value
Weight (without two motors)	0.95 kg
Length*Width*Height	64*70*85 mm
Motion Space	$\pm 360^\circ$
Max. Speed	600°/s
Max. allowable Torque	20.2 Nm
Max. continuous Torque	3.08 Nm
Max. Deflection	$\pm 30^\circ$
Max. Stiffness	Equivalent to rigid joint stiffness
Min. Stiffness	0.085Nm/deg
Leaf spring (thickness* width)	1.2*10 mm

* The input motors used in this prototype design are Faulhaber DC-micromotor 3257W024CR.

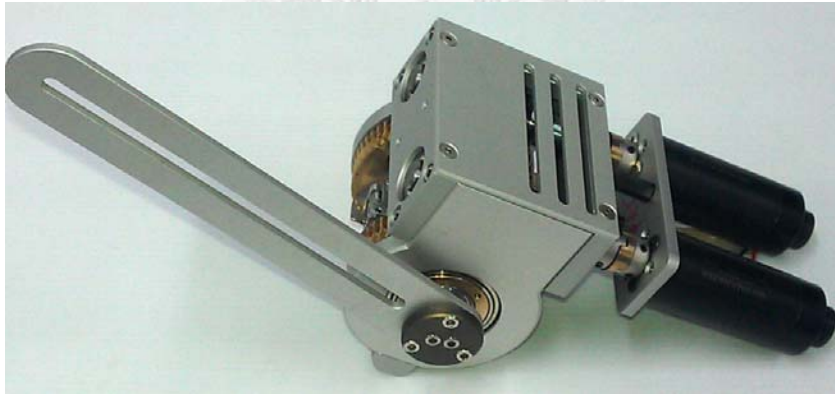


Figure 6-10 Active Variable Stiffness Differential Elastic Actuator (ADEA).

6.4.1. Adaptive Compliant Property of ADEA

An experiment was designed to interpret the adaptive compliant property of the

ADEA. The experiment comprises four stages. First, by using a simple PID controller, the output link of the ADEA was rotated and kept in a vertical direction. Second, the output link of ADEA was manually deflected in a counterclockwise direction away from the 0° (equilibrium point) with the situation whereby the motor was still working. Third, the output link was deflected in a clockwise direction. Fourth, the link was released. As shown in Figure 6-11, the result is a plot of the angle with time and the photograph shows the beginning and finishing position of the ADEA.

The experiment shows that an adaptive compliant configuration was used to make the interaction between robots and humans safer and more natural and that ADEA has the ability to interact with people or unknown environments under safety constraints by an adaptive compliance configuration.

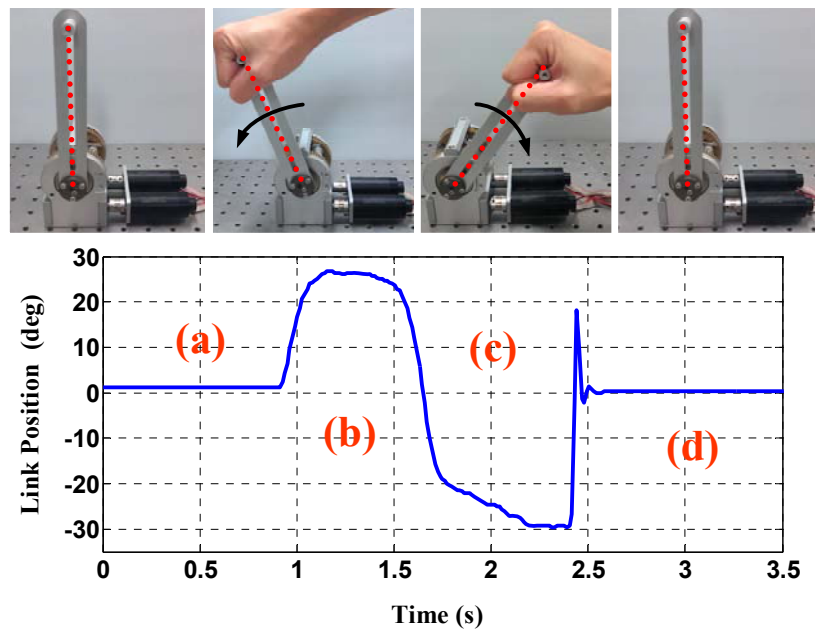


Figure 6-11 Adaptive compliant property for the ADEA.

6.4.2. Active Variable Stiffness Property of ADEA

By changing the effective length of leaf spring, the ADEA is able to vary the stiffness. In this experiment, a force sensor is used to measure the external force at the end-point of the output link and an encoder is used to measure the angular deflection of the output link. As shown in Figure 6-12, L is the effective length of leaf spring. The stiffness of the ADEA is changed with the effective length of leaf spring.

6.4.3. Response to Position Command with Variable Stiffness

The step response of the designed ADEA system with different length of leaf

spring (maximum and minimum) is given in Figure 6-13. The position of the ADEA changes from 0° to 30° by using a simple PID controller; the result is a plot of the angle with time. As shown in Figure 6-13, when the length of the leaf spring of the ADEA is maximum (stiffness is minimum), vibration due to the position command over 0.72 sec and the actuator is at a 4.5° angle offset because of the gravity, the precise position movement ability is worse. If the length of the leaf spring of the ADEA is minimum (stiffness is maximum), vibration does not occur, and the ADEA has good precise position movements. The experiment shows that the ADEA has the ability to obtain different stiffness by changing the length of the leaf spring of the ADEA, and the ADEA with maximum stiffness shows better response than the ADEA with minimum.

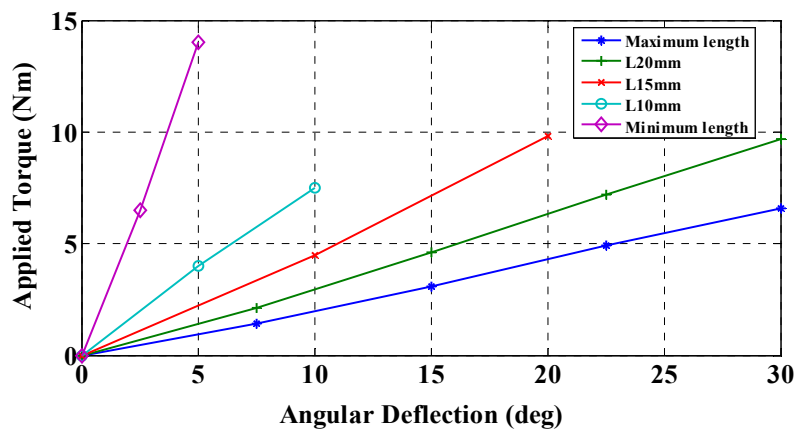


Figure 6-12 Measure stiffness of the ADEA.

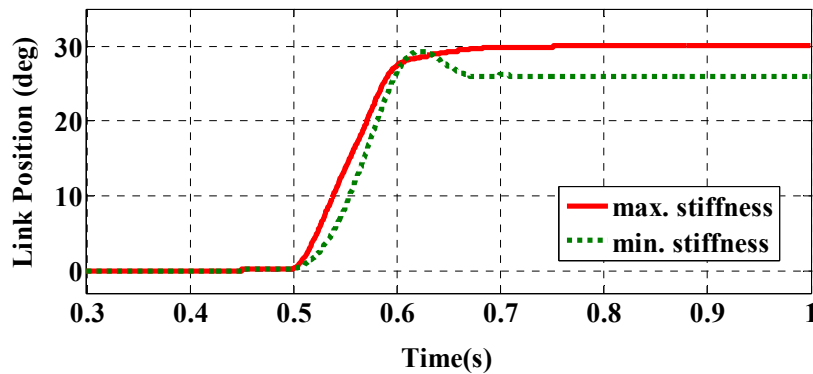


Figure 6-13 Response to position command with variable stiffness.

6.4.4. Head Injury Criterion (HIC)

For a typical robot, the margin available for designing to satisfy both safety and performance requirements is the intersection of the ranges of tip-velocity and payload values of acceptable designs. Since the tip-velocity and payload values determine how to design a safe robot, several safety criteria based on these two factors have been developed. For example, to represent human safety associated with the dynamic collision, the HIC, quantitatively measuring head injury risks in car crash situations, was used to evaluate the tolerant level of human-robot impact in many researches. HIC value equal to or greater than 1000 is typically associated with extremely severe head injury. The value less than 100 is considered suitable for normal operation of a machine physically interacting with humans. The HIC for compliant manipulators and

the acceptable velocity under the safety constraint can be written as:

$$v_{\max} = \left[\frac{HIC_{\max}}{2 \left(\frac{2}{\pi}\right)^2 \left(\frac{K_{\text{cov}}}{M_{\text{oper}}}\right)^{\frac{3}{4}} \left(\frac{M_{\text{rob}}(K_{\text{transm}})}{M_{\text{rob}}(K_{\text{transm}}) + M_{\text{oper}}}\right)^{\frac{7}{4}}} \right]^{\frac{2}{5}} \quad (6.9)$$

Where the maximum tolerant max HIC can be chosen less than 100, a suitable value for normal operation of a machine physically interacting with humans. As shown in Figure 6-14, we can see that when $v_{\max}=1\text{m/s}$, the HIC of ADEA is much better than the SEA.

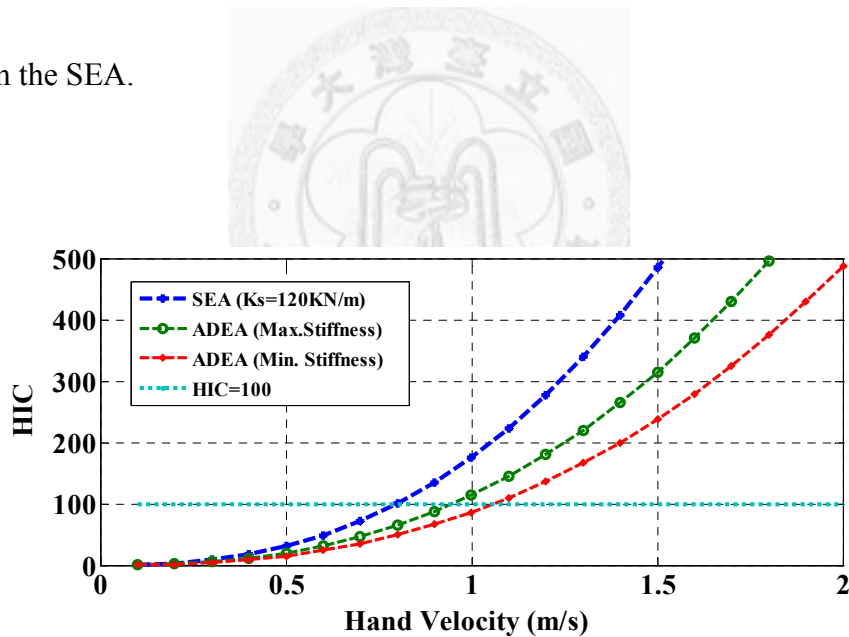


Figure 6-14 The head Injury Criterion (HIC) for SEA and ADEA. An HIC of 100 is a suitable value to normal operation of a machine physically interacting with humans. The model parameters for ADEA are: Maximum $K_{\text{transm}}=3000\text{kN/m}$ (Equivalent to rigid joint stiffness), Minimum $K_{\text{transm}}=0.95\text{kN/m}$, $\gamma=3000\text{kN/m}$, $K_{\text{cov}}=25\text{kN/m}$, $M_{\text{oper}}=4\text{kg}$, $M_{\text{rotor}}=0.7\text{kg}$ and $M_{\text{link}}=0.5\text{kg}$.

6.5. Summary

In this chapter, an Active Variable Stiffness Differential Elastic Actuator design and application to safe robotics is presented. By changing the synchronisation and differentiation of angle displacement of these two antagonistic worm gears, ADEA has the capacity to minimize large impact forces due to shocks, to safely interact with the user or become as stiff as possible to make precise position movements.



CHAPTER 7. APPLICATION : REHABILITATION SYSTEM

The chapter introduces an active variable stiffness exoskeleton robotic system (AVSER) with the active variable stiffness elastic actuator (AVSEA), which improves the safety *for* human-robot interaction and produces unique adjustable stiffness capacity to meet the demand for safe active-passive elbow rehabilitation. The AVSEA consists of two DC-motors: One is used to control the position of the joint, and the other is used to adjust the stiffness of the system. The stiffness is generated by a leaf spring. By shortening the effective length of the leaf spring, the AVSEA is able to reduce the stiffness automatically, which makes the AVSER from active (assistive) motion to passive (resistance) rehabilitation during the process of therapy. In the dissertation, the mechanical design, modeling, and control algorithms are described in details. The capacity of the proposed AVSER with electromyogram (EMG) signal feedback is verified by rehabilitation exercise experiments for a subject to demonstrate the efficacy of the developed system.

7.1. Introduction

Rehabilitation robotics emerges from mechatronics as a focused effort to design rehabilitation systems, since successful motor rehabilitation of traumatic brain-injured, spinal cord-injured, and stroke patients usually require a task-specific therapy approach. In reality, budget constraints and therapist shortages limit a hand-to-hand therapy approach throughout the world. Thus, intelligent machines not only offer a good solution to promote motor recovery, but also provide a better understanding of motor control [82].

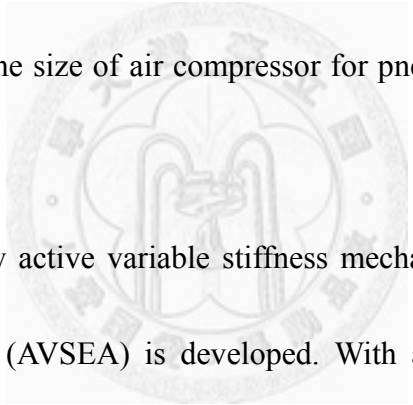
Achieving the intensive automatic treatment must employ manifold strategies, involving all aspects of the mechatronics system design, such as the mechanical, electrical, and control and software architectures. In general, two different kinds of rehabilitation robots, **active assistive robots** and **passive constrained robots** are developed as successful rehabilitation tools. An active assistive robot serves as a force source, transmitting power to a body segment to actively guide a patient passively following the desired rehabilitative motions. Assistive robots in [83]-[89], prosthetic devices in [90]-[92] and even exoskeletons in [93]-[96] fall into this category. On the other hand, a passive constrained robot serves as a passive constraint. The robot can actively change preset constraints of a patient's motions to allow the patient to move

spontaneously according to the given motion pattern of the passive treatment. The devices and robots proposed in [97][98] are passive constrained robots. Determining to utilize what kind of robots to improve motor capacity depends upon quantitative evaluation of different rehabilitation training for different patients. For instance, in the early stages of therapy, passive rehabilitation is often the preferred method for reducing swelling, alleviating pain, and restoring range of motion [99].

Up to now, most of robotic systems, consisting of rigid components, are heavy, fast, strong and powerful. Most of them are without any capacity for interaction with humans under safe constraints. In order to work, cooperate, assist, and interact with human, the new generation of safe robot systems have been devised to efficiently build a robot with intrinsically safe robot actuation, such as series elastic actuators (SEA) [83][100] or Safe joint mechanism (SJM) [79][80][81][101][102]. However, the safe robot actuator, SEA, SJM cannot generate a desired stiffness to satisfy specified tasks in advance. In order to obtain the ideal stiffness to satisfy the functions of human-robot interaction, active variable stiffness actuators used a variable stiffness transmission mechanism to active vary mechanical stiffness of the given system were proposed. The active variable stiffness actuators can be classified into several groups.

(1) Antagonistic actuation with nonlinear spring: two actuators connect same block

[56][103][104]. (2) Antagonistic actuation using a pneumatic artificial muscle [105]–[108]. (3) Serial actuation: most implementations used two actuators to control the position and stiffness of the joint [109]–[112]. (4) Serial actuation with leaf springs: leaf springs were also used to vary mechanical stiffness [53]–[57][113]. Although, these active variable stiffness actuator are advantageous to dexterous manipulation and their compliant component is good for collection safety. However, for antagonistic actuation, the control theory for two antagonistic motors move synchronous is complex, the size of air compressor for pneumatic artificial muscle is huge.



In this chapter, a new active variable stiffness mechanism, the Active Variable Stiffness Elastic Actuator (AVSEA) is developed. With a special AVSEA actuator design, the particular Active Variable Stiffness Exoskeleton Robot (AVSER) system is applied to safe active-passive elbow rehabilitation, as shown in Figure 7-1. The AVSER is defined as a robotic system using the concept of the AVSEA. Herein, the AVSER is designed and applied to elbow rehabilitation to generate either directly positive actuation force to guide the human user or indirectly negative resistive force to resist the human user to achieve versatile desired motion patterns.

To sum up, the AVSER has the following characteristics and advantages:

- Energy efficiency: The leaf spring structure of the AVSEA has solved the energy waste problem because of dispensable dynamic adjustment.
- Functional: The AVSER has elastic elements and functions of variable stiffness to meet the demand for safe active-passive elbow rehabilitation.
- Safety: The elastic elements are used to improve the safety and *security for* human-robot interaction. Beside, the bounded joint limited and the emergency stop are used to prevent an abnormal or uncomfortable elbow rehabilitation.
- Cheap: With the AVSER, the torque/force sensor can be replaced with a potential meter to lower costs.
- Portable: The *convenient AVSER* is *small enough to carry* easily.
- Convenient: The complete rehabilitation robot system (with computer user interface, control system, AVSER) is developed for users to set it up and use it more conveniently.

The chapter is organized as follows. Section 7.2 presents an overview of the AVSER. The AVSEA, its properties, and the design topology are introduced in Section 7.3. The design and principle of the proposed AVSER based on the Active Variable Stiffness Elastic Actuator (AVSEA) is addressed in Section 7.4. Experiments

are provided to demonstrate that the proposed AVSER can provide different rehabilitation exercises. The results are given in Section 7.5. Finally, the summary are made in Section 7.6.

7.2. New Rehabilitation Robot System—Active Variable Stiffness Exoskeleton Robot (AVSER)

As a possible application, an AVSER using an Active Variable Stiffness Elastic Actuator (AVSEA) provides an adjustable stiffness capacity to execute the particular tasks for active-passive elbow rehabilitation.

Considering that EMG signals of human muscles are crucial to understanding a patient's intention of movement, this AVSER is also integrated with EMG signal feedback capacity. This signal feedback can be used as important information to investigate the patient's muscle condition with other quantity signal feedback for the control system to generate suitable training strategies, whereas we only use EMG signals to allow occupational therapists to investigate the muscle condition with other feedback signals in this work. Anyhow, we use two encoders, one linear potentiometer, and two active electrodes as the feedback sensors for the AVSEA; that is to say, two encoders are used to measure the motor angle and the elbow angle; the linear

7.2 NEW REHABILITATION ROBOT SYSTEM—ACTIVE VARIABLE STIFFNESS EXOSKELETON ROBOT (AVSER)

potentiometer is used to measure the deflection of linear springs; two active electrodes are used to measure EMG signals. The overall Rehabilitation Robot System using AVSER is shown in Figure 7-2.

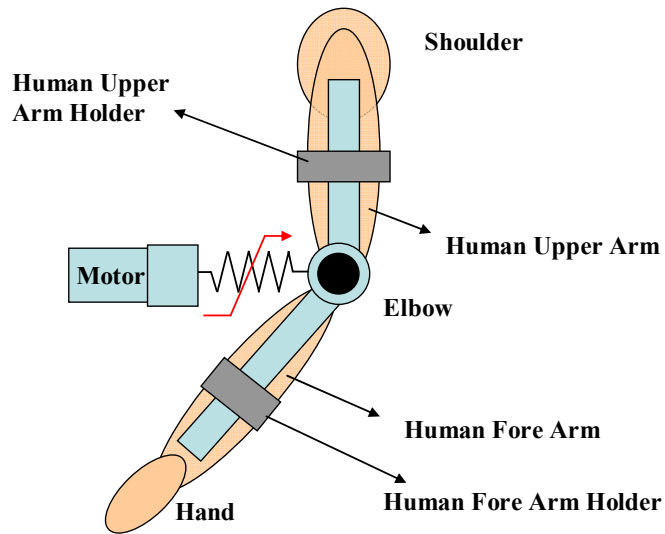


Figure 7-1 The Active Variable Stiffness Exoskeleton Robot System

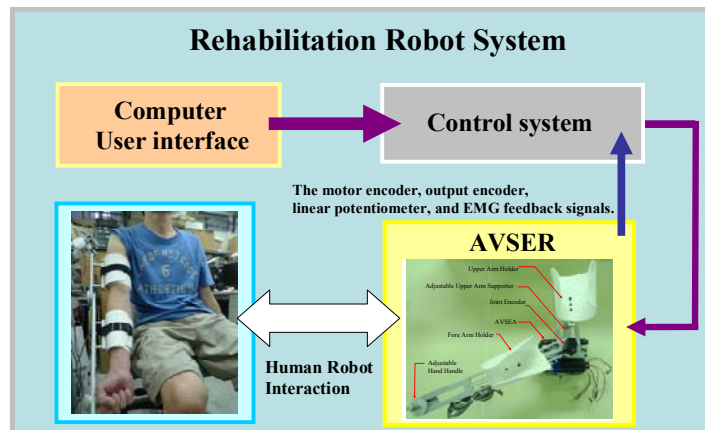
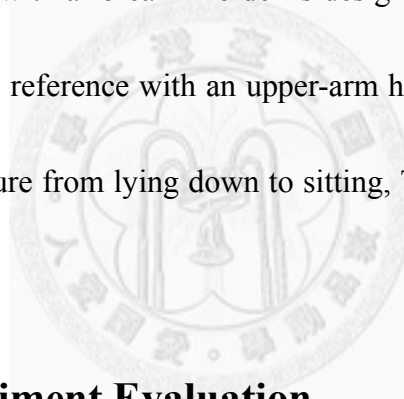


Figure 7-2 Rehabilitation Robot System

7.3. Principle and Design of the Active Variable Stiffness

Elastic Exoskeleton Robot (AVSER)

Based on the results in the previous section, an Active Variable Stiffness Elastic Actuator (AVSEA) is built the 3D model of AVSEA is shown in Figure 7-3. And design, modeling, and analysis of the AVSER (AVSEA with exoskeleton structure) are also explained in this section. In order to satisfy individual needs of the elbow rehabilitation, a level arm with a forearm holder is designed to move with a subject's forearm, and an adjustable reference with an upper-arm holder is designed to allow a subject to change the posture from lying down to sitting, The 3D model of AVSER is shown in Figure 7-4.



7.4. System Experiment Evaluation

In this section, experiments were conducted to evaluate the properties and abilities of the Active Variable Stiffness Exoskeleton Robot System (AVSER), as shown in Figure 7-5. The rotation of the axis is measured by an encoder which is fixed on the output link. The dimensions of the AVSER, design parameters and some detailed specification are listed in the Table 7-1. In the following experiments, EMG signals from two muscles, the biceps and triceps, were measured from a 34-year-old subject. Active surface electrodes were placed on the biceps and triceps by an

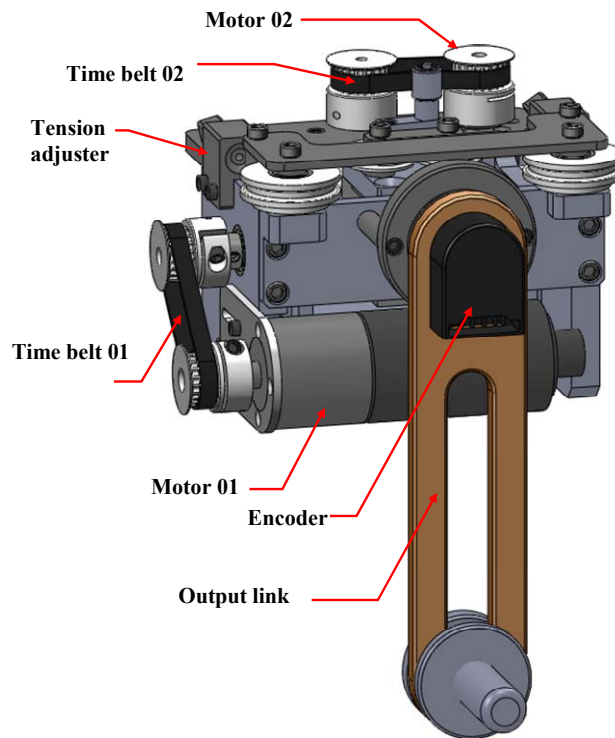


Figure 7-3 3D model of AVSEA

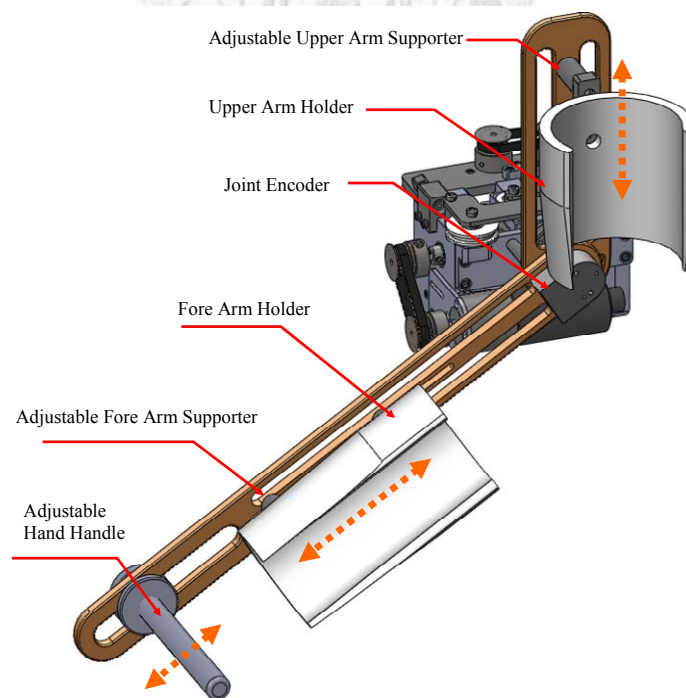


Figure 7-4 3D model of AVSER.

occupational therapist. Those data were sampled at 8000 Hz by a sbRIO-9642 and filtered with a band-pass fourth-order Butterworth filter in which the low cutoff frequency is 100 Hz and the high cutoff frequency is 1000 Hz. The Rehabilitation exercise setup as shown in Figure 7-6.

AVSER demonstrated its capacity of realizing different rehabilitation exercises. Four kinds of rehabilitation exercise modes—(a)Active rehabilitation, (b)Active-assistive rehabilitation, (c)Passive-resistance rehabilitation, and (d)Zero resistance—were examined, as shown in Figure 7-7.

Table 7-1 Specification of the AVSER

PARAMETERS	Value
Weight (without two motors)	0.95 kg
Length*Width*Height	64*70*85 mm
Motion Space	$\pm 360^\circ$
Max. Speed	600°/s
Max. allowable Torque	20.2 Nm
Max. continuous Torque	3.08 Nm
Max. Deflection	$\pm 30^\circ$
Max. Stiffness	Equivalent to rigid joint stiffness
Min. Stiffness	0.085Nm/deg
Leaf spring (thickness* width)	1.2*10 mm

* The input motors used in this prototype design are Faulhaber DC-micromotor 3257W024CR.

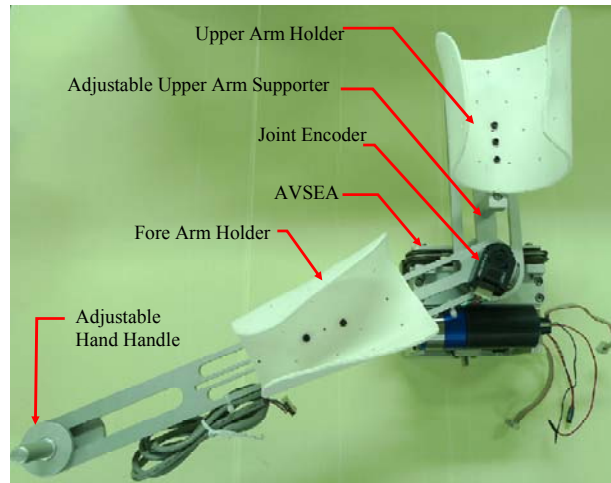


Figure 7-5 Active Variable Stiffness Exoskeleton Robot System (AVSER).

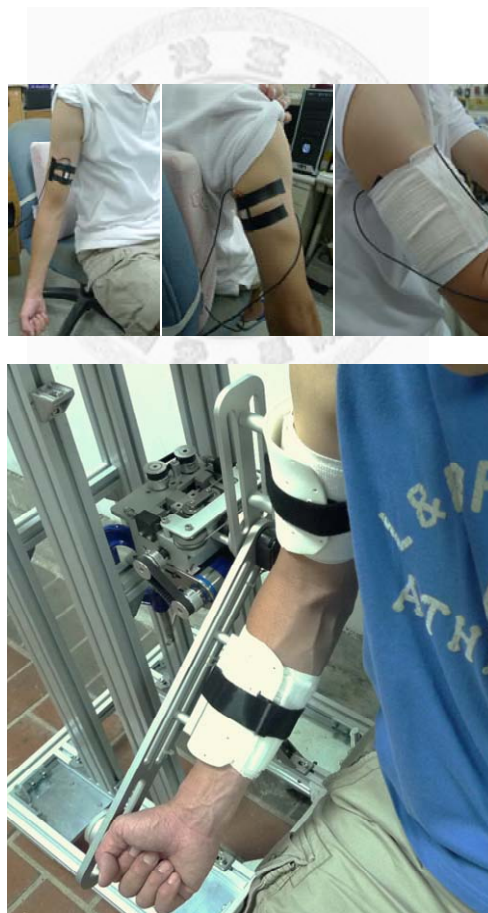


Figure 7-6 Rehabilitation exercise setup.

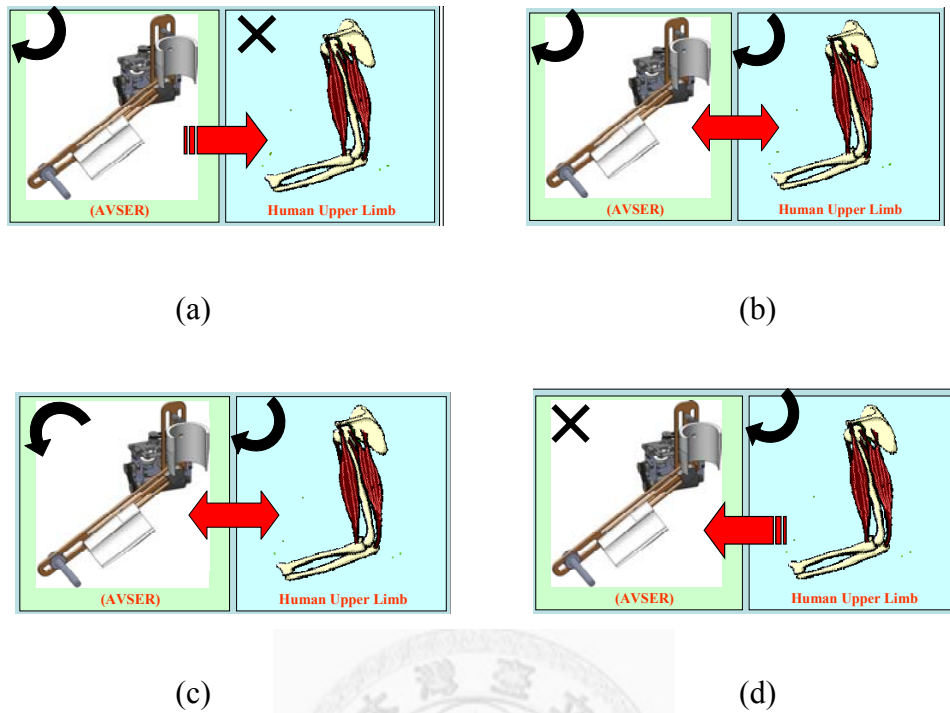


Figure 7-7 Active Variable Stiffness Exoskeleton Robot System (AVSER).

Experimental results of the elbow angle, assistive torque, resistance torque, and EMG signals from biceps and triceps during each test are shown in Figure 7-8.

Active Rehabilitation

Figure 7-8(a) shows that in the range-of-motion exercise mode and under joint position control, the muscles were relaxed and the EMG signals were flat. In this active training, the movement will be entirely induced by the AVSER and the subject will not exert any force.

Active-assistive Rehabilitation

Figure 7-8(b) shows that in active-assistive rehabilitation mode and under force control, the AVSER provided assistive torque in the same direction during the elbow flexion and the biceps relaxed. In reverse, this exercise mode can be seen as an interactive mode in that the subject can induce the movement himself without any side effects when the AVSER assists.

Passive-resistance Rehabilitation

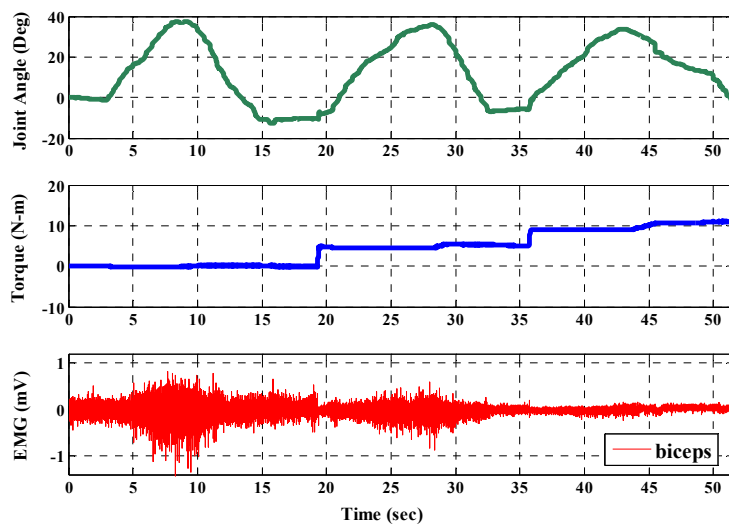
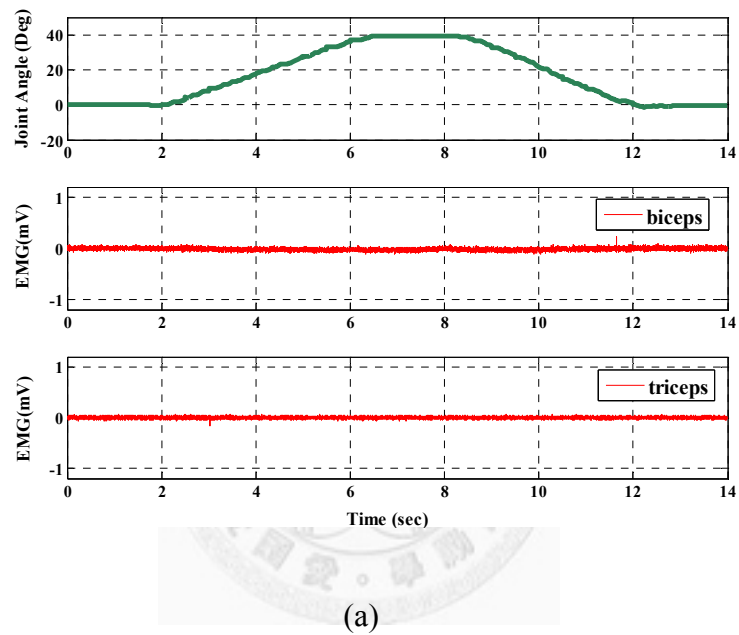
In passive-resistance rehabilitation mode and under force control, as shown in Figure 7-8(c), biceps contracted in the elbow flexion motion because of the direction of the set resistive torque. With the resistive torque, triceps will contract more in the elbow resistance rehabilitation motion. The results show that the AVSER can generate constant load torque while a subject spontaneously moves.

Zero resistance

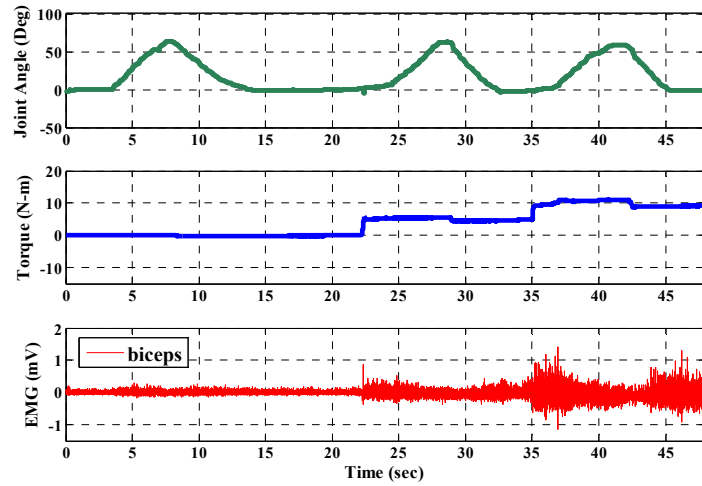
In zero resistance and under force control, as shown in Figure 7-8(d), the EMG signals of biceps was induced by the gravity component generated by the weight of the level arm and the subject.

In those experiments, EMG signals implying the subject's intention provide

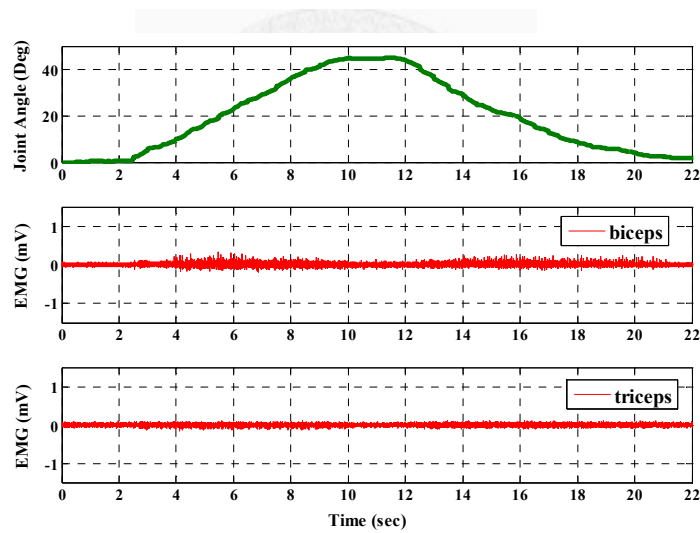
therapists a better understanding of the subject's motor condition, and can be used to modify the therapy with other information, like elbow angles, elbow torque, etc. It could be used to automatically provide physical therapy for different rehabilitation exercises in the future as well.



(b)



(c)



(d)

Figure 7-8 Experiment results of different rehabilitation exercise modes.

7.5. Summary

This chapter presents the rehabilitation system (AVSER) with the safety component (AVSEA). The working principle, construction, properties, and the

possible application to the AVSER were provided as well. The AVSER improves the safety *for* human-robot interaction and produces unique adjustable stiffness capacity to meet the demand for safe active-passive elbow rehabilitation. Compared with other rehabilitation systems, the proposed AVSER possesses several important advantages such as energy efficiency, safety, cheap, portable, and convenient. The experimental results show that the AVSER is capable of realizing different rehabilitation exercises.



CHAPTER 8. CONCLUSIONS AND FUTURE WORKS

8.1. Conclusions

This dissertation describes the development of an integrated humanoid robot arm system that can cooperate, assist, and even interact with humans in different fields and environments. Issues related to the safety level of human-robot interaction are also explored.

In the first part of the dissertation, a vertically-intersected DAMA is developed and applied to a 6-axis humanoid robot arm, without careful consideration of the safety level of human-robot interaction. The DAMA structure is refined using finite element analysis. Based on simulations with ADAMS and MATLAB software packages, the system's dynamic properties are observed. The hardware and software systems of the DAMA and the 6-axis humanoid robot arm are also developed. The experimental results show that for an S curve and circle trajectory input position command, the DAMA and the 6-axis humanoid robot arm can effectively track commands.

The second part of the dissertation discusses actuation design, ensuring an appropriate level of safety in human-robot interaction. It proposes a new approach to actuation, active variable stiffness elastic actuation, and discusses the design of several active variable stiffness elastic actuators (APVSEA, AVSEA, ADEA), arriving at a compromise between proper human-robot interaction safety and high manipulation performance. This part ends by describing another application to the active variable stiffness elastic actuators – the elbow rehabilitation system (AVSER).

The dissertation describes the invention of a prototype AVSER, with adjustable characteristics adaptable to unfamiliar environments, and explains how its application to the humanoid robot arm system allows for both safety and high performance.

8.2. Future Works

The efforts described in this dissertation allow for the design of a robot that looks and moves like a human being, and which can be used to help people. However, much work is still needed to allow for the building of a high-level humanoid robot, such as the development of a more functional AVSEA, and of a safer humanoid robot system design. In addition to the current applications to the AVSEA, rehabilitation systems and exoskeleton systems could be developed in the future.

8.2.1. Active Variable Stiffness Elastic Actuator

The AVSEAs which are mentioned in this dissertation are designed to control the position and the stiffness of the system with two motors, allowing them to interact with people and environments and comply with safety constraints. However, even with two motors, these AVSEAs still have several defects, such as overly high value, heaviness, expensiveness, and energy inefficiency. In the future, an AVSEA could be designed that offers the ability to control the system's position and stiffness independently, just using only one motor and power input. This new AVSEA would offer low value, energy efficiency, safety, affordability, and increased functionality.

8.2.2. Humanoid Robot System Design

This integrated humanoid robot system consists of rigid links, electrical servo actuators, tough covers, high-ratio reduction devices, and position sensors, making it hard for the robot to safely interact with people and environments and causing it to move slowly, through careful motion planning and multiple control strategies. Since an intrinsic safety actuator has already been invented, the next step to be taken is to integrate the actuator design into the multi-DOF humanoid robot arm design and determine the ideal use of active variable stiffness elastic actuation through experimentation.

8.2.3. Rehabilitation System

This dissertation presents the design of an AVSER, which improves the safety of human-robot interaction and produces a unique type of adjustable stiffness capacity that meets safe active-passive elbow rehabilitation demands. In the future, it is expected that a multi-axial rehabilitation system can be developed, as shown in Figure 8-1(a). A multi-axial rehabilitation system would offer elastic elements and variable stiffness functions, meeting demand for safe upper-limb rehabilitation, as shown in Figure 8-1(b).

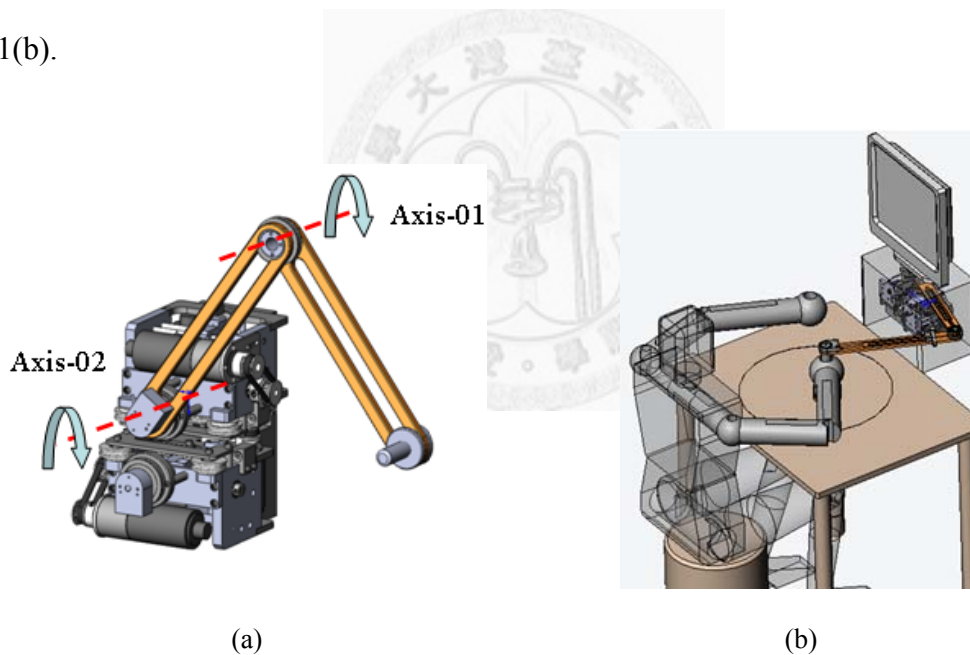


Figure 8-1 The multi-Axial rehabilitation system (a) 3D model of the system, (b) The system has elastic elements and functions of variable stiffness to meet the demand for safe upper limbs rehabilitation.

8.2.4. Exoskeleton System

The development of robots as mechanical workers that can support human labor and assist humans in their daily activities through means such as physical and

8.2 FUTURE WORKS

informational interaction, has been long anticipated. In the future, a prototype AVSEA could be developed that has adjustable characteristics made possible by a torque switch mechanism, which would allow it to adapt to applied input and output force. This AVSEA can used to develop an exoskeleton system for assisting humans in their daily activities.



REFERENCES

- [1] T. Fukuda and Y. Kawauchi, "Cellular robotic system(CEBOT) as one of the realization of self-organizing intelligent universal manipulator," *Proc. IEEE International Conference on Robotics and Automation*, University of Tsukuba, Japan, pp. 662-667. 1990.
- [2] M. Yim, "New locomotion gaits," *Proc. IEEE International Conference on Robotics and Automation*, San Diego, California, USA, pp. 2508-2514. 1994.
- [3] M. Yim, D.G. Duff and K.D. Roufas, "Polybot: a MODULAR reconfigurable robot," *Proc. IEEE International Conference on Robotics and Automation*, San Francisco, CA, USA, pp. 514-520. 2000.
- [4] G.J. Hamlin, and A.C. Sanderson, "Tetrobot: a modular system for hyper-redundant parallel robotics," *Proc. IEEE International Conference on Robotics and Automation*, Nagoya, Aichi, Japan, pp. 154-159. 1995.
- [5] H. Sawada, and S. Matunaga, "Dynamics and control of space robot brachiating motion using handrails," *Proc. IEEE/RSJ International Conference on Intelligent Robots and Systems*, Las Vegas, Nevada, pp. 3065-3070. 2003.
- [6] A. Brunete, J. E. Torres, M. Hernando and E. Gambao, "A 2 Dof servomotor-based module for pipe inspection modular micro-robots," *Proc. IEEE/RSJ International Conference on Intelligent Robots and Systems*, Beijing, China, pp. 1329-1334. 2006.
- [7] W.H. Zhu, T. Lamarche, and P. Barnard, "Modular robot manipulators with preloadable modules," *Proc. IEEE International Conference on Mechatronics and Automation*, Harbin, China, pp. 7-12. 2007.
- [8] A. Lyder, R.F.M. Garcia and K. Stoy, "Mechanical design of odin, an extendable heterogeneous deformable modular robot," *Proc. IEEE/RSJ International Conference on Intelligent Robots and Systems*, Acropolis convention center, Nice, France, pp. 883-888. 2008.
- [9] M.D.M. Kutzer, M. S. Moses, C. Y. Brown, D. H. Scheidt, G. S. Chirikjian and M. Armand, "Design of a new independently-mobile reconfigurable modular robot," *Proc. IEEE International Conference on Robotics and Automation*, Anchorage, Alaska, USA, pp. 2758-2764. 2010.
- [10] M.C. Gray, and D. Rus, "Self-reconfigurable molecule robots as 3D metamorphic robots," *Proc. IEEE/RSJ International Conference on Intelligent Robots and Systems*, Victoria, B. C., Canada, pp. 837-842. 1998.
- [11] H. Murata, A. Kamimura and S. Kokajiet, "Hardware design of modular robotic system," *Proc. IEEE/RSJ International Conference on Intelligent Robotics and*

- Systems*, Kagawa university, Takamatsu, Japan, pp. 2210-2217. 2000.
- [12] H. Bojinov, A. Casal and T. Hogg, "Multiagent control of self-reconfigurable robots," *Proc. 4th International Conference on Multi Agent Systems*, Boston, MA, USA, 143-150. 2000.
- [13] E. Yoshida, S. Murata, and A. Kamimura, "Evolutionary synthesis of dynamic motion and reconfiguration process for a modular robot M-TRAN," *Proc. IEEE International Conference on Computational Intelligence in Robotics and Automation*, Kobe Portopia Hotel, Kobe, Japan, pp. 1004-1012. 2003.
- [14] P. White and M. Yim, "Scalable modular self-reconfigurable robots using external actuation," *Proc. IEEE/RSJ International Conference on Intelligent Robotics and Systems*, San Diego, California, USA, pp. 2773-2778. 2007.
- [15] A. Sproewitz, M. Asadpour, Y. Bourquin and A. J. Ijspeert, "An active connection mechanism for modular self-reconfigurable robotic systems based on physical latching," *Proc. IEEE International Conference on Robotics and Automation*, Pasadena, California, USA, pp. 3508-3513. 2008.
- [16] A. Sproewitz, A. Billard, P. Dillenbourg and A. T. Ijspeert, "Roombots-mechanical design of self-reconfiguring modular robots for adaptive furniture," *Proc. IEEE International Conference on Robotics and Automation*, Kobe, Japan, pp. 4259-4264. 2009.
- [17] K. Kaneko, F. Kanehiro, S. Kajita, K. Yokoyama, K. Akachi, T. Kawasaki, S. Ota and T. Isozumi, "Design of prototype humanoid robotics platform for HRP," *Proc. IEEE/RSJ International Conference on Intelligent Robots and Systems*, Lausanne, Switzerland, Vol.3, pp. 2431-2436. 2002.
- [18] Q. Liu, Q. Huang, W. Zhang, X. Wang and C. Wu, "Manipulation of a humanoid robot by teleoperation," *Proc. 5th World Congress on Intelligent Control and Automation*, Hangzhou, China, pp. 4894-4898. 2004.
- [19] I. W. Park, J. Y. Kim, J. Lee and J. H. Oh, "Mechanical design of humanoid robot platform KHR-3(KAIST) humanoid robot-3: HUBO," *Proc. IEEE-RAS International Conference on Humanoid Robots*, Tsukuba, Japan, pp. 321-326. 2005.
- [20] S. Kim, CH. Kim and J. H. Park, "Human-like arm motion generation for humanoid robots using motion capture Database," *Proc. IEEE/RSJ International Conference on Intelligent Robots and Systems*, Beijing, China, pp. 3486-3491. 2006.
- [21] D. Jia, Q. Huang, W. Zhang, H. Xin, Z. Yu and K. Li, "Mechanical design of a light weight and high stiffness arm for humanoids," *Proc. 9th IEEE-RAS International Conference on Human Robots*, Paris, France, pp. 337-342. 2009.

- [22] Z. Yu, Q. Huang, J. Li, Q. Shi, X. Chen and K. Li, "Distributed control system for a humanoid robot," *Proc. IEEE International Conference on Mechatronics and Automation*, Harbin, China, pp. 1166 – 1171. 2007.
- [23] Q. Liu, X. Tang and J. Zhou, "Delay and stability analysis of networked robot system," *Proc. IEEE International Conference on Control and Automation*, Guangzhou, China, pp.2903 – 2906. 2007.
- [24] C. L. Lai, P.L. Hsu, B. C. Wang, "Design of the adaptive smith predictor for the time-varying network control system," *Proc. SICE Annual Conference*, The University Electro-Communication, Japan, pp. 2933 – 2938. 2008.
- [25] A. L. Edsinger "Robot manipulation in human environments," *Doctoral Dissertation*, Department of Electrical Engineering and Computer Science, Massachusetts Institute of Technology, 2007.
- [26] A. De Luca, A. Albu-Schaffer, S. Haddadin, and G. Hirzinger, "Collision detection and safe reaction with the DLR-III lightweight manipulator arm," *Proc. IEEE/RSJ International Conference on Intelligent and Systems*, Beijing, China, pp. 1623-1630, 2006.
- [27] M. Lauria, M.-A. Legault, M.-A. Lavoie, and F. Michaud, "High performance differential elastic actuator for robotic interaction tasks," *Proc. AAAI Spring Symposium-Multidisciplinary Collaboration for Socially Assistive Robotics*, Stanford University, CA, USA, vol. SS-07-07, pp. 39-41, 2007.
- [28] D. W. Robinson, J. E. Pratt, D. J. Paluska, and G. A. Pratt, "Series elastic actuator development for a biomimetic walking robot," *Proc. IEEE/ASME International Conference on Advanced Intelligent Mechatronics*, Atlanta, GA, USA, pp. 561-568, 1999.
- [29] G. A. Pratt and M. M. Williamson, "Series elastic actuators," *Proc. IEEE/RSJ International Conference on Intelligent Robotics and Systems*, Pittsburgh, PA, pp. 399-406, 1995.
- [30] C.-M. Chew, G.-S. Hong, and W. Zhou, "Series damper actuator: a novel force/torque control actuator," *Proc. 4th IEEE-RAS International Conference on Humanoid Robots*, Santa Monica, CA, USA, pp. 533-546, 2004.
- [31] G. B. Andeen and R. Kombluh, "Design of Compliance in Robotics," *Mechanical Research Laboratory, SRI International Menlo Park*, California, USA, pp. 276-281, 1988.
- [32] W. S. Jonathon and F. f. W. Richard, "Improvements to series elastic actuators," *Proc. 2nd IEEE/ASME International Conference on Mechatronic and Embedded Systems and Applications*, pp. 1-7, 2006.
- [33] J. E. Pratt and B. T. Krupp, "Series elastic actuators for legged robots," *Proc.*

- the SPIE*, Orlando, FL, United States, vol.5422, pp. 135-144, 2004.
- [34] D. W. Robinson, "Design and analysis of series elasticity in closed-loop actuator force control," *Doctoral Dissertation*, Department of Mechanical Engineering, Massachusetts Institute of Technology, 2000.
- [35] W. T. Townsend and J. A. Guertin, "Teleoperator slave - WAM design methodology," *Industrial Robot: An International Journal*, vol. 26, pp. 167-177, 1999.
- [36] "How Do You Choose a Haptic Device?" [Online]. Available: http://www.mpb-technologies.ca/mpbt/haptics/hand_controllers/freedom/resources/How%20do%20you%20choose%20a%20haptic%20device.pdf.
- [37] J. Versace, "A Review of the Severity Index," *Proc. 15th Stapp Car Crash Conference, Society of Automotive Engineers*, New York, USA, pp. 771-796, 1971.
- [38] A. Bicchi and G. Tonietti, "Fast and soft-arm" *IEEE Robotics and Automation Magazine*, vol. 11, pp. 22-33, 2004.
- [39] J.-J. Park, B.-S. Kim, J.-B. Song, and H.-S. Kim, "Safe link mechanism based on passive compliance for safe human-robot collision," *Proc. IEEE International Conference on Robotics and Automation*, Rome, Italy, pp. 1152-1157, 2007.
- [40] M. Zinn, O. Khatib, B. Roth, and J. K. Salisbury, "Playing it safe," *IEEE Robotics and Automation Magazine*, vol. 11, pp. 12-21, 2004.
- [41] W. T. Townsend and J. K. Salisbury, "Mechanical bandwidth as a guideline to high-performance manipulator design," *Proc. IEEE International Conference on Robotics and Automation*, Scottsdale, AZ, USA, pp. 1390-1395, 1989.
- [42] B. Rooks, "The harmonious robot," *Industrial Robot: An International Journal*, vol. 33, pp. 125-130, 2006.
- [43] A. Edsinger-Gonzales and J. Weber, "Domo: a force sensing humanoid robot for manipulation research," *Proc. IEEE-RAS International Conference on Humanoid Robots*, Santa Monica, CA, USA, pp. 273-291, 2004.
- [44] E. a. B. Torres-Jara, J., "A simple and scalable force actuator," *Proc. the 35th International Symposium on Robotics*, Paris, France, pp. 1-5, 2004.
- [45] J. W. Sensinger and R. F. Weir, "Design and analysis of a non-backdrivable series elastic actuator," *Proc. International Conference on Rehabilitation Robotics*, Chicago, IL, USA, pp. 390-393, 2005.
- [46] N. G. Tsagarakis, M. Laffranchi, B. Vanderborght and D. G. Caldwell, "A compact soft actuator unit for small scale human friendly robots," *Proc. IEEE International Conference on Robotics and Automation*, Kobe, Japan, pp.

- 4356-4362, 2009.
- [47] G. Rosati, S. Cenci, G. Boschetti, D. Zanotto and S. M. MD, "Design of a single-dof active hand orthosis for neurorehabilitation," *Proc. IEEE International Conference on Rehabilitation robotics*, Kyoto International Conference Center, Japan, pp. 161-166, 2009.
 - [48] K. kong, J. Bae and M. Tomizuka, "Control of rotary series elastic actuator for ideal force-mode actuation in human-robot interaction application," *IEEE/ASME Transactions on Mechatronics*, vol.14, no 1, pp. 105-118, 2009.
 - [49] H. K. Kwa, J. H. Noodren, M. Missel and T. Craig, "Development of the IHMC mobility assist exoskeleton," *Proc. IEEE International Conference on Robotics and Automation*, Kobe, Japan, pp. 2556-2562, 2009.
 - [50] S. K. Au, J. Weber and H. Herr, "Powered ankle-foot prosthesis improves walking metabolic economy," *IEEE Transactions on Robotics*, vol. 25, no 1, pp. 51-66, 2009.
 - [51] B. Bigge and I. R. Harvey, "Programmable springs: developing actuators with programmable compliance for autonomous robots," *Robotics and Autonomous Systems*, vol. 55, pp. 728-734, 2007.
 - [52] J. E. C. Jonathan W. Hurst, and Alfred A. Rizzi, "The actuator with mechanically adjustable series compliance," *IEEE Transactions on Robotics*, vol. 26, no 1, pp. 597-606, 2010.
 - [53] A. Bicchi, M. Bavaro, G. Boccadamo, D. De Carli, R. Filippini, G. Grioli, M. Piccigallo, A. Rosi, R. Schiavi, S. Soumen, and G. Tonietti, "Physical human-robot interaction: dependability, safety, and performance," *Proc. IEEE International Workshop on Advanced Motion Control*, Trento, Italian, pp. 9-14, 2008.
 - [54] H. Iwata, S. Kobashi, T. Aono, and S. A. S. S. Sugano, "Design of anthropomorphic 4-DOF tactile interaction manipulator with passive joints," *Proc. IEEE/RSJ International Conference on Intelligent Robots and Systems*, Tokyo, Japan, pp. 1785-1790, 2005.
 - [55] R. M. Kolacinski and R. D. Quinn, "A novel biomimetic actuator system," *Robotics and Autonomous Systems*, vol. 25, pp. 1-18, 1998.
 - [56] K. F. Laurin-Kovitz, J. E. Colgate, and S. D. R. Carnes, "Design of components for programmable passive impedance," *Proc. IEEE International Conference on Robotics and Automation*, Sacramento, California, pp. 1476-1481, 1991.
 - [57] A. Bicchi, G. Tonietti, M. Bavaro, and M. Piccigallo, "Variable stiffness actuators for fast and safe motion control," *Proc. International Symposium of Robotics Research*, Siena, Italy, pp. 527-536, 2003.

- [58] J. Choi, S. Hong, W. Lee and S. Kang, "A variable stiffness joint using leaf spring for robot manipulators," *Proc. IEEE International Conference on Robotics and Automation*, Tokyo, Japan, pp. 4363-4368, 2009.
- [59] N. G. Tsagarikis, A. Jafari, and D. G. Caldwell, "A novel variable stiffness actuator: minimizing the energy requirements for the stiffness regulation," *Proc. Annual International Conference of the IEEE Engineering in Medicine and Biology Society(EMBC)*, Buenos Aires, Argentina, pp. 1275-1278, 2010.
- [60] F. Petit, M. Chalon, W. Fried, M. Grebentein, A. A. Schaffer and G. Hirzinger, "Bidirectional antagonistic variable stiffness actuation: analysis, design and implementation," *Proc. IEEE International Conference on Robotics and Automation*, Anchorage, Alaska, USA, pp. 4189-4196, 2010.
- [61] A. A. Schaffer, S. Wolf, O. Eiberger, S. Haddadin, F. Petit and M. Chalon, "Dynamic modeling and control of variable stiffness actuators," *Proc. IEEE International Conference on Robotics and Automation*, Anchorage, Alaska, USA, pp. 2155-2162, 2010.
- [62] B. S. Kim and J. B. Song, "Hybrid dual actuator unit: a design of a variable stiffness actuator based on an adjustable moment arm mechanism," *Proc. IEEE International Conference on Robotics and Automation*, Anchorage, Alaska, USA, pp. 1655-1660, 2010.
- [63] J. Choi, S. Hong, W. Lee and S. Kang, "A robot joint with variable stiffness using leaf springs," *IEEE Transactions on Robotics*, vol.27, no 2, pp. 229-238, 2011.
- [64] S. A. Migliore, E. A. Brown, and S. P. DeWeerth, "Novel nonlinear elastic actuators for passively controlling robotic joint compliance," *Journal of Mechanical Design*, vol. 129, pp. 406-412, 2007.
- [65] A. D. Luca, F. Flacco, A. Bicchi and R. Schiavi, "Nonlinear decoupled motion-stiffness control and collision detection/reaction for the VSA-II variable stiffness device," *Proc. IEEE International Conference on Intelligent Robotics and Systems*, St. Louis, USA, pp. 5487-5494, 2009.
- [66] M. Laffranchi, N. G. Tsagarakis and D. G. Caldwell, "Safe human robot interaction via energy regulation control," *Proc. IEEE International Conference on Intelligent Robotics and Systems*, St. Louis, USA, pp. 35-41, 2009.
- [67] K. Koganezawa and H. Yamashita, "Stiffness control of multi-DOF joint," *Proc. IEEE International Conference on Intelligent Robotics and Systems*, St. Louis, USA, pp. 363-370, 2009.
- [68] M. Grebenstein, M. Chalon, G. Hirzinger and R. Siegwart, "Antagonistically driven finger design for the anthropomorphic DLR hand arm system," *Proc.*

- IEEE-RAS International Conference on Humanoid Robotics*, Nashville, TN, USA, pp. 609-616, 2010.
- [69] K. W. Hollander, T. G. Sugar, and D. E. Herring, "Adjustable robotic tendon using a jack spring trade," *Proc. International Conference on Rehabilitation Robotics*, Chicago, IL, USA, pp. 113-118, 2005.
- [70] T. W. Secord, A. Mazumdar and H. H. Asada, "A multi-cell piezoelectric device for tunable resonance actuation and energy harvesting," *Proc. IEEE International Conference on Robotics and Automation*, Anchorage, Alaska, USA, pp. 2169-2176, 2010.
- [71] M. Laffranchi, N. G. Tsagarakis and D. G. Caldwell, "Safe human robot interaction via energy regulation control," *Proc. IEEE International Conference on Intelligent Robotics and Systems*, St. Louis, USA, pp. 35-41, 2009.
- [72] J. B. Morrell, "Parallel coupled micro-macro actuators," Department of Mechanical Engineering, Massachusetts Institute of Technology, Technical Report, no. 1563, 1996.
- [73] M. Zinn, B. Roth, O. Khatib, and J. K. Salisbury, "A new actuation approach for human friendly robot design," *Proc. IEEE International Conference on Robotics and Automation*, New Orleans, LA, pp. 249-254, 2004.
- [74] R. Van Ham, B. Vanderborght, M. Van Damme, B. Verrelst, and D. Lefeber, "MACCEPA, the mechanically adjustable compliance and controllable equilibrium position actuator: design and implementation in a biped robot," *Robotics and Autonomous Systems*, vol. 55, pp. 761-768, 2007.
- [75] R. C. G. K.S. Fu, and C.S.G. Lee, *Robotics: Control, Sensing, Vision, and Intelligence*. New York: McGraw-Hill Book Company, 1987.
- [76] I. Sardellitti, G. Palli, N. G. Tsagarakis, and D. G. Caldwell, "Antagonistically actuated compliant joint: torque and stiffness control," *Proc. IEEE International Conference on Intelligent Robots and Systems*, Taipei, Taiwan, pp. 1909-1914, 2010.
- [77] S. Jien, S. Hirai, Y. Ogawa, M. Ito and K. Honda, "Pressure control valve for McKibben artificial muscle actuators with miniaturized unconstrained pneumatic on/off valves," *Proc. IEEE/ASME International Conference on Advanced Intelligent Mechatronics*, Singapore, pp. 1383-1388, 2009.
- [78] R. Schiavi, A. Bicchi, and F. Flacco, "Integration of active and passive compliance control for safe human-robot coexistence," *Proc. IEEE International Conference on Robotics and Automation*, Kobe, Japan, pp. 259-264, 2009.
- [79] J.-J. Park, B.-S. Kim, J.-B. Song, and H.-S. Kim, "Safe link mechanism based

- on nonlinear stiffness for collision safety," *Mechanism and Machine Theory*, vol. 43, pp.1332-1348, 2007.
- [80] J.-J. Park, J.-B. Song, and H.-S. Kim, "Safe joint mechanism based on passive compliance for collision safety," *Lecture Note in Control and Information Sciences*, pp. 49-61, 2008.
- [81] J.-J. Park, H.-S. Kim, and J.-B. Song, "Safe robot arm with safe joint mechanism using nonlinear spring system for collision safety," *Proc. IEEE International Conference on Robotics and Automation*, Kobe, Japan, pp. 3371-3397, 2009.
- [82] Y. Morita, M. Nagasaki, H. Ukai, N. Matsui, and M. Uchida, "Development of rehabilitation training support system of upper limb motor function for personalized rehabilitation," *Proc. IEEE International Conference Robotics and Biomimetics*, Bangkok, Thailand, pp. 300-305, 2009.
- [83] K. Kong, J. Bae, and M. Tomizuka, "Control of rotary series elastic actuator for ideal force-mode actuation in human-robot interaction applications," *IEEE/ASME Transaction on Mechatronics*, vol. 14, no.1, pp. 105-118, 2009.
- [84] P. R. Culmer, A. E. Jackson, S. Makower, R. Richardson, J. A. Cozens, M. C. Levesley, and B. B. Bhakta, "A control strategy for upper limb robotic rehabilitation with a dual robot system," *IEEE/ASME Transactions on Mechatronics*, vol. 15, no. 4, pp. 575-585, 2010.
- [85] L. Masia, H. I. Krebs, P. Cappa, and N. Hogan, "Design and characterization of hand module for whole-arm rehabilitation following stroke," *IEEE/ASME Transactions on Mechatronics*, vol. 12, no. 4, pp. 399-407, 2007.
- [86] S. K. Banala, S. H. Kim, S. K. Agrawal, and J. P. Scholz, "Robot assisted gait training with active leg exoskeleton (ALEX)," *IEEE Transactions on Neural Systems and Rehabilitation Engineering*, vol. 17, no.1, pp. 2-8, 2009.
- [87] H. van Der Kooij, "Compliant actuation of rehabilitation robots," *IEEE Robotics and Automation Magazine*, vol. 15, pp. 60-69, 2008.
- [88] K. Kong and D. Jeon, "Design and control of an exoskeleton for the elderly and patients," *IEEE/ASME Transactions on Mechatronics*, vol. 11, no.4, pp. 428-432, 2006.
- [89] J. A. Blaya and H. Herr, "Adaptive control of a variable-impedance ankle-foot orthosis to assist drop-foot gait," *IEEE Transactions on Neural Systems and Rehabilitation Engineering*, vol. 12, no.1, pp. 24-31, 2004.
- [90] J. W. Sensinger and R. F. F. Weir, "User-modulated impedance control of a prosthetic elbow in unconstrained, perturbed motion," *IEEE Transactions on Biomedical Engineering*, vol. 55, no.2, pp. 1043-1055, 2008.

- [91] Vanderniepen, R. Van Ham, M. Van Damme, and D. Lefeber, "Design of a powered elbow orthosis for orthopaedic rehabilitation using compliant actuation," in *Proc. 2nd Biennial IEEE/RAS-EMBS International Conference Biomedical Robotics and Biomechanics*, Scottsdale, AZ, USA, pp. 801-806, 2008.
- [92] K. Kim, J. E. Colgate, J. J. Santos-Munn'e, A. Makhlin, and M. A. Peshkin, "On the design of miniature haptic devices for upper extremity prosthetics," *IEEE/ASME Transactions on Mechatronics*, vol. 15, no. 1, pp. 27-39, 2009.
- [93] A. B. Zoss, H. Kazerooni, and A. Chu, "Biomechanical design of the Berkeley lower extremity exoskeleton (BLEEX)," *IEEE/ASME Transactions on Mechatronics*, vol. 11, no.4, pp. 128-138, 2006.
- [94] S. K. Agrawal, S. K. Banala, A. Fattah, V. Sangwan, V. Krishnamoorthy, J. P. Scholz and W. L. Hsu, "Assessment of motion of a swing leg and gait rehabilitation with a gravity balancing exoskeleton," *IEEE Transactions on Neural Systems and Rehabilitation Engineering*, vol. 15, no.3, pp. 410-420, 2007.
- [95] S. K. Agrawal, S. K. Banala, K. Mamkala, V. Sangwan, J. P. Scholz, V. Krishnamoorthy, and W. L. Hsu, "Exoskeletons for gait assistance and training of the motor impaired," *Proc. IEEE International Conference on Rehabilitation Robotics*, Noordwijk, The Netherlands, pp. 1108-1113, 2007.
- [96] C. J. Walsh, D. Paluska, K. Pasch, W. Grand, A. Valiente, and H. Herr, "Development of a lightweight, underactuated exoskeleton for load-carrying augmentation," *Proc. IEEE International Conference Robotics and Automation*, Orlando, FL, USA, pp. 3485-3491, 2006.
- [97] T. Kikuchi, X. Hu, K. Fukushima, K. Oda, J. Furusho, and A. Inoue, "Quasi-3-DOF rehabilitation system for upper limbs: Its force-feedback mechanism and software for rehabilitation," *Proc. IEEE International Conference Rehabilitation Robotics*, Noordwijk, The Netherlands, pp. 24-27, 2007.
- [98] A. Khanicheh, D. Mintzopoulos, B. Weinberg, A. A. Tzika, and C. Mavroidis, "Evaluation of electrorheological fluid dampers for applications at 3-T MRI environment," *IEEE/ASME Transactions on Mechatronics*, vol. 13, no.3, pp. 286-294, 2008.
- [99] C. Mavroidis, J. Nikitczuk, B. Weinberg, G. Danaher, K. Jensen, P. Pelletier, J. Prugnarola, R. Stuart, R. Arango, M. Leahey, R. Pavone, A. Provo, and D. Yasevac, "Smart portable rehabilitation devices," *Journal of NeuroEngineering and Rehabilitation*, vol. 2, pp. 18, 2005.

- [100] G. A. Pratt and M. M. Williamson, "Series elastic actuators," *Proc. IEEE/RSJ International Conference on Intelligent Robots and Systems*, Pittsburgh, USA , pp. 399–406, 1995.
- [101] K. S. Kim, J. J. Park and J. B. Song, "Safe joint mechanism using double slider mechanism and spring for humanoid robot arm," *Proc. 8th IEEE/RAS International Conference on Human Robots*, Daejeon, Korea, pp. 73–78. 2008.
- [102] J. J. Park, H. S. Kim, J. B. Song and H. S. Kim, "Safe robot arm with safe joint mechanism using nonlinear spring system for collision safety," *Proc. IEEE International Conference on Robotics and Automation*, Kobe, Japan, pp. 3371–3376, 2009.
- [103] S. A. Migliore, E. A. Brown and S. P. D. Weerth, "Biologically Inspired joint stiffness control," *Proc. IEEE International Conference on Robotics and Automation*, Barcelona, Spain, pp.4508–4513, 2005.
- [104] G. Tonietti, R. Schiavi and A. Bicchi, "Design and control of a variable stiffness actuator for safe and physical human/robot interaction," *Proc. IEEE International Conference Robotic Automation*, Barcelona, Spain, pp. 526–531, 2005.
- [105] D. G. Caldwell, G. A.M. Cerda, and M. J. Goodwin, "Braided pneumatic actuator control of a multi-jointed manipulator," *Proc. IEEE International Conference on Systems, Man and Cybernetics, Systems Engineering in the Service of Humans*, Le Touquet, France, pp.423-428, 1993.
- [106] F. Daerden, and D. Lefeber, "The concept and design of pleated pneumatic artificial muscles," *International Journal Fluid Power*, vol.2, no.3, pp. 41–50, 2001.
- [107] N. Saga, T. Saikawa and H. Okano, "Flexor mechanism of robot arm using pneumatic muscle actuators," *Proc. IEEE International Conference on Mechatronics and Automation*, Niagara Falls, Canada, pp. 1261–1266, 2005.
- [108] D. Shin, I. Sardellitti, and O. Khatib, "A hybrid actuation approach for human-friendly robot design," *Proc. IEEE International Conference on Robotic Automation*, Pasadena, CA, USA, pp. 1747–1752, 2008.
- [109] S. Wolf and G. Hirzinger, "A new variable stiffness design Matching requirements of the next robot generation," *Proc. IEEE International Conference on Robotic Automation*, Pasadena, CA, USA, pp. 1741–1746, 2008.
- [110] R. Schiavi, G. Grioli, S. Sen and A. Bicchi, "VS-II: a novel prototype of variable stiffness actuator for safe and performing robots interacting with humans," *Proc. IEEE International Conference on Robotic Automation*, Pasadena, CA, USA, pp. 19–23, 2008.

- [111] B. S. Kim, J. B. Song, and J. J. Park, "A serial-type dual actuator unit with planetary gear train: basic design and application," *IEEE/ASME Transactions on Mechatronics*, vol. 15, no.1, pp.108–116, 2010.
- [112] B. S. Kim and J. B. Song, "Hybrid dual actuator unit: a design of a variable stiffness actuator based on an Adjustable moment arm mechanism," *Proc. IEEE International Conference on Robotic Automation*, Anchorage, Alaska, USA, pp. 1655–1660, 2010.
- [113] T. Morita and S. Sugano, "Development of one-D.O.F. robot arm equipped with mechanical impedance adjuster," *Proc. IEEE International Conference on Mecharonics and Automation*, Niagara Falls, Canada, pp. 1261–1266, 2005.

